Intracellular delivery of radioimmunoconjugates that target the cancer testis antigen, NY-ESO-1

Hin Lun Chu

Linacre College

Gray Institute for Radioation Oncology and Biology

Department of Oncology

Supervisor:

Professor Katherine Vallis

A thesis submitted for the degree

Doctor of Philosophy

Michaelmas Term 2013

Intracellular delivery of radioimmunoconjugates that target the cancer testis antigen, NY-ESO-1

Hin Lun Chu

Linacre College, University of Oxford

Doctor of Philosophy, Michaelmas Term 2013

Abstract

Cancer testis antigens (CTA) represent attractive targets for targeted radiotherapy and imaging as their expression is restricted to cancer and germ cells. NY-ESO-1, a member of the CTA family, is highly immunogenic and expressed in multiple tumor types including carcinoma of bladder, liver lung. The aim of this study was to develop radioimmunoconjugates (RIC) to target NY-ESO-1 protein in cancer cells. Anti-NY-ESO-1 antibodies were modified by addition of DTPA for ^{111}In-labelling or, in the presence of Iodogen, were ^{123}I-labelled. . Delivery of radiolabeled immunoconjugates across the cell membrane was achieved using a protein transfection (PT) reagent (SAINT-PhD) and by chemical linkage with the cell-penetrating and nuclear-localizing peptide, TAT (YGRKKRRQRRR). Cellular internalization, distribution and efflux of ^{111}In-DTPA-anti-NY-ESO-1-TAT-PT and ^{123}I-anti-NY-ESO-1-TAT-PT were investigated in cell fractionation and retention assays. It was shown that protein transfection reagent has promoted the cellular uptake of RICs into SK-MEL-37 and both of ^{111}In-DTPA-anti-NY-ESO-1-TAT-PT and ^{123}I-anti-NY-ESO-1-TAT-PT was retained longer in SK-MEL-37 cells in comparison to their isotope control RIC. In clonogenic assays, ^{111}In-DTPA-anti-NY-ESO-1-TAT-PT significantly reduced surviving fraction of SK-MEL-37 cells. Cytotoxicity was inversely proportional to specific activity and

the concentration of cells exposed to ^{111}In-DTPA-anti-NY-ESO-1-TAT-PT. siRNA knock down of NY-ESO-1 resulted in partial reversal of ^{111}In-DTPA-anti-NY-ESO-1-TAT-PT associated cytotoxicity. These promising results obtained from the *in vitro* study has brought the probe further into *in vivo* study. In preliminary biodistribution studies in SK-MEL-37 xenograft-bearing mice, tumour:muscle ratio for ^{111}In-DTPA-anti-NY-ESO-1-TAT-PT was statistically significant compared to the control RIC 48 h post injection. This clearly indicated that the probe can be delivered into tumour in *in vivo* model and the successful uptake of radioactivity increased the chance of causing cytotoxicity to tumour cells through DNA damage. All of these findings have suggested that intracellular cancer associated antigen NY-ESO-1 can be reached by protein transfection reagent and cell penetrating peptide and initiates DNA damage through radio-isotope mediated cytotoxicity. Therefore, it represents a novel approach not just to the treatment of CTA-expressing cancers but also any of the possible intracellular expressing oncoprotein.

Acknowledgements

I am very grateful to my supervisor, Professor Katherine Vallis, for her invaluable advice, supervision, support, guidance and encouragement over four years that eventually came into this thesis. More importantly, she set a very good example on being a clinician as well as a successful researcher which is the career path that I want to pursue in the future. She is very enthusiastic and puts tremendous effort on helping and guiding me throughout my research. I am extremely thankful to her that she is always being patient in pushing me to understand everything related to my research area. Furthermore, I don't think I can achieve my dream in getting into medical school in Hong Kong without a well written reference provided by my supervisor. Thank you very much for everything, Kate!

I am also grateful to Dr. Bart Cornelissen who has always been there explaining all the scientific mysteries to me. Basically, he taught me almost everything on how to radiolabel an antibody and everything related to radioactivity. He has been my hero in the past 4 years.

Sarah Able, our research assistant, will be helping me to complete my experiments that I could not finish during my time in Oxford. She is always helpful and generous to offer her help when we need her in the lab all the time. She is also the one who helped to prove-read the first draft of my thesis. Thank you so much!

All other current and past members in the group including, Philip Waghorn, Mark Jackson, Ketan Shah, Neel Patel, Sam Terry, have provided countless useful tips

and a very friendly atmosphere in the lab. I cannot believe that I have already spent 4 years in the lab. Time flies so quickly because of you all!

Finally, I would like to thank my family and friends. There would have been no way through without my friends and family. I would not have been able to pursue my dream without their support and encouragement. Thank you very much!

Table of Contents

List of Abbreviations

ADCC	Antibody-dependent cell-mediated cytotoxicity
γH2AX	Phosphorylated histone H2A subtype X
ATM	Ataxia telangiectasia mutated
BORIS	Brother Of the Regulator of Imprinted Sites
BSA	Bovine serum albumin
CDC	Complement dependent cytotoxicity
CEA	Carcinoembryonic antigen
CPM	Counts Per Minute
CPP	Cell Penetrating Peptides
CTA	Cancer Testis Antigens
CT	Computerised tomography
DAC	5-aza-2'-deoxycitidine
DAPI	2-(4-amidinophenyl)-1H -indole-6-carboxamidine
DC	Dendritic cells
DLBCL	Diffuse large B-cell lymphoma

DTPA	Diethylenetriaminepentaacetic acid
EDC	1-Ethyl-3-[3-dimethylaminopropyl]carbodiimide Hydrochloride
FACS	Fluorescence-activated cell sorter
FDA	Food and Drug Administration
HER2	Human Epidermal Growth Factor-2 Receptor
HIF	Hypoxia-inducble factor
HIV	Human Immunodeficiency Virus
HLA	Human histocompatibility leukocyte antigen
ICC	Immunocytochemistry
IHC	Immunohistochemistry
Iodogen	1,3,4,6-tetracholoro-3α,6α-diphenylglycouril
ITLC	Instant thin layer chromatography
LET	Linear energy transfer
mAb	Monoclonal Antibody
MES	2-(*N*-morpholino)ethanesulfonic acid
MHC	Major histocompatibility complex
NLS	Nuclear localization sequence
NK	Natural killer
qPCR	quantitative polymerase chain reaction

PI3K	Phosphatidylinositol 3-kinase
$PI(4,5)P_2$	Phosphatidylinositol-4,5-bisphosphate
PT	Protein transfection
PTD	Protein transduction domains
p-SCN-Bn-DTPA	2-(4-isothiocyanatobenzyl)-diethylenetriaminepentaacetic acid
RIPA	Radioimmunoprecipitation Assay
RIC	Radioimmunoconjugate
RIT	Radioimmunotherapy
RT	Room Temperature
RT-PCR	Reverse-transcriptase polymerase chain reaction
VEGF	Vascular endothelial growth factor
SDS-PAGE	Sodium dodecyl sulfate polyacrylamide gel electrophoresis
SEC	size-exclusion chromatography
SEREE	Serological identification of antigens by recombinant cDNA expression libraries
SF	Surviving fraction
SPECT	Single Photon Emission Computerised Tomography
Sulfo-NHS	*N*-hydroxysulfosuccinimide
TAT	Trans-Activator of Transcription

Chapter 1

Introduction

Chapter 1: Introduction

1.1. Cancer

1.1.1. Cancer Statistics,

The term cancer is used to describe diseases in which there is uncontrolled growth of abnormal cells, which have the ability to invade other tissues. In a non-disease state, cells are subject to mitogenic growth signals, which regulate transition from a quiescent state into an active proliferative state. Hence cell division is tightly regulated under normal conditions (Hanahan and Weinberg, 2000). However, mutations in genes encoding critical cell regulatory proteins can cause changes in cell behaviour, resulting in an expansion of abnormal cells that infiltrate surrounding normal tissue and acquire the capacity to metastasize (Alison, 2001).

According to national statistics provided by Cancer Research UK, more than 324,500 people diagnosed with cancer in the UK in 2010, with cancer being the second biggest killer following heart disease (2010 http://www.cancerresearchuk.org/cancer-info/cancerstats/incidence/). The European age standardised rate for cancer in the UK is significantly higher in males than females (426 per 100,000 vs. 374 per 100,000, respectively) (2012 http://www.cancerresearchuk.org/cancer-info/cancerstats/incidence/all-cancers-combined/#UK). The majority of cancers are non-hereditary, and are attributed to environmental factors such as smoking, life style and infections (Hanahan and Weinberg, 2000). Inherited genetic defects account for 5-10% cases of cancer. Cancer incidence is increasing globally and hence cancer therapy is an active field of scientific research.

1.1.3. The phenotype of cancer cells

DNA damage occurs at a rate of $1x10^3$ to $1x10^6$ molecular lesions per cell per day, in response to environmental factors and normal metabolic processes inside cells. Unrepaired DNA lesions in critical genes could lead to defects in the regulatory pathways that control normal cell proliferation and homeostasis. The behaviour of cancer cells does not depend only on changes in gene expression but is also influenced by external signals from surrounding cells in the tissue and microenvironment. It has been proposed that in the majority of cases, cancer cell phenotype is a manifestation of six common modifications in cell biology: self-sufficiency in growth signals (e.g. activation of H-Ras or myc oncogene), insensitivity to growth inhibitory signals (e.g. mutation in retinoblastoma protein), evasion of programmed cell death (e.g. over-expression of survival signals such as IGF-1), activation of telomerase, sustained angiogenesis (e.g. upregulation of VEGF expression), and tissue invasion and metastasis (e.g. inactivation of E-cadherin molecules) (Malumbres and Barbacid, 2003, Parrizas et al., 1997, Hanahan and Weinberg, 2000). Most human cancers exhibit at least one of these physiological alterations and evolve to acquire further abnormalities.

1.1.3. Current therapeutic approaches to cancer

There are more than 200 different types of cancer and there are over 60 different organs in the body in which cancer can develop. The survival rates for most types of cancer have improved in developed nations in recent years, as understanding of the biological mechanisms that underlie cancer has increased (2009 http://www.cancerresearchuk.org/cancer-info/cancerstats/survival/latestrates/survival-statistics-for-the-most-common-

cancers). Currently, primary tumours are treated using a combination of therapies, such as surgery, local radiotherapy, chemotherapy and immunotherapy. It is necessary to use the optimum combination of these therapies to reduce the chance of cancer cell survival and the occurrence of micrometastases that frequently lead to tumour relapse (Zitvogel et al., 2008).

1.1.7. Chemotherapy

The use of chemotherapy to treat cancer began in the 1940s with the use of nitrogen mustards and antifolate drugs. The complete regression of a tumour through the use of chemotherapy in humans was first documented in 1958 when Roy Hertz *et al.* observed that choriocarinoma, a germ cell malignancy derived from trophoblastic cells of the placenta, was successfully treated using methotrexate, which acts via inhibition of DNA synthesis (Chabner and Roberts, 2005, Li et al., 1958). Since that time, advances in laboratory techniques and innovations in biotechnology have led to the identification of new signalling pathways that regulate cellular activities such as proliferation and programmed cell death. The wealth of research into the mechanisms underlying tumour development has led to the design of novel chemotherapeutic agents to treat cancer.

There are several cytotoxic compounds that are widely used in chemotherapy for treating cancers, which act via inhibition of DNA synthesis or interference of the signalling pathways. For example, 5-fluorouracil and gemcitabine, termed antimetabolites, are analogues of pyrimidine nucleoside that disrupt DNA and RNA synthesis. Another potent cytotoxic compound, oxaliplatin, a platinum agent,

has a synergic effect with 5-fluorouracil against colon cancer (Bleiberg and de Gramont, 1998). Oxaliplatin forms both inter-and intra-strand platinum DNA crosslinks leading to inhibition of DNA replication. The DNA methyltransferase inhibitor 5-aza-2'-deoxycitidine (DAC), which is used in the treatment of leukemias and myelodysplastic syndrome, is thought to exert an anti-tumour effect via reactivation of tumour suppressor genes that had been silenced by methylation in cancer cells (Zitvogel et al., 2008, Lubbert, 2000). The development of imatinib mesylate was one of the breakthroughs in chemotherapy as it was the first cytotoxic compound that could be described as a targeted therapy. This molecule is widely used in the treatment of chronic myelogenous leukemia and exerts its anti-cancer effect by preventing the tyrosine kinase BCR-ABL, which is solely expressed in tumour cells, from phosphorylating downstream signalling molecules, thus inhibiting cancer growth and leading to apoptosis (Chabner and Roberts, 2005, Stegmeier et al.).

1.1.5. Radiotherapy

Radiation, in the form of alpha (α) particles, beta (β) particles or gamma (γ) rays, is released by unstable atomic nuclei to achieve an energetically stable state. Instability of nuclei generally increases with atomic size, with the largest stable nucleus being that of Bismuth (atomic number 83). Alpha particles, which are comprised of two protons and two neutrons, are generally released by larger radioactive atomic nuclei. Beta particles are high-energy electrons or positrons released from nuclei with an excess of neutrons or protons respectively. Gamma rays, high-energy electromagnetic radiation, can be produced following alpha or beta decay. When a nucleus emits an alpha or beta particle, the daughter nucleus

is usually left in an excited state. It can then move to a lower energy state by emitting a gamma ray.

Exposure to ionising radiation has a variety of cellular consequences, including changes in protein expression, activation of signalling pathways such as DNA repair mechanisms, and apoptosis (Hall, 1997). Exposure of cells to ionising radiation leads to DNA damage, which activates the ataxia telangiectasia mutated (ATM) protein kinase, and triggers different downstream signal transduction pathways responsible for regulating cell survival (Valerie et al., 2007). Exposure to ionising radiation can induce different forms of DNA damage, including single-strand breaks, double-strand breaks, and DNA-DNA and DNA-protein crosslinks. Double-strand DNA breaks are thought to be the most important for inducing cell death, and their incidence increases with absorbed radiation dose (Prise et al., 2005).

Ionising radiation has played an important role in the treatment of cancers for over 100 years. Nearly 50% of all cancer patients are treated with radiotherapy, either alone or in combination with other cancer therapies (Delaney et al., 2005). There are three main methods used in the clinic to administer radiotherapy. External beam radiotherapy uses an external source of radiation directed at the tumour, and is the most common form of radiotherapy used in clinical practise. Internal radiotherapy (brachytherapy) involves the placement of a sealed radioactive source in proximity to the tumour site. This type of radiotherapy is commonly used in the treatment of carcinoma of cervix, prostate, and skin (Baskar et al., 2012). The third method, molecular targeted radiotherapy, is discussed in detail in a subsequent section of the introduction.

In addition to its use in cancer therapy, gamma radiation is also used in medical imaging to determine the location of tumours within the body. The patient is dosed with a tracer amount of gamma emitting radionuclide, and a gamma camera is then used to take 2D images from multiple angles by rotation around the patient. In a single-photon emission computerised tomography (SPECT) scan, a computerised tomographic algorithm is then applied to the 2D image projections, to generate a 3D data set. SPECT scans are commonly co-registered with x-ray computerised tomography (CT) scans, to combine the 3D imaging capabilities of SPECT with the precise anatomical information provided by CT.

1.1.6. Immunotherapy

The aim of cancer immunotherapy is to induce an immune response against tumour cells. The ‘magic bullet’ concept proposed by Paul Ehrlich over a century ago was realised in part by the discovery of monoclonal antibodies, which bind tumour antigens selectively and with high affinity. Initially, monoclonal antibodies were produced in mice, but these failed to produce effective cancer remission for several reasons, including ustimulation of a human immune response, short circulating half-life, poor ability to induce human effector responses and limited penetration into tumour sites (Stern and Herrmann, 2005). Advances in antibody engineering in the 1990s provided flexible platforms for generating chimeric, humanised and fully human monoclonal antibodies to overcome some of the problems associated with murine antibodies. Monoclonal antibodies (mAb) exert anti-tumour effects via a variety of mechanisms, such as interrupting signalling pathways involved in cell proliferation, tumour progression and survival (Slamon et al., 1989). Trastuzumab (Herceptin), a humanised mAb against the Human Epidermal Growth Factor-2 (HER2) receptor, was approved

by the Food and Drug Administration (FDA) in 1998 for use in patients with HER2 overexpressing breast cancer (Stern and Herrmann, 2005, Valabrega et al., 2007). Trastuzumab binds the extracellular domain of the HER2 protein, leading to disruption of receptor dimerisation and thus inhibiting the downstream phosphatidylinositol 3-kinase (PI3K) signalling pathway (Nahta et al., 2006).

Antibody targeted immunotherapy also has the ability to elicit an immune response against tumours via interaction with the antibody-dependent cellular cytotoxicity (ADCC) and complement dependent cytotoxicity (CDC) pathways (illustrated in Figure 1.1). ADCC is a mechanism of cell-mediated immune response in which effector cells, including granulocytes and macrophages, actively lyse target cells through interaction of their Fcγ receptors with the Fc portion of the antibody bound on the surface of the antigen. Rituximab, an anti-CD20 chimeric mAb approved by the FDA in 1997 for treatment of B cell non-Hodgkin Lymphoma, has been demonstrated to mediate ADCC. In a B16 mouse melanoma model, mice lacking activating Fcγ receptor, or dosed with antibodies engineered to disrupt Fc binding to Fcγ receptors, showed a lack of response to rituximab therapy (Clynes et al., 2000).

There is the potential to further improve the efficacy of antibody-based therapies using the strategies illustrated in Figure 1.2, one of which is attaching a radionuclide to the antibody, the basis for radioummunotherapy (RIT).

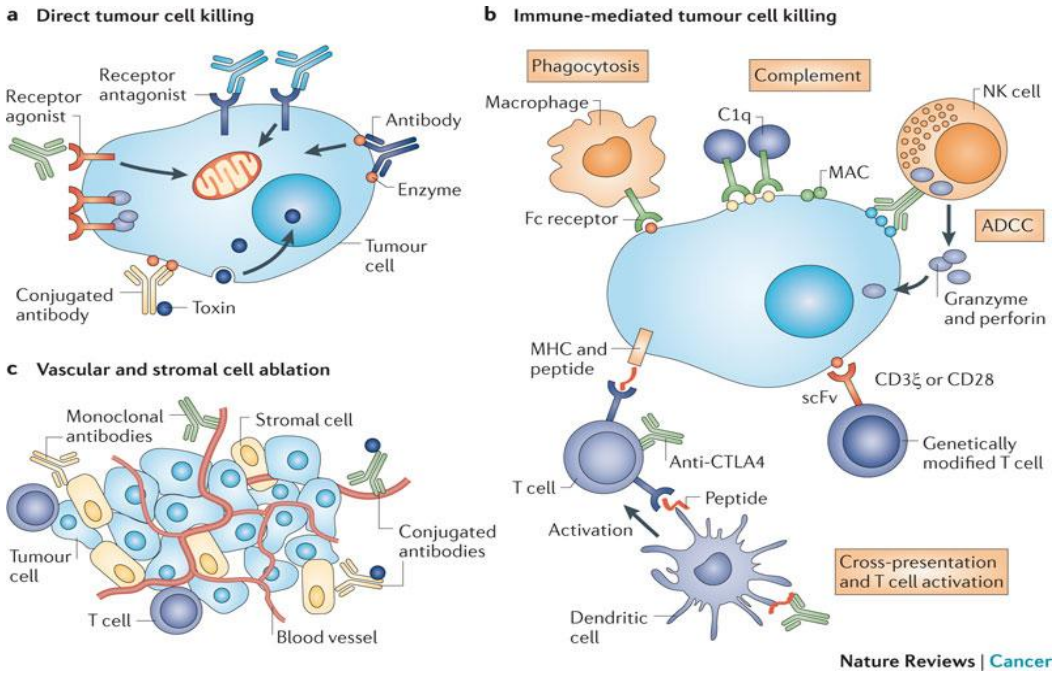

Figure 1.1. Mechanisms of antibody mediated tumour cell killing (adapted by permission from Nature Publishing Group) (Scott et al., 2012).

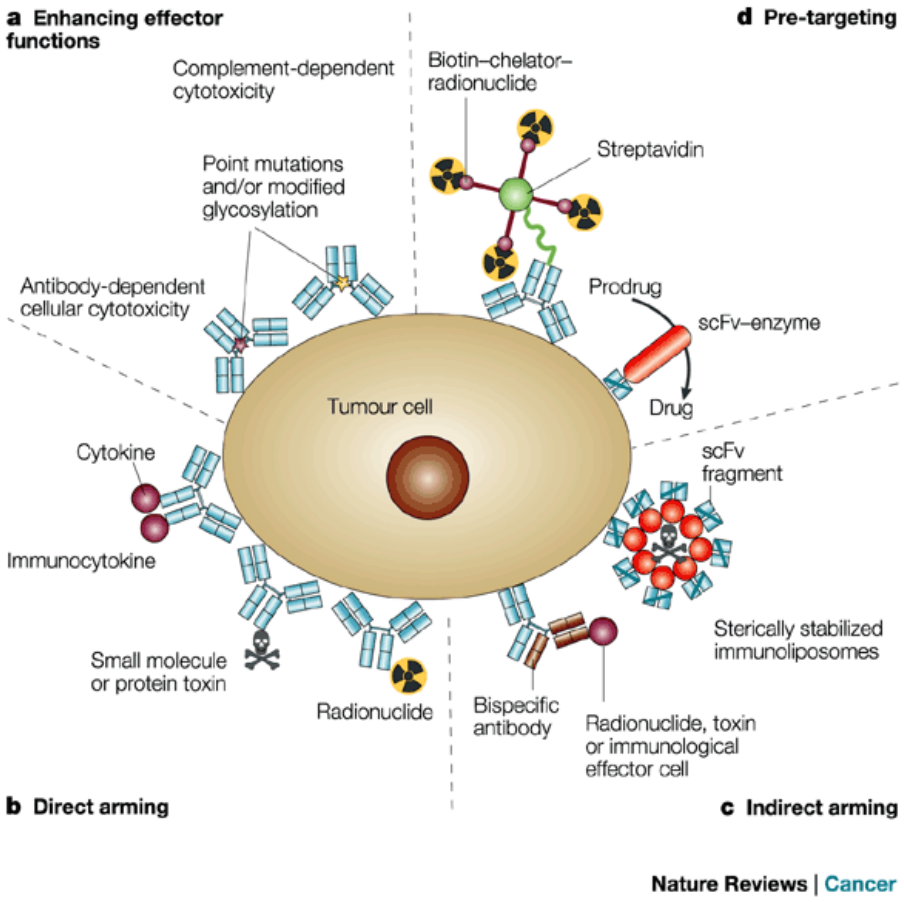

Figure 1.2. Strategies for monoclonal antibody antitumour targeting (adapted by permission from Nature Publishing Group). (Carter, 2001)

1.1.7. Radioimmunotherapy

Radioimmunotherapy is based on the use of monoclonal antibodies (mAb) to deliver radioisotopes to cancer cells. The concept of labelling an antibody with a radionuclide was first introduced by Pressman *et al.* in 1948, who developed a technique for radioiodinating a polyclonal antibody with ^{131}I (Pressman et al., 1949, Pressman, 1949). In 1953, Pressman *et al.* successfully localised tumours using a radiolabelled polyclonal antibody against osteogenic sarcoma (Pressman and Korngold, 1953). This was the first published literature demonstrating *in vivo* tumour imaging using a radiolabelled antibody. The development of hybridoma techniques enabled the large-scale production of mAb, which led, in turn, to an expansion in research into radioimmunotherapy.

To date two radioimmunotherapy treatments for cancer have been approved for use in patients. ^{90}Y-ibritumomab tiuxetan (zevalin®) and ^{131}I-tositumomab (Bexxar®) were approved by the FDA in 2002 and 2003 for the treatment of relapsed or refractory low grade, follicular or transformed B-cell lymphoma (Goldsmith, 2010). These radionuclide-conjugated antibodies act primarily by killing malignant cells via β-particle emission. It was demonstrated that the overall survival (OS) and progression free survival (PFS) times were improved in patients treated with ^{90}Y-ibritumomab tiuxetan or ^{131}I-tositumomab after first line induction treatments in comparison to patients treated with first line treatments only (Witzig et al., 2007, Buchegger et al., 2006a, Morschhauser et al., 2008). A comparison between ^{90}Y-ibritumomab tiuxetan and the anti-CD20 antibody rituximab was carried out in a Phase III trial involving patients with relapsed or refractory low-grade follicular or transformed B-cell non-Hodgkin lymphoma. It was shown that both the overall response rate and complete response rate were

higher for ^{90}Y-ibritumomab tiuxetan than rituximab (80% v 56% and 30% v 16%,respectively) (Witzig et al., 2002). Radioimmunotherapy represents a promising treatment option for cancer patients and is the focus of the experiments described in this thesis.

1.1.8. Auger electron therapy

Auger electron-emitters represent a class of radionuclides with potential for use in RIT. Auger electrons are emitted from the electronic shells of radionuclides that decay by electron capture, which is characteristic of atoms with an excess of protons versus neutrons. Electron capture is initiated when an inner shell electron transfers to the nucleus, and results in transformation of a proton into a neutron. The inner shell vacancy is then filled by electron transitions from a shell of higher energy. The energy released as electrons move from outer to inner shells may be sufficient to allow other electrons to be ejected from the atom. These have low energy and are know as Auger electrons . Auger electrons have a short range compared to other particles (Figure 1.3). The release of Auger electrons results in highly localised energy deposition in the immediate vicinity of the decaying radionuclide. The ionising effect of Auger electrons on DNA molecules is illustrated in Figure 1.4, in comparison to alpha and beta particles. High-energy alpha particles produce high density ionisations in the DNA molecule along a linear path. In comparison, ionisation events are less frequent along the track of energetic beta particles. Low energy Auger electrons, localised in close proximity to DNA molecules, frequently ionise along an irregular (zigzag) path leading to a cluster of high ionisation density, thereby generating dsDNA which may ultimately cause apoptosis (Buchegger et al., 2006b, Karagiannis, 2007). The

rationale for the use of Auger electron-emitting isotopes for radioimmunotherapy is that their short range allows ionising radiation to be delivered to tumour cells with minimal damage to surrounding tissue. In this study, the Auger electron-emitters, ^{111}Indium (^{111}In) and ^{123}Iodine (^{123}I), with decay half-lives of 2.8 days and 13.2 hours respectively, were utilised in a radioimmunotherapy strategy. ^{123}I is more suitable for imaging purpose due to its relatively short half life whereas ^{111}In is appropriate for Auger electron emitters type therapy.

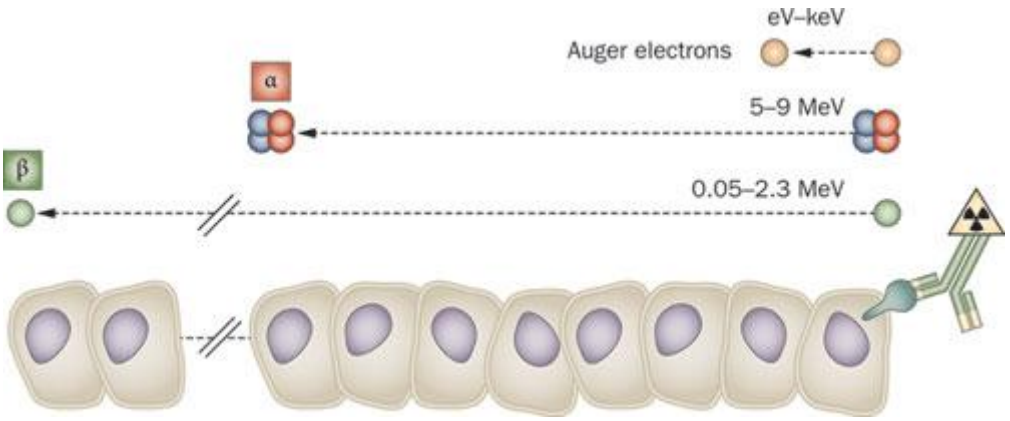

Figure 1.3. Schematic diagram illustrating the path length of alpha (α) particles, beta (β) particles and Auger electrons relative to the scale of mammalian cells (adapted by permission from Nature Publishing Group). (Pouget et al., 2011)

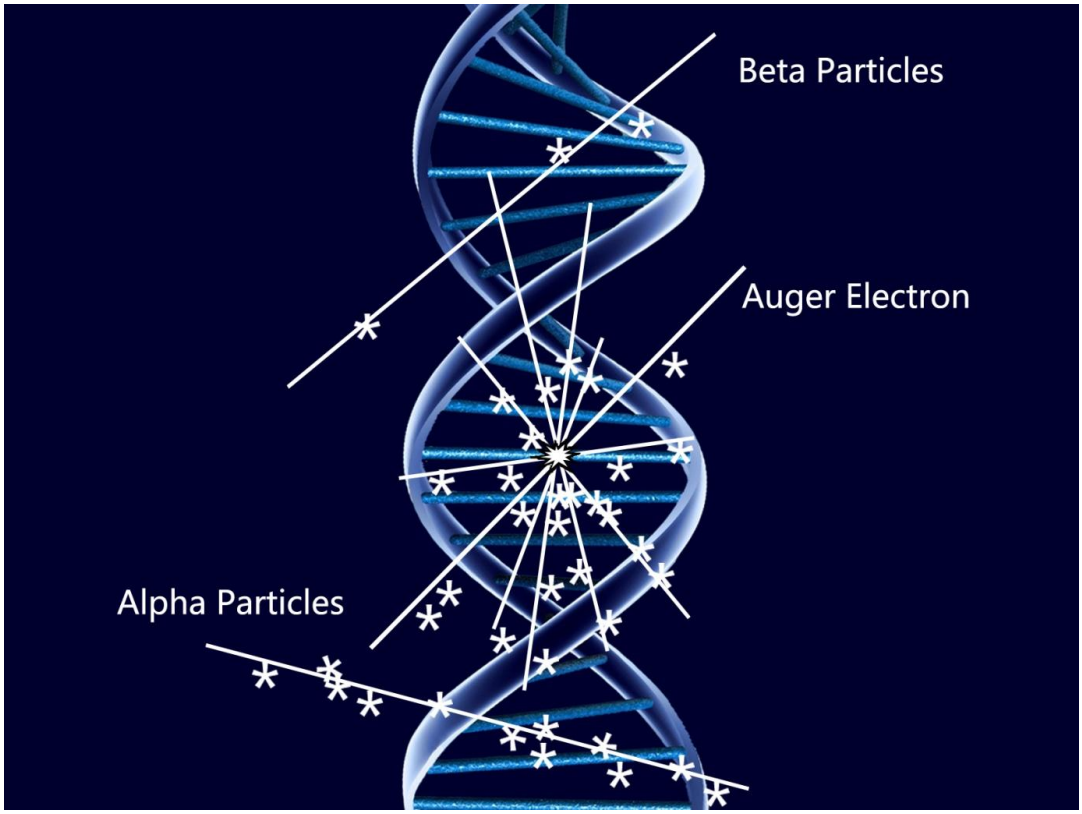

Figure 1.4. Schematic illustration of the ionising effect of different types of radioactive particles.

1.2. Cancer testis antigens

Cancer testis (CT) antigens can be defined as a class of proteins with normal expression restricted to germ cells in the testis, ovary and trophoblast, but which are also aberrantly activated and expressed in a range of human cancers. Although several CT antigens have been detected in somatic tissues including pancreas, liver and spleen, quantitative polymerase chain reaction (qPCR) showed that mRNA levels of CT antigens in these tissues are less than 1 % of their expression in testis (Caballero and Chen, 2009, Scanlan et al., 2004). Boon *et al.* successfully cloned the first human cancer testis antigen from a melanoma patient in in 1991 using the technique of autologous typing, in which cultured tumour and

normal cells from a patient are used as targets for specific immune recognition by the patient's own antibodies and T cells. This antigen was designated melanoma antigen-1 (MAGE-1, later renamed MAGE-A1) (van der Bruggen et al., 1991, Chen et al., 1994). The autologous typing approach led to the discovery of other CT antigens including B melanoma antigen (BAGE) and G antigen 1 (GAGE-1) which share no structural similarities with the MAGE gene (Scanlan et al., 2002). The discovery of other CT antigens was extended by the development of the technique known as SEREX (serological identification of antigens by recombinant cDNA expression libraries), in which cDNA expression libraries are screened using antibodies instead of T cells (Chen et al., 1997). Several CT antigens, including SSX2, NY-ESO-1, SCP-1 and CT-7, were identified by this strategy (Caballero and Chen, 2009). The technique of massive parallel signature sequencing (MPSS) was utilised to compare the mRNA expression profiles between testis, melanoma cell lines and other somatic tissues, which led to the discovery of more than 20 CT antigen-like genes including CT45 (Caballero and Chen, 2009).

CT antigens can be classified into two different groups: those that are encoded on the X-chromosome, termed CT-X antigens (Figure 1.5), and those that are located on other chromosomes, designated non-X CT antigens. More than 150 CT genes have been identified so far, and just over half of them are located on the X-chromosome, clustering between Xq24 and Xq28. Analysis of the DNA sequence of the X-chromosome suggests that approximately 10% of the genes are of CT antigen type, and they tend to form expanded families associated with inverted DNA repeats (Ross et al., 2005, Dobrynin et al.). In contrast, the genes for non-X

CT antigens are spread throughout the genome and do not generally form gene families or reside within genomic repeats (Simpson et al., 2005).

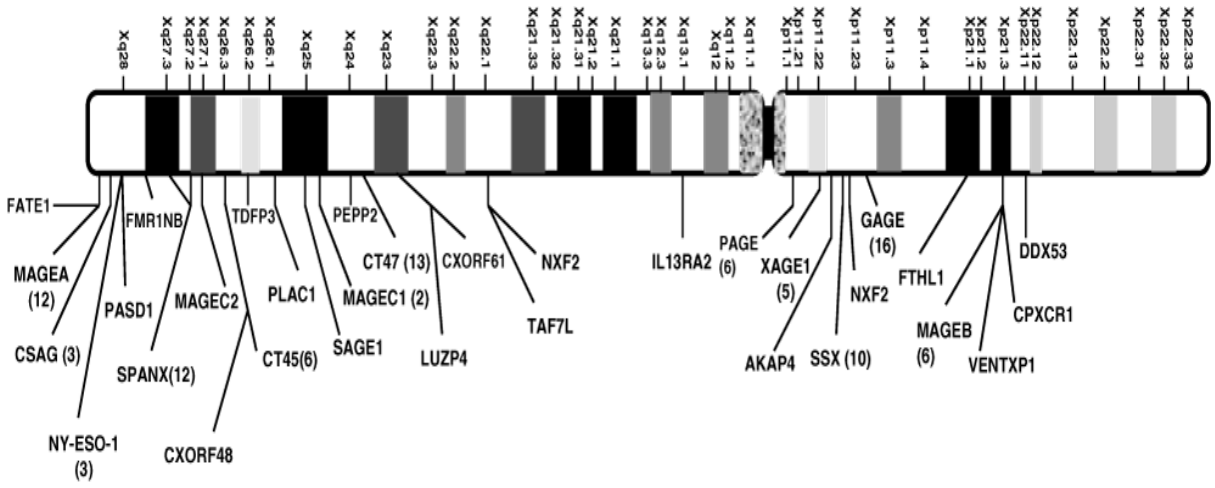

Figure 1.5. The distribution of CT antigens on the X-chromosome (Caballero and Chen, 2009).

The biological function of CT antigens remains poorly understood. In normal testis, CT-X antigens, such as MAGE and NY-ESO-1, are expressed in spermatogonia, whereas non-X CT antigens including SCP-1 and BORIS, are dominantly expressed in later stages of spermatogenesis, such as in spermatocytes (Figure 1.6) (Simpson et al., 2005). It is possible that CT antigens affect some key cellular processes involving cell-cycle, signalling pathway, and chromosomal recombination (Chiriva-Internati et al., 2012, Park et al., 2003, Simpson et al., 2005, Hayama et al., 2006). The extensive MAGE family of CT antigens, some of the most widely studied of the CT-X antigens, possesses a large central region, known as the MAGE homology domain (MHD) which is an important site of protein-protein interaction (Taniura et al., 2005). Moreover, MAGE-A1 was found to be involved in the NOTCH1 signalling pathway by interacting with SKIP

and recruiting histone deacetylase, thereby acting as a transcriptional repressor (Laduron et al., 2004). It is therefore possible that MAGE-A1 might have a regulatory role in early stages of spermatogenesis. Another member of MAGE family, MAGE-A11, was found to inhibit prolyl 4-hydroxylases 2 (PHD2) which results in maintenance of the stability of hypoxia-inducble factor (HIF) α subunit, thereby upregulating VEGF expression by increasing levels of HIF (Aprelikova et al., 2009). Retinoblastoma tumour suppressor protein can be destabilised by an oncoprotein gankyrin, contributing to the escape from cell cycle arrest. It was shown that MAGE-A4 is the binding partner of gankyrin and can suppress the activity of gankyrin by inducing p-53 dependent and p-53 independent apoptosis (Nagao et al., 2003). Other experiments have also indicated that overexpression of MAGE-A3 was associated with drug resistance (Simpson et al., 2005).

Non-X CT antigens are thought to be associated with meiosis, gametogensis, and fertilisation. For instance, it was shown in yeast that SPO11 causes double-stranded DNA breaks, initiating recombination events during meiosis (Keeney et al., 1997). Research into CT antigens continues, with the aim of further elucidating their structure and role in cell signalling pathways.

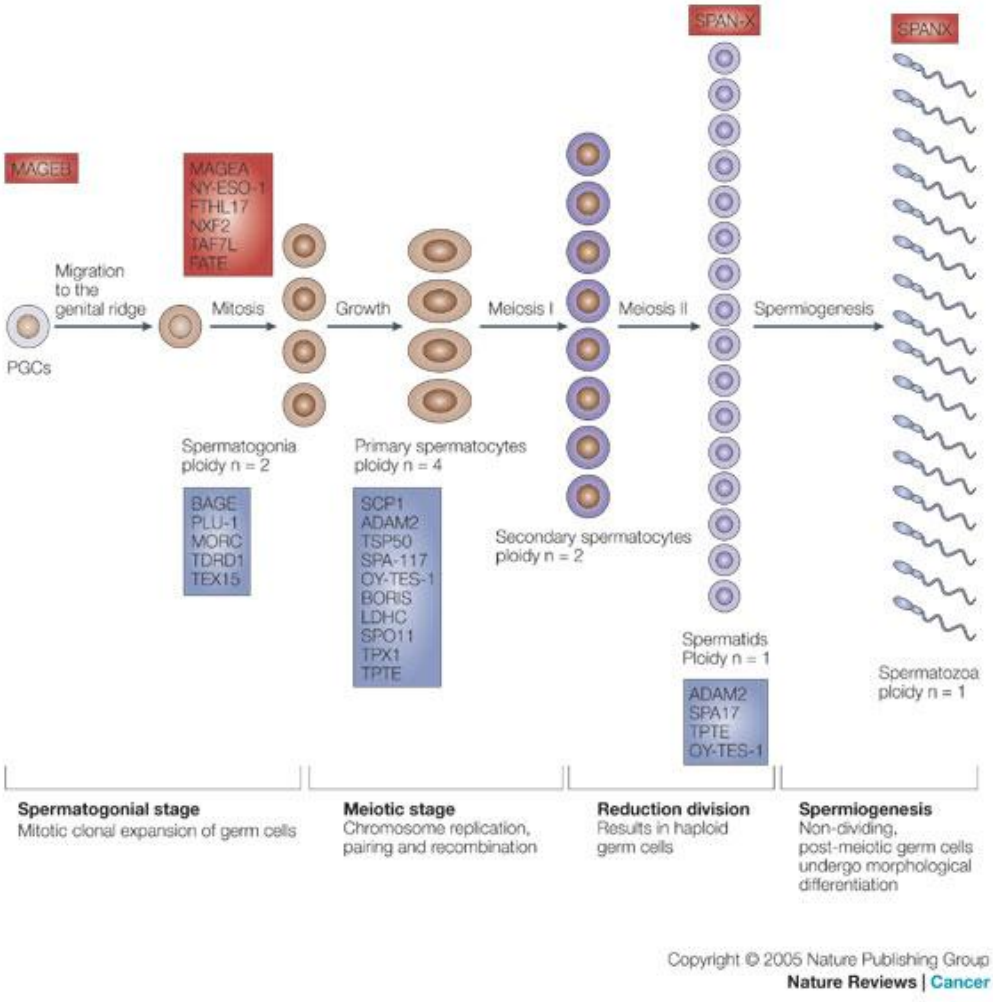

Figure 1.6. Summary of stages of spermatogenesis in humans (adapted by permission from Nature Publishing Group). (Simpson et al., 2005)

1.3. NY-ESO-1

NY-ESO-1 is a CT antigen that was first identified by applying SEREX to an oesophageal squamous cell carcinoma from a 58-year old female patient (Chen et al., 1997). The protein was termed NY-ESO-1 because it was identified in New York (NY) from an oesophageal cancer patient (ESO), and was the first member of a new gene family. The NY-ESO-1 gene is located on chromosome Xq28 (Figure 1.5) and encodes a protein of 180 amino acids with a molecular weight of 17,995 Da. Glycine is abundant at the N-terminal portion of the protein,

contributing hydrophilicity, whereas a long hydrophobic region is present near the C-terminal (amino acids 152-172) followed by a short hydrophilic region at the end of the C-terminal, suggesting the possibility of a transmembrane domain (Chen et al., 1997). LAGE-1, also located on chromosome Xq28, shares approximately 84%-89% homology with NY-ESO-1 at the protein level (Lethé et al., 1998).

A recent genome-wide analysis of the gene expression of 153 CT antigens led the authors to conclude that although these genes are generally highly expressed in testis, they exhibit heterogeneous gene expression profiles, allowing their classification into testis-restricted (39 genes), testis/brain-restricted (14 genes), and a testis-selective group of genes (85 genes) that show additional expression in somatic tissues. The majority of genes in the testis-restricted category are CT-X genes, including NY-ESO-1 (Hofmann et al., 2008). Similar to other CT-X antigens, the function of NY-ESO-1 has remained poorly understood. No gene knockout or transgenic studies have as yet been reported in the published literature and there are no known species homologues. Recently it has been shown that transcriptional regulation of NY-ESO-1 in lung cancer cells can be modulated by a non-X CT antigen termed Brother Of the Regulator of Imprinted Sites (BORIS). Upregulation of BORIS expression was shown to result in the nuclear translocation of the transcription factor SP-1 which led to an increase in NY-ESO-1 promoter activity (Kang et al., 2007).

NY-ESO-1 is a promising candidate for targeted immunotherapy due to its restricted expression in normal tissue but frequent occurrence in various types of cancers, which indicates that off-target effects of antibody-based therapy should be minimal. High levels of NY-ESO-1 mRNA, detected by reverse-transcriptase

polymerase chain reaction (RT-PCR), have been reported for cancers of the prostate, ovary, oesophagus, stomach, bladder and breast as well as in multiple myeloma, hepatocellular and non-small cell lung carcinoma. At the protein level, immunohistochemical staining (IHC) analysis indicates that the protein is expressed frequently in neuroblastoma, synovial sarcoma, melanoma, and epithelial ovarian cancer (Gnjatic et al., 2006, Nicholaou et al., 2006). NY-ESO-1 protein expression was demonstrated in the cytoplasm and nucleus of malignant melanoma tumour cells, and the median overall survival time for patients whose tumour cells were positive for NY-ESO-1 expression was 2 years shorter than those who were negative for NY-ESO-1 expression. The frequency of expression of NY-ESO-1 at the mRNA and protein level in various cancers has been summarised in Table 1.1. The expression of NY-ESO-1 in cancers affecting several different organs suggests the possibility that NY-ESO-1-targeted therapies would have efficacy in multiple tumour types.

NY-ESO-1 is reported to be highly immunogenic, although the immunological response varies by individual, type and stage of cancer. For instance, consistent with the frequency of NY-ESO-1 protein detection by IHC, autoantibodies against NY-ESO-1 were detected at higher levels in advanced neuroblastoma and melanoma, indicating immunogenicity of NY-ESO-1 is associated with the advanced stage of disease (Rodolfo et al., 2003, Jäger et al., 1999). For lung cancer patients, it has been reported that levels of autoantibody against NY-ESO-1 antigen were significantly higher in patients suffering from non-small cell lung cancer (23%) in comparison to small cell lung cancer (9%), and were found more frequently in undifferentiated tumours (40%) than in more differentiated adenocarcinoma or squamous cell carcinoma (15% and 29%) (Türeci et al., 2006).

However, the clinical significance of anti-NY-ESO-1 autoantibody remains unclear, as circulating autoantibodies would not be expected to gain access to the intracellular NY-ESO-1 protein.

Further evidence of the immunogenicity of NY-ESO-1 was obtained in a study involving a metastatic melanoma patient with a high titre antibody against NY-ESO-1. A cytotoxic T ($CD8^+$) cell line from the patient was established and reacted with autologous melanoma cells and with the allogeneic human histocompatibility leukocyte antigen (HLA-A2) molecule. The CTL cell line was found to recognise peptides 157-165, 157-167, and 155-163 of NY-ESO-1 presented by HLA-A2 of T2 cells (Jäger et al., 1998). Furthermore, a NY-ESO-1 specific T helper ($CD4^+$) cell response was observed and recognised 157-170 of NY-ESO-1 presented by HLA-DP4 molecules (Zeng et al., 2001).

Types of cancer	% of mRNA expression	% of protein expression	References
Bladder	33	25	(Sharma et al., 2003, Kurashige et al., 2001, Bolli et al., 2005)
Breast	23		(Sugita et al., 2004, Mashino et al., 2001)
Colorectal	6		(Mashino et al., 2001, Li et al., 2005)
Oesophagus	22	32	(Fujita et al., 2004, Mashino et al., 2001, Akcakanat et al., 2004)
Gastric	10		(Wang et al., 2004a,

			Mashino et al., 2001)
HCC	34	19	(Zhang et al., 2005, Xing et al., 2004, Korangy et al., 2004, Chen et al., 2003, Peng et al., 2005)
Head and neck		24	(Prasad et al., 2004)
Melanoma		44	(Gnjatic et al., 2006, Nicholaou et al., 2006)
Multiple myeloma	37		(van Rhee et al., 2005)
Myeloma and plasmoctoma		27	(Dhodapkar et al., 2003)
NSCLC	21	15	(Konishi et al., 2004, Wang et al., 2004b, Jungbluth et al., 2001b, Tajima et al., 2003, Bolli et al., 2005)
Ovarian	30	43	(Odunsi et al., 2003)
Pancreas	0		(Kubuschok et al., 2004)
Prostate	38	15	(Nakada et al., 2003, Fossa et al., 2004)
Sarcoma	36		(Ayyoub et al., 2004)
Synovial sarcoma		80	(Jungbluth et al., 2001a)

Table 1.1. Percentage of cancers expressing NY-ESO-1 at the molecular and protein level. (HCC – heptacarcinoma; NSCLC - non-small cell lung cancer).

1.3.1. Clinical trials with NY-ESO-1

Due to its immunogenicity, researchers are trying to develop therapeutic NY-ESO-1 vaccines. The first clinical trial of NY-ESO-1 vaccine was initiated by intradermal injection of three HLA-A2-binding NY-ESO-1 peptides in 12 patients with NY-ESO-1 positive tumours. A $CD8^+$ T cell and delayed-type hypersensitivity response was triggered in four of seven NY-ESO-1 auto-antibody negative patients and was associated with regression and disease stabilisation. In contrast, no significant change in $CD8^+$ T cell response was detected in the five patients with anti-NY-ESO-1 serum antibody, suggesting that patients with pre-existing NY-ESO-1 autoantibodies may not be suitable candidates for a vaccine approach (Jäger et al., 2000). Although disease stabilisation was initially observed in five of the NY-ESO-1 seronegative patients, three of these patients did demonstrate disease progression later in the study. The authors postulate that this could be due to the emergence of NY-ESO-1 antigen loss or MHC-loss variants. To date, there have been over 30 clinical trials involving NY-ESO-1, with more than 300 patients recruited to them (Gnjatic et al., 2006).

1.3.2. Rationale for NY-ESO-1 as a target for radioimmunotherapy

There are several criteria that a target antigen should fulfil in order for a monoclonal antibody to exert an efficient anti-tumour response. Ideally, the target antigen should be accessible, stably expressed, highly immunogenic, and consistently and exclusively found in cancer cells. Moreover, antigen secretion should be minimal, to avoid the antibody being depleted through binding to circulating antigens in the blood (Scott et al., 2012). NY-ESO-1 appears to fulfil

several of these criteria, and therefore represents a promising target for radioimmunotherapy.

1.4. Challenges involved in use of NY-ESO-1 for radioimmunotherapy

The targets for immunotherapy are commonly cell surface antigens; for example trastuzumab is directed against the cell-surface receptor, HER2. Alternatively, therapeutic antibodies can be directed against tumour antigens in the circulation which promote angiogenesis. An example is bevacizumab which binds vascular endothelial growth factor (VEGF). In contrast, NY-ESO-1 protein has an intracellular location, in the cytoplasm and nucleus. The inability of large antibody molecules to cross the cell membrane presents a challenge for the development of therapeutic antibodies against intracellular targets. However this problem may be overcome through the use of cell-penetrating peptides to deliver antibodies across the cell membrane.

1.5. Cell-penetrating peptides

The cell membrane is the barrier that separates the interior of the cell from the external environment. It possesses the property of selective permeability, which allows the controlled movement of substances, including ions and organic molecules, in and out of cells. A significant challenge for achieving therapeutic efficacy with antibody-based compounds is their delivery and passage across the cell membrane.

Cell-penetrating peptides (CPPs), also sometimes referred to as protein transduction domains (PTD), Trojan peptides, or membrane-translocating sequences, can be defined as short sequences of amino acids (usually less than 30 amino acid residues) capable of passing across the cell membrane in an apparently energy independent manner without the necessity of recognition by surface receptors. The use of CPPs to deliver a range of bioactive materials - including proteins, peptides, oligonucleotides, and nanoparticles - across the membranes of various different cell types, as well as into different cellular compartments, has been reported in *in vitro* and *in vivo* experiments (Järver and Langel, 2006). CPPs can be classified according to their peptide origin or physicochemical properties. Using the former classification scheme, CPPs can be categorised as short sequences of peptides derived from proteins, chimeric peptides derived from the fusion of two natural peptides, or synthetic CPPs which are designed based on information from structure-activity studies. (Bechara and Sagan). Alternatively, the latter scheme categorises CPPs as cationic, amphipathic or hydrophobic (Milletti, 2012).

1.6. Mechanisms of cell penetration by CPPs

Despite the successful use of CPPs in a range of cell lines, the cellular uptake mechanisms of CPPs have not been fully elucidated. Initially, many reports suggested that internalisation of CPPs was not significantly inhibited by incubation at low temperature (4 ℃), or by depletion of the ATP cellular pool, suggesting that uptake of CPPs across the cell membrane was a endocytosis-independent process (Vivès et al., 1997, Suzuki et al., 2002). Furthermore,

Wender *et al.* demonstrated that the charge of CPPs was sufficient to enhance their cellular uptake, implying that binding to surface receptors was not required for internalisation of CPPs (Wender et al., 2000). However, most of these experiments were performed using fluorescence-activated cell sorter (FACS) analysis. The use of methanol in the fixation step of FACS was shown to be associated with artifactual redistribution of CPP, thus raising concerns about the validity of the data obtained by FACS (Richard et al., 2003). Since then, many studies have reported that internalisation of CPPs is mediated by endocytosis. The first contact of CPPs with the cell surface appears to be via electrostatic interactions with proteoglycans in the extracellular matrix. This triggers actin remodelling and activation of the small GTPases RhoA or Rac1 (Couchman, 2003, Heitz et al., 2009). Thereafter, the cellular uptake pathway is influenced by several parameters, including the physicochemical properties of the CPP. The majority of the cationic CPPs were primarily found to be associated with macropinocytosis. However, one of the well-studied cationic CPPs, known as the Trans-Activator of Transcription (TAT) protein of the Human Immunodeficiency Virus, was reported to be taken up into the cells by both clathrin-and caveolin-dependent endocytosis (Richard et al., 2005, Jones et al., 2005). Other factors which influence the uptake of CPPs include their ability to interact with cell surface and membrane lipid components, the nature of the cargo, and the cell type

and membrane composition. Moreover, different mechanisms of membrane translocation and endocytosis may occur simultaneously for most CPPs. This is especially true for amphipathic peptides, which can interact with lipids and adopt secondary structures within the membrane that modify membrane integrity (Deshayes et al., 2008, Heitz et al., 2009). The potential mechanisms of cellular uptake and intracellular trafficking of CPPs are summarised in Figure 1.7.

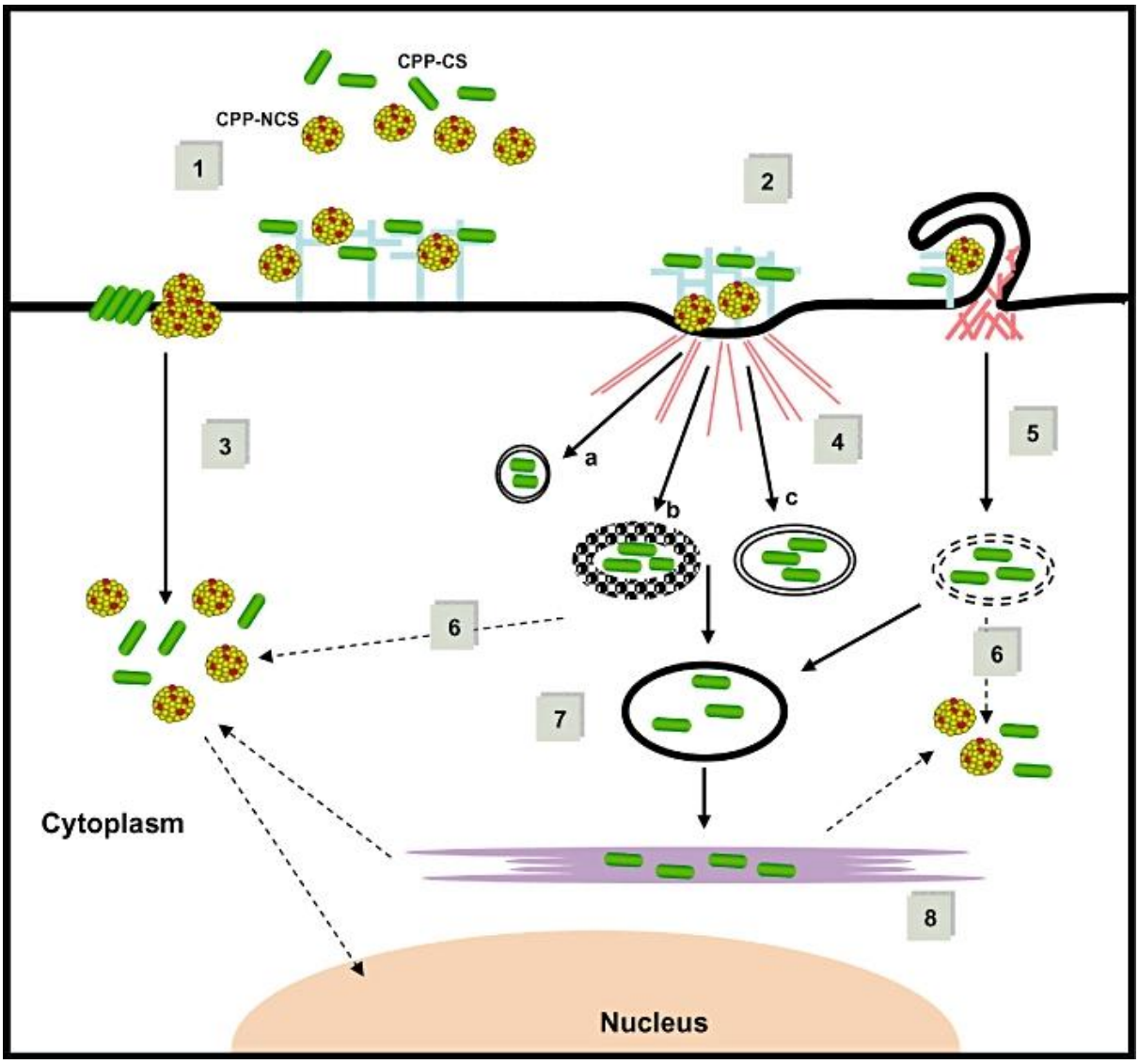

Figure 1.7. Schematic diagram of different uptake and intracellular trafficking mechanisms of cell penetrating peptides (adapted by permission from John Wiley and Sons Publishing Group). (Heitz et al., 2009)

1.7. TAT peptide

The cell-penetrating peptide TAT is an α-helical domain derived from the transcription activating factor of human immunodeficiency virus (HIV-1) that is readily taken up by cells (Cornelissen et al., 2007, Brooks et al., 2005). It is a small basic peptide which is able to deliver a variety of cargoes including, peptides, proteins, oligonucleotides, plasmid DNA and liposome into cells without affecting their function (Dietz and Bδhr, 2004). TAT peptide (GRKKRRQRRRPPQGYGC) possesses a nuclear localization sequence (NLS, underlined), which was shown to facilitate the internalisation and nuclear uptake of radiolabeled antibody in human breast cancer cells *in vitro*, and in xenograft and normal tissues *in vivo* in athymic mice (Hu et al., 2006). TAT was chosen for use in the experiments described in this thesis to deliver radiolabelled anti-NY-ESO-1 antibody to the nucleus of tumour cells.

1.8. Protein transfection reagent

Experiments revealed that conjugation to TAT did not adequately improve internalisation of radiolabelled anti-NY-ESO-1 antibody in the tumour cells used in this study (see Section 4.4). Hence, the radioimmunoconjugates were transfected into the cells using a protein transfection reagent SAINT-PhD. This reagent consists of a cationic amphiphile and helper lipid. Cationic liposomes can enter cells via different pathways. It was demonstrated in Raji cells, which do not express proteoglycans, that DNA material could not be successfully transfected without the expression of the proteoglycan, syndecan-1 (Mounkes et al., 1998). In the same publication, the researchers showed both in cultured cells and mice that the transfection efficiency depends on the net positive charge of the liposomal complex. In addition, a reduction in transfection efficiency has been shown to

result after treatment of cells with an inhibitor of caveolae-mediated endocytosis termed filipin III. Localisation of liposomal complexes with the Tf receptor, a marker of clathrin-coated endosomes, has been shown in the literature. Inhibition of the internalisation of liposomal complexes has also been demonstrated in cells with a dominant negative mutation of Eps15 (epidermal growth factor receptor pathway substrate clone 15) or following potassium depletion, which both arrest coated pit formation. Thus the published evidence suggests that both caveolae-mediated and clathrin-mediated endocytosis contribute to liposome entry into cells (Castanho et al., 1999, Zuhorn et al., 2002).

Fusion of liposome and endosomal membrane, a process known as endosomolysis, is thought to be the mechanism by which liposomal complexes evade lysosomal degradation, and is summarised in Figure 1.8. In brief, the endosomal membrane becomes destabilised when contact is made with the cationic liposome (step 1), thus triggering the anionic lipids facing the cytoplasmic side of the membrane to transfer to the endosomal side (step 2). The mixture of these anionic lipids and the cationic lipids of the liposome forms charge-neutral ion pairs (step 3) which displace the material incorporated by the liposome and release it into cytoplasm (step 4) (Zelphati and Szoka, 1996, Medina-Kauwe et al., 2005). The transfection reagent used in this study is a cationic liposome, which suggests it releases its attached material into the cytoplasm via this method.

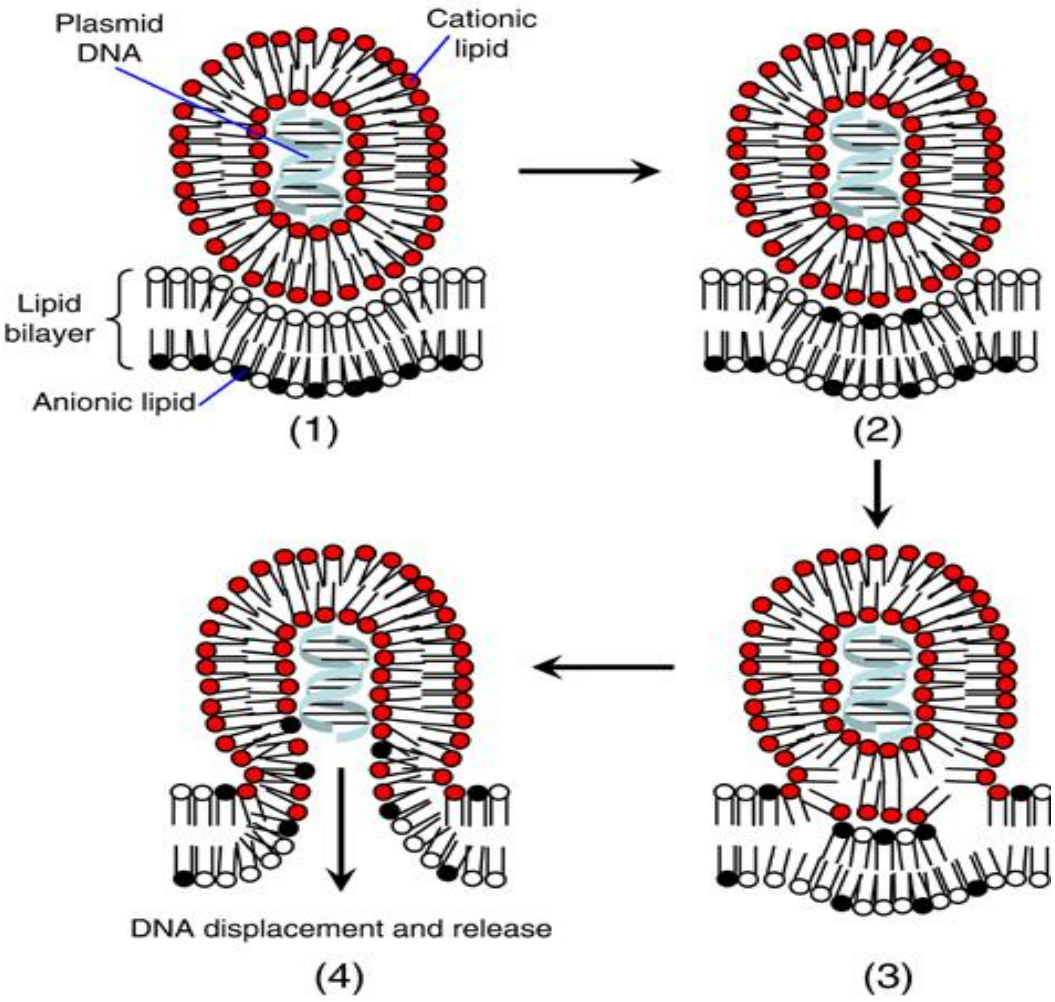

Figure 1.8. Mechanisms of liposomal transfer of DNA across the cell membrane.

1.9. Conclusion

The CT antigen NY-ESO-1 represents a viable target for radioimmunotherapy, given its immunogenicity and expression in a wide range of tumours. The challenge of delivering a radiolabelled antibody across the cell membrane to reach the intracellular NY-ESO-1 molecule can be overcome via a strategy involving the use of a cell-penetrating peptide and protein transfection reagent. The presence of the nuclear localisation sequence in TAT should ensure nuclear delivery of the radiolabelled antibody. Use of Auger electron-emitting radioisotopes, which

generate high linear energy transfer (LET) radiation within a very short distance of the decay site, should ensure DNA damage is localised to tumour cells.

1.10. The aim and objectives of the study

The aims of the study were to develop radiopharmaceuticals that target the CT antigen, NY-ESO-1. The objectives were therefore:

1. To synthesise a radiolabeled antibody to NY-ESO-1 capable of cellular internalisation and confirm preserved binding affinity after conjugation to TAT.
2. To evaluate the cellular uptake and cytotoxicty of the radioimmunoconjugate *in vitro*.
3. To evaluate the biodistribution of radioimmunoconjugate using SPECT *in vivo*.

Chapter 2

Materials and Methods

Chapter 2: Materials and methods

2.1. Cell Culture

The human bladder cancer cell lines, T24, J82 and 5637 (gift from Dr. Anne Kiltie); the human melanoma cancer cell lines, Trombelli (gift from Prof. Vincenzo Cerundolo), SK-MEL-37, SK-MEL-23 (gift from Ms Anna Pagotto) and the human breast cancer cell line, MDA-MB-468 (obtained from American Type Culture Collection) were cultured in Dulbecco's modified Eagle's medium (DMEM, Sigma) supplemented with 10% fetal bovine serum (FBS; Invitrogen, Paisley, UK), 100 units/mL penicillin, and 100 μg/mL streptomycin at 37 ℃ in an atmosphere of 5 % CO_2.

2.2. Western blot analysis

Cells were lysed using radioimmunoprecipitation assay (RIPA) buffer. The protein concentration of the lysates was measured by BCA assay (Pierce, Thermo Scientific, IL). Lysates were incubated for 10 min at 70 ℃ to denature the proteins. Cell lysate (20 μg) was added to 4-12.5% gradient gels for sodium dodecyl sulfate polyacrylamide gel electrophoresis (SDS-PAGE) under reducing conditions (160V, 70 min). After electrophoresis, proteins were transferred from the gel to a nitrocellulose membrane (Amersham Bioscience, UK) using a wet transfer technique (100V, 60 min). The membrane was then blocked using blocking buffer (skimmed milk [5%, Marvel] in PBS containing 0.1% Tween-20). Subsequently, anti-NY-ESO-1 mouse monoclonal antibody (mAb) (Sigma, E978 clone, 1:1000) in blocking buffer was added to the membrane and was incubated with shaking overnight at 4 ℃. Following 3x15 min washes with PBS Tween-20 (0.1%), membranes were incubated with Horse Radish Peroxidase-conjugated

anti-mouse IgG secondary antibody (Promega, UK; 1:5000) for 1 h at room temperature (RT). Following 3x15 min with PBS Tween-20 (0.1%), proteins were detected using an enhanced chemiluminescence detection system (Pierce, Thermo Scientific).

2.3. Immunocytochemistry (ICC)

Cells (10^5) were cytospun (7 min, 800 rpm) or grown on glass slides and subsequently fixed in 4% formaldehyde in PBS for 15 min. After 3 washes with PBS, slides were treated with 1% Triton-100 in PBS (PBST). Slides were blocked with 2% bovine serum albumin (BSA, Sigma) in 0.1% PBST for 1 h. Slides were incubated overnight with mouse anti-human NY-ESO-1 antibody (Sigma, E978 clone, 1:200 dilution) in 2% BSA and 0.1% PBST. After 3 washes in PBS, slides were incubated with goat anti-mouse IgG antibody conjugated to Alexa Fluor 488 (1:500; Invitrogen) for 45 min at RT. After 3 washes in PBS, coverslips were mounted using Vectashield mounting medium containing 2-(4-amidinophenyl)-1H -indole-6-carboxamidine DAPI (Vector Laboratories, UK) and cells visualised using a Zeiss confocal fluorescence microscope (Carl Zeiss Ltd., Welwyn Garden City, UK).

2.4. Synthesis of radioimmunoconjugates (RIC)

The conjugation of TAT to anti-NY-ESO-1 (mouse monoclonal, Sigma E978 clone) or mouse IgG (mIgG) antibody was accomplished by a series of chemical reactions utilising several cross-linking reagents. Anti-NY-ESO-1 or mIgG antibody (100 µg) was first buffer-exchanged into 2-(*N*-

morpholino)ethanesulfonic acid (MES) buffer (0.1 M, pH 6.0) to give a concentration of approximately 1 µg/µL using a Microcon YM-30 ultrafiltration column. 1-Ethyl-3-[3-dimethylaminopropyl] carbodiimide hydrochloride (EDC, Pierce) (3 µg) and N-hydroxysulfosuccinimide (Sulfo-NHS, Pierce) (10 µg), both dissolved in 0.1 M MES buffer (pH 6.0), were added to the antibody and incubated for 15 min at RT to yield an amine-reactive NHS ester for the sequential steps of the conjugation of TAT peptides. The antibody was then buffer-exchanged into PBS (pH 7.0) and TAT (4 µg in PBS, pH 7.0) was added to the antibody and incubated for 2 h at RT. Unbound free TAT was removed through size-exclusion chromatography (SEC) using a Sephadex G-50 gel filtration column (Sigma) and was eluted with sodium bicarbonate (0.1 M, $NaHCO_3$, pH 8.2). The TAT-conjugated antibody was then either labelled directly with ^{123}I using iodogen, or reacted with a metal chelator for subsequent labelling with ^{111}In.

For ^{123}I labelling, 1,3,4,6-tetrachloro-3α,6α-diphenylglucoluril (iodogen, 150 µg) was dissolved in chloroform (400 µL) and added to an Eppendorf tube. The tube was placed in a fume hood overnight with the lid open to allow the complete evaporation of the organic solvent, leaving a coating of iodogen on the tube. The tube was briefly rinsed with iodogen buffer (0.1 M, Na_2HPO_4, pH 8.4) to remove any unbound iodogen. The TAT conjugated antibody was incubated with ^{123}I in the iodogen coated tube for 15 min at room temperature. A G-50 gel filtration column was used to separate radiolabelled antibody from unbound ^{123}I.

For ^{111}In-labelling, the TAT conjugated antibody was incubated with 2-(4-isothiocyanatobenzyl)-diethylenetriaminepentaacetic acid (benzyl-DTPA) (5 µg) or cyclic diethylenetriaminepentaacetic acid (cDTPA) (8 µg) for 1 h at RT. The

molar ratio of antibody to DTPA was 1 in 20 to achieve the optimal antibody conjugation. The DTPA-conjugated TAT-modified antibody was separated from any excess DTPA using a Sephadex G-50 gel filtration column and was eluted with sodium citrate (0.1 M, $NaH_2C_6H_5O_7$, pH 5.0). The antibody was incubated with ^{111}In for 1 h at RT. A G-50 gel filtration column was used to separate radiolabelled antibody from unbound ^{111}In.

Following ^{123}I- or ^{111}In-labelling, the radiolabelled antibody was buffer-exchanged into PBS (pH 7.4) using a Sephadex G-50 gel filtration column or a Microcon YM-30 ultrafiltration column. Finally, protein transfection reagent (Synvolux Therapeutics, BV, Groningen, Netherlands) was added and mixed gently and incubated for 20 min at RT. The ratio of protein (μg) to protein transfection reagent (μL) was 1: 10. The radiochemical purity was $\geqslant$95%.

2.5. Validation of the conjugation of TAT to mouse IgG

To confirm that TAT peptide was successfully conjugated to mouse IgG, TAT was radiolabelled with ^{123}I to allow the tracking of chemical reactions in each step of the process. TAT peptide (20 μg) dissolved in sodium bicarbonate (0.1 M, $NaHCO_3$, pH 8.2) and ^{123}I (8 MBq) were added to an iodogen coated tube and incubated for 15 min at RT. Radioiodinated TAT was separated from free, unbound ^{123}I using a P-2 gel filtration column. The fractions corresponding to radioiodinated TAT were combined and incubated with mouse IgG (100 μg) for 2 h. Radioiodinated TAT bound to mIgG was then separated from unbound radioiodinated TAT using a Sephadex G-50 gel filtration column. Assuming a 30% loss of TAT protein during the purification procedure (based on previous

experience in the laboratory), the number of TAT molecules conjugated to one mIgG antibody molecule was then calculated as follows:

(amount of TAT conjugated antibody)/ (total amount of radioiodinated TAT peptide) x molar ratio of radioiodinated TAT to mIgG antibody.

The molar ratio of radioiodinated TAT to mIgG antibody=number of moles of radioiodinated TAT/number of moles of mIgG antibody, that is, 14 μg/1780/100 μg/150000=11.8. Next, the amount of TAT conjugated antibody and the total amount of radioiodinated TAT peptide times could be worked out by the area of corresponding to mIgG-123I-TAT and the area of mIgG-123I-TAT plus free unbound radioiodinated TAT. The number of TAT peptide= [608466/ (608466+2356656)]*11.8=2.42.

2.6. Clonogenic survival assays

Cells ($1x10^5$) were harvested and aliquoted into Eppendorf tubes containing RIC or appropriate controls. After 24 h incubation at 37 °C, fresh medium was added to a final volume of 1 mL. Cell suspension (10 μL) was transferred to 12-well plates containing 1 mL of fresh medium. Following 10 days incubation at 37 °C, cells were washed 2 x 10 min with PBS and 1 x 10 min with water. Cells were then stained with methylene blue (1%) in water:methanol (1:1), and colonies were counted. The surviving fraction (SF) was calculated by dividing the number of colonies by the number of cells seeded multiplied by the plating efficiency (Franken et al., 2006). Data were normalized to SFs of untreated controls.

2.7. Radioimmunoassay

NY-ESO-1 protein lysate (2 ng/mL, Pierce, Thermo Scientific) was coated onto a high affinity radioimmunoassay plate (96-well, Costar) and incubated overnight at

4 ℃. Wells were washed 3 x 100 µl PBST (0.1% Tween-20 in PBS) and blocked with bovine serum albumin (2% BSA, 0.1% PBST) for 2 h at RT (Cornelissen et al., 2011a). After 3 x 5 min washes with PBST, anti-NY-ESO-1 or anti-NY-ESO-1-TAT conjugate (0.01 nM-1000 nM) was added and incubated for 2 h at RT in the presence of radiolabelled ^{123}I-anti-NY-ESO-1 (5 nM). Supernatant was removed and wells washed twice with PBS (100 µL) to remove any unbound ^{123}I-anti-NY-ESO-1. Glycine (100 µL, 0.1 M, pH 2.5) was added to dissociate bound ^{123}I-anti-NY-ESO-1 from the cell lysates, and radioactivity was measured in a Gamma counter (PerkinElmer Wizard 1470, Waltham, MA).

2.8.Inhibition of protein expression by siRNA knockdown

Three small inhibitory RNAs (27mer siRNA duplexes, Origene, Rockville) targeting NY-ESO-1 transcript were used for down-regulating the expression of NY-ESO-1 protein. siRNA sequence 1 and sequence 2 spanned the NY-ESO-1 mRNA transcript at position 442 to 467, targeting sequence 5'-gcaacatactgactatccgactgac-3', and position 696 to 723, targeting sequence 5'-ggaggaggacggcttacatgtttgtttc-3'. Sequence 3 was designed to bind to NY-ESO-1 mRNA transcript at position 343 to 367, targeting sequence 5'-cgacacccatggaagcagagctggc-3'. siRNA duplexes (30 pmol) were incubated with Lipofectamine 2000 (5 µL, Invitrogen) in 500 µl OptiMem medium for 20 min. SK-MEL-37 melanoma cells ($1x10^5$), in normal growth medium (DMEM, Sigma) without serum or antibiotics, were incubated with the siRNA/Lipofectamine for 6 h. Medium was removed and replaced by fresh medium containing serum (10% FBS) and antibiotics (100 units/mL penicillin, and 100 µg/mL streptomycin) and

cells were incubated for 48 h or 72 h at 37 ℃. A Western blot was performed to confirm NY-ESO-1 protein knockdown.

2.9. Internalisation and nuclear localisation of radiopharmaceuticals

SK-MEL-37 cells ($1x10^5$) were seeded in 24-well plates and incubated overnight to allow cells to adhere. RICs (0.33 nM, 0.5 MBq/μg) or appropriate controls were added and incubated for selected times. For internalisation assays, the supernatant containing the unbound antibody was removed and cells were washed twice with PBS (500 μL). To strip away the membrane-bound radiolabelled antibody, glycine (0.1 M, pH 2.5) was added and incubated for 6 min at 4 ℃. The tubes were centrifuged at 1000xg for 3 min, supernatant containing the membrane-bound antibody was removed, and cells were washed twice with PBS (500 μL). Cells were then lysed with NaOH (0.1 M) followed by 2 washes with PBS (500 μL) to obtain the internalised antibody fraction. Radioactivity in the fractions containing unbound, membrane bound and internalised radiolabeled antibody was counted using a Gamma counter (Wizard, PerkinElmer, Waltham, MA, USA) (Hu et al., 2006, Cornelissen et al., 2011b).

To quantify the radioactivity in the cytoplasmic or nuclear fraction, cells were exposed to RICs or controls as detailed above. At selected time points, cells were removed from the plate using trypsin and transferred into Eppendorf tubes ($9x10^5$ cells). The tubes were centrifuged at 500xg for 2 min, and supernatant containing the unbound antibody fraction was removed. The cells were washed twice in PBS. Glycine (0.1 M, pH 2.5) was added and incubated for 6 min at 4 ℃. The tubes were centrifuged at 1000xg for 3 min, supernatant containing the membrane-bound antibody was removed, and cells were washed twice with PBS (500 μL). Cell pellets were resuspended in cell membrane lysis buffer (500 μL, 25 mM KCl,

5 mM $MgCl_2$, 10 mM Tris–HCl and 0.5% NP-40) and incubated for 6 min at 4 ℃. The tubes were centrifuged at 1000xg for 3 min and supernatant containing the cytoplasmic fraction was removed. After 2 x washes in PBS, the nuclear fraction was obtained by incubation of the nuclear pellet with NaOH (500 μL, 0.1 M) for 20 min at RT. Radioactivity in the fractions containing unbound, membrane-bound, cytoplasmic and nuclear radiolabelled antibody was counted using a Gamma counter (Wizard, PerkinElmer, Waltham, MA, USA) (Hu et al., 2006).

2.10. Retention of radiopharmaceuticals

To evaluate the retention of RICs in SK-MEL-37 and SK-MEL-23 melanoma cell lines, cells ($1x10^5$) were seeded in 24-well plates and incubated overnight to allow the cells to adhere. RICs (0.33 nM, 0.5 MBq/μg) were added and incubated at 37 ℃ for either 4 h (for ^{123}I-labelled agents) or 24 h (for ^{111}In-labelled agents). After incubation, medium was removed for counting in a Gamma counter. Cells were washed twice with PBS (500 μL), and fresh growth medium (DMEM, 10% fetal bovine serum, 100 units/mL penicillin, and 100 μg/mL streptomycin) was then added. Cells were incubated at 37 ℃ for selected times, ranging from 1 to 48 h. At these selected time points, medium was discarded and cells washed twice with PBS (500 μL). Cells were incubated with glycine (0.1 M, pH 2.5) to remove any membrane-bound radioactivity. NaOH (0.1 M) was added to the cells and incubated for 20 min at RT, following by washing twice with PBS (500 μL), to obtain the internalised fraction. All data was calculated as the percentage of radioactivity retained in the cells at the zero time point.

2.11. Investigation of cell viability by WST-1 assay

SK-MEL-37 cells ($1x10^4$) were seeded in 96-well plates and incubated overnight to allow the cells to adhere. Cells were then washed twice with PBS (150 μL),

followed by the addition of fresh growth medium. RICs or appropriate controls (0.05 nM-500 nM) were added. After incubation for 24 h, supernatant was removed, cells washed twice with PBS, and fresh medium added (90 μL). WST-1/ECS solution (Millipore) was added to each well and the absorbance of the samples at 450 nM was measured using a microplate reader. Blank wells were treated with the WST-1/ECS solution but did not contain cells. The percentage of cell viability was calculated by absorbance of (treated sample – blank) / (untreated sample – blank) x 100%.

2.12. γH2AX assay

SK-MEL-37 cells ($5x10^5$) were seeded into 96-well plates and incubated overnight to allow cells to adhere. Cells were then washed twice with PBS (100 μL), followed by the addition of fresh growth medium. RICs or appropriate controls were added (200 nM, 0 MBq/μg - 3 MBq/μg). After incubation for 4 h at 37 ℃, cells were washed twice with PBS (100 μL) and fixed in 4% formaldehyde in PBS for 15 min. After washing the cells twice with PBS to remove residual formaldehyde, cells were incubated in 1% Triton-100 in PBS for 15 min. Cells were washed twice in PBS, followed by incubation in blocking buffer (5% bovine serum albumin in 0.1% Triton-100 in PBS) overnight at 4 ℃. Cells were then incubated with rabbit anti-human γH2AX antibody (1 in 800, Merck Millipore, Watford, UK) at 4 ℃. After incubation and washing twice with PBS to remove any unbound antibody, goat anti-rabbit IgG antibody conjugated to Alexa Fluor 488 (AF488; Invitrogen, Paisley, UK) was added to the cells and incubated for 1 h at RT. After 2 washes in PBS, fluorescence images were acquired using an INCell analyser (GE Healthcare, Pittsburgh, PA, USA). Cells exposed to 4 Gy X-irradiation using a Caesium irradiator were used as a positive control. The number

of γH2AX foci per cell was counted using the INCell analyser software. The data in each group was normalised by subtracting the number of γH2AX foci/cell in control samples (treated with PBS instead of radiopharmaceuticals) from the number of foci/cell in test samples.

2.13. Mouse models and inoculations

Animal procedures were carried out in accordance with the UK Animals (Scientific Procedures) Act 1986 and with local ethical committee approval. SK-MEL-37 xenografts were established in male/female BALB/c nude mice (Harlan). In brief, SK-MEL-37 melanoma cells were removed from flasks using trypsin, and resuspended in serum free fresh growth medium (DMEM). SK-MEL-37 cells ($1.5x10^6$) were mixed with matrigel (1:1) and injected subcutaneously (s.c.) in the right hind flank of mice under brief isoflurane anaesthesia (2.5%). Tumour growth was measured using callipers twice a week.

2.14. Tumour harvest and immunohistochemistry

When the diameter of tumours reached approximately 6.5 mm, mice were euthanized. Tumours were harvested and immersed in OCT (tissue tek. polyvinyl alcohol, polyethylene glycol) in cryomoulds on dry ice. The tumours were sectioned (10 μm) using a cryostat, and sections were adhered to glass slides and stored at -20 °C.

The sections on the glass slide were rehydrated in PBS for 5 min at RT. The sections were then fixed in 4% formaldehyde in PBS for 30 min. Slides were washed with PBS (3x 5 min), and incubated in 1% Triton in PBS for 15 min at RT. After washing for 3 x 5 min with PBS, the slides were blocked with blocking

buffer (5% bovine serum albumin in 0.1% Triton-100 in PBS) for 2 h at RT. After washing for 3 x 5 min with PBS, slides were incubated with rabbit anti-human NY-ESO-1 polyclonal antibody (1 in 500, Abcam, Cambridge, UK) overnight at 4℃ with gentle shaking. Rabbit IgG was used as isotype control. After washing for 3 x 5 min with PBS, slides were incubated with goat anti-rabbit IgG conjugated to AF488 (1 in 500) for 1 h at RT. Slides were washed for 3 x 5 min with PBS, coverslips mounted using Vectashield mounting medium containing DAPI (Vector Laboratories, UK), and sections visualised using a Zeiss confocal fluorescence microscope (Carl Zeiss Ltd., Welwyn Garden City, UK).

2.15. Biodistribution of radioimmunoconjugates

SK-MEL-37 or SK-MEL-23 xenografts were established in BALB/c nude mice as previously described. When tumours reached a diameter of approximately 10 mm (measured by calliper), mice received an intravenous (i.v.) injection of ^{111}In-labelled anti-NY-ESO-1 antibody (10 μg, 5 MBq). ^{111}In-labelled mIgG was used as a non-specific isotype control. SPECT/CT images were acquired at 24, 48 and 72 h post-injection (p.i.). During acquisition of images, mice were anesthetised using isoflurane (2%, oxygen flow rate of 1 L/min). The respiratory rate of mice was closely monitored. After the 72 h scan, animals were euthanized, and tissues and organs (bladder, large intestine, small intestine, pancreas, spleen, stomach, liver, lung, kidney, heart, skin, muscle, brain and testis) were removed. Blood was aspirated from the heart (left ventricle) and retained for subsequent analysis. After dissection, tissues were briefly rinsed with water to remove blood, and air dried on tissue paper. Each tissue/organ was placed in a separate counting tube and radioactivity was counted using a Gamma counter (Wizard, PerkinElmer, Waltham, MA, USA).

Chapter 3

Synthesis of NY-ESO-1 targeting radiopharmaceuticals

Chapter 3: Synthesis of NY-ESO-1 targeting radiopharmaceuticals

The methods used in the synthesis of radiopharmaceuticals are detailed in Section 2.4. The current section illustrates and discusses data obtained during the synthesis process, and provides details of the optimisation procedures that were followed to arrive at the final methodology.

3.1. Conjugation of anti-NY-ESO-1 to TAT

Section 2.4 details the procedure used to calculate the number of molecules of TAT that can be bound to one mouse IgG (mIgG) antibody molecule. These experiments were carried out using the ^{123}I radioisotope, because of the ability to conjugate the isotope directly to the antibody without the need for a metal chelator. After incubation of TAT with ^{123}I, a P2 gel filtration column was carried out to separate ^{123}I-TAT from free ^{123}I (Figure 3.1). In this separation technique, larger molecules elute earlier, while smaller molecules are retained in the pores of the gel and elute at a later stage. This indicates that the peak between fractions 9 and 14 corresponds to ^{123}I-TAT, and the peak between fractions 16-21 to the free unbound ^{123}I.

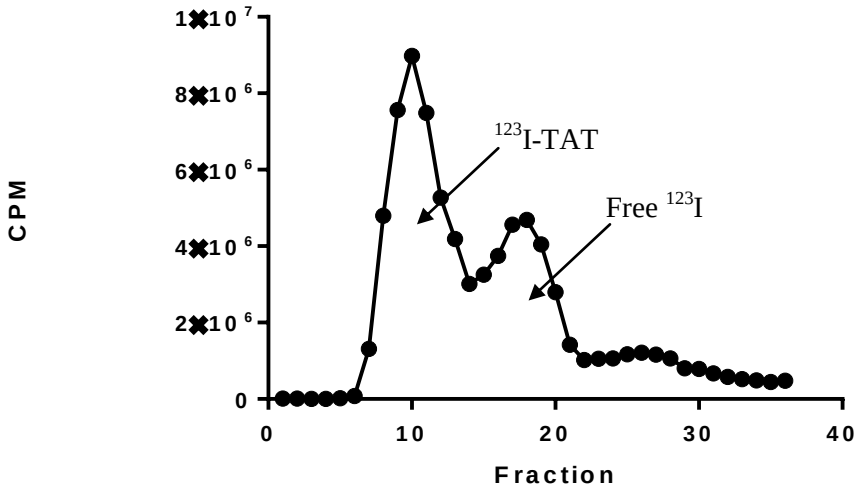

Figure 3.1. Separation of ^{123}I-TAT from unbound ^{123}I. TAT peptide in $NaHCO_3$ was incubated with 8 MBq ^{123}I for 15 min. ^{123}I-TAT was separated from unbound ^{123}I using a P-2 column, and eluted fractions were counted in a γ-counter (CPM refers to counts per minute).

Fractions 9-14 corresponding to ^{123}I-TAT were combined and incubated with EDC/sNHS activated mIgG. EDC activates carboxyl groups for direct reaction with primary amines via amide bond formation. The addition of *N*-hydroxysulfosuccinimide (sNHS) improves coupling efficiency by creating dry-stable amine-reactive intermediates.

After reaction of the activated antibody with ^{123}I-TAT, a Sephadex G-50 gel filtration column was used to separate ^{123}I-TAT bound to mIgG from unbound ^{123}I-TAT (Figure 3.2). The peak between fractions 10 and 14 in Figure 3.2 corresponds to the antibody bound ^{123}I-TAT and the peak between fractions 20 and 27 corresponds to the free unbound ^{123}I-TAT.

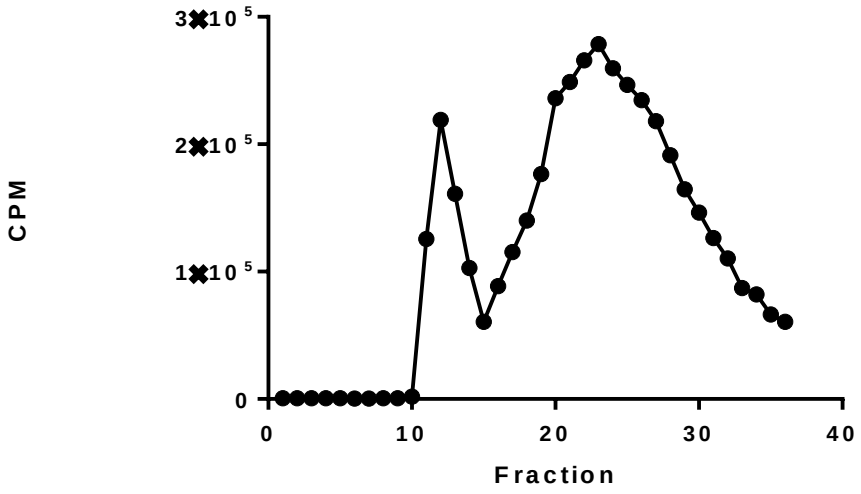

Figure 3.2. Separation of ^{123}I-mIgG-TAT from ^{123}I-TAT. ^{123}I-TAT was incubated with 100 µg sNHS/EDC-activated mIgG for 2 h. ^{123}I-mIgG-TAT was separated from unconjugated ^{123}I-TAT using a G-50 column, and eluted fractions were counted in a γ-counter (cpm refers to counts per minute)

The calculations described in Section 2.5 were performed, and it was shown that 2.42 molecules of TAT could be conjugated to one mIgG antibody molecule. The activation of the antibody by incubation of EDC and sNHS at pH 6.0 and the optimum pH for the forming the amide bond is pH 7.0 thus eliminating the possibility of cross-linking antibodies after the incubation of EDC and sNHS. The pattern of the elution profile was also similar to those performed by other colleagues in the lab.

3.2. Radiolabelling of anti-NY-ESO-1 with 111In

Section 2.4 details the final optimised conditions used for the synthesis of the ^{111}In-labelled RICs. However several challenges were faced during the method development, which are discussed here. Most proteins, including antibodies, do not possess metal binding functional groups, which prevents formation of a strong stable bond between the antibody and metal isotopes such as ^{111}In. To overcome this, a metal chelator can be attached to the antibody to aid covalent conjugation to metals, thereby generating a stable radionuclide-chelate-antibody molecule (Yuanfang and Chuanchu, 1991). Two chelators were investigated for suitability for use in this study; 2-(4-isothiocyanatobenzyl)-diethylenetriaminepentaacetic acid (bnDTPA) or the cyclic diethylenetriaminepentaacetic acid (cDTPA) anhydride. The organic solvent dimethyl sulfoxide (DMSO) was used to dissolve the metal chelators. There are several advantages of using DMSO compared to the other widely used organic solvent chloroforms for this process. These include the excellent solubility of anhydride in DMSO, improved coupling efficiency, and the miscibility of DMSO with water to avoid evaporation of organic solvent (Yuanfang and Chuanchu, 1991, Blend et al., 1988). cDTPA is commonly used as a bifunctional chelating reagent for ^{111}In-labelling of antibody due to the simplicity of its conjugation reaction with proteins (Arano et al., 1996). However,

some studies have demonstrated that antibodies conjugated to radioisotopes with cDTPA are less stable than those conjugated using benzyl-DTPA (BnDTPA). *In vivo*, this instability could lead to the release of ^{111}In from the chelate into blood, followed by binding to transferrin and accumulation in the liver (Arano et al., 1996, Brechbiel et al., 1986). Therefore, BnDTPA was initially selected for use in this study. In initial optimisation studies, an attempt was made to calculate the number of BnDTPA molecules conjugated to an antibody molecule, using a method similar to that described in section 2.4. However, after incubation of ^{111}In-BnDTPA with anti-NY-ESO-1 and purification using a G-50 filtration column, a single peak was observed (Figure 3.3). This result indicates that conjugation of BnDTPA with anti-NY-ESO-1 was not successful, as two distinct peaks should have resulted; corresponding to ^{111}In-BnDTPA-anti-NY-ESO-1 antibody and unbound ^{111}In-Bn-DTPA respectively. Attempts to optimise the experimental conditions were made, such as varying the pH of sodium bicarbonate buffer (ranging from 8.0 to 8.5), changing the incubation time of BnDTPA with antibody, and using a different molar excess of BnDTPA; but ultimately BnDTPA could not be conjugated to the antibody.

Due to the lack of success using BnDTPA for conjugation, a decision was made to investigate whether cyclic diethylenetriaminepentaacetic acid (cDTPA) anhydride would be a suitable chelating agent in this study. The interaction between ^{111}In and cDTPA is formed by coordination of the metal with the five deprotonated carboxylate group and the three tertiary amino groups of the cDTPA molecule, resulting in a very stable octadentate. The linkage of cDTPA to antibody involves bond formation between lysine residue of the protein and one of the carboxylate groups in DTPA. It has been shown that cDTPA is approximately ten-fold more

reactive than BnDTPA for antibody conjugation (Reilly et al., 1992). After incubation of ^{111}In-cDTPA with anti-NY-ESO-1 and purification using a G-50 filtration column, 2 peaks were observed (Figure 3.4); corresponding to ^{111}In-cDTPA-anti-NY-ESO-1 and excess unbound ^{111}In-cDTPA. The number of cDTPA molecules bound to one antibody molecule was calculated as previously described, and results summarised in Table 3.1. A decision was made to incubate the antibody with 20-fold molar excess of cDTPA in subsequent experiments.

To determine the labelling efficiency of cDTPA-anti-NY-ESO-1-TAT with ^{111}In, the antibody conjugate was reacted with ^{111}In (1 MBq/ µg) for 1 h at RT, and radiolabelled antibody separated from free ^{111}In using a G-50 column. The labelling efficiency was calculated to be greater than 95% (Figure 3.5).

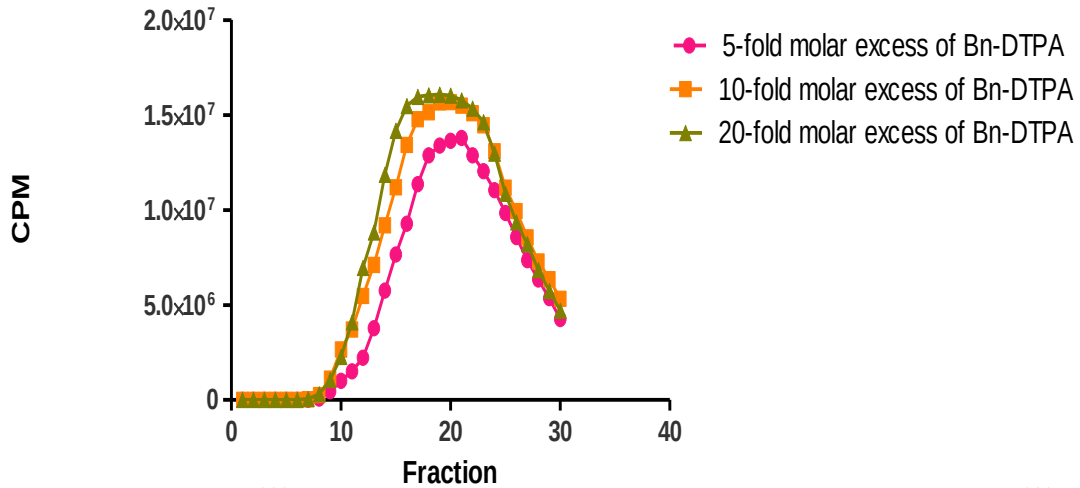

Figure 3.3. Separation of ^{111}In-BnDTPA-NY-ESO-1 antibody from free unbound ^{111}In-BnDTPA using a sephadex G-50 column. Anti-NY-ESO-1 antibody (10 µg) was incubated with increasing amounts of BnDTPA dissolved in DMSO (0.2 µg, 0.4 µg and 0.8 µg) at RT for 1 h to achieve a 5-20 fold molar excess of BnDTPA. Antibody conjugate was labelled with ^{111}In for 1 h at RT followed by G-50 column purification.

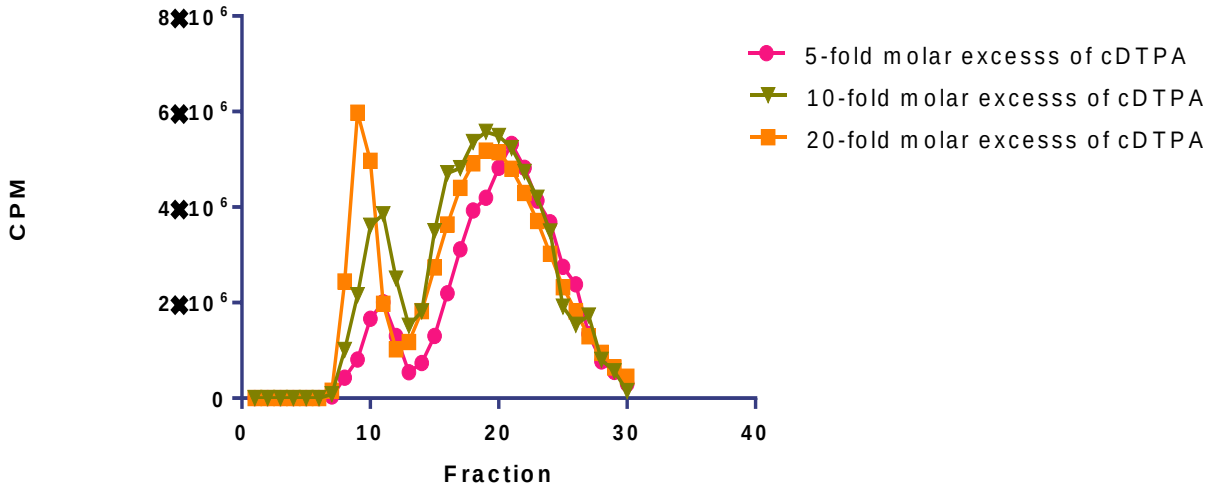

Figure 3.4. Separation of ^{111}In-DTPA-NY-ESO-1 antibody from free unbound ^{111}In-cDTPA using a sephadex G-50 filtration column. Anti-NY-ESO-1 antibody (10 µg) was incubated with increasing amounts of cDTPA dissolved in DMSO (0.15 µg, 0.3 µg, 0.6 µg and 1.2 µg) at RT for 1 h to achieve a 5-20 fold molar excess of cDTPA. Antibody conjugate was labelled with ^{111}In for 1 h at RT followed by G-50 column purification.

	5-fold	10-fold	20-fold
^{111}In-DTPA-NY-ESO-1 (CPM)	4913102	13129374	17571213
^{111}In-DTPA-NY-ESO-1+ ^{111}In-DTPA (CPM)	23300933	40127271	44189178
Number of DTPA per antibody	0.87	2.47	5.69

Table 3.1. Summary of number of cDTPA molecules conjugated to an antibody molecule following incubation of antibody with increasing molar excess of cDTPA (5-fold, 10-fold and 20-fold).

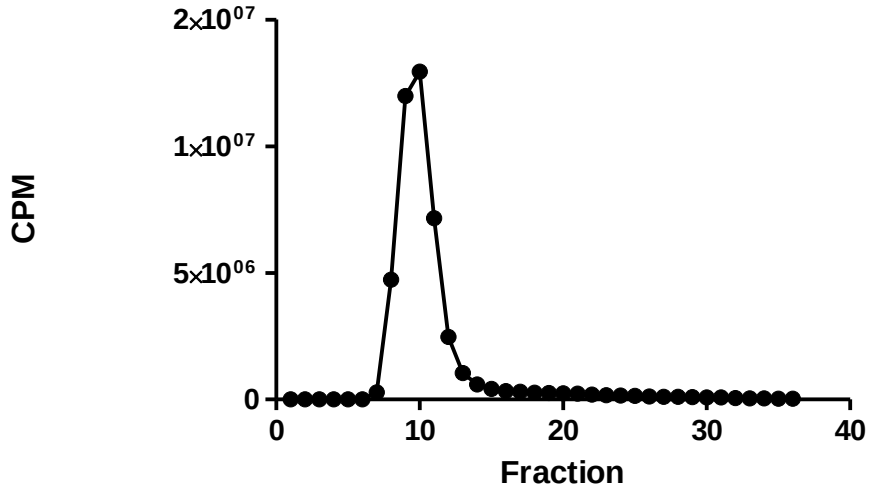

Figure 3.5. Separation of ^{111}In-cDTPA-anti-NY-ESO-1-TAT from unbound ^{111}In. cDTPA-anti-NY-ESO-1-TAT (10 µg) was radiolabeled with 10 MBq of ^{111}In for an hour at RT before purification using a G-50 column. Labelling efficiency was >95%. A single peak was observed and represented ^{111}In-DTPA-anti-NY-ESO-1-TAT.

Chapter 4

In Vitro Studies of NY-ESO-1 Targeting Radiopharmaceuticals: Results and Discussion

Chapter 4: *In Vitro* Studies of NY-ESO-1 Targeting Radiopharmaceuticals: Results and Discussion

4.1.Introduction

This chapter presents and discusses the results of *in vitro* studies using the anti-NY-ESO-1 RICs. Before characterising the RICs in *in vitro* systems, it was necessary to confirm that conjugation to TAT did not affect the binding affinity of the anti-NY-ESO-1 antibody to the NY-ESO-1 antigen. This was carried out using a radioimmunoassay. Subsequently, studies were carried out to ensure the choice of cell line was suitable to study the *in vitro* characteristics of the RICs. After the identification of a suitable cell line, the internalisation and retention of the RICs in these cells was determined. Cell viability following treatment with RICs was investigated using WST-1 and clonogenic assays. Finally, a γH2AX assay was carried out to confirm that the RICs induced of DNA damage, the likely predominant determinant of their cytotoxicity.

4.2. Radioimmunoassay

The radioimmunoassay was conducted to determine whether the binding affinity of the anti-NY-ESO-1 antibody to the NY-ESO-1 antigen was impaired following conjugation of the antibody to TAT and DTPA. ^{123}I-anti-NY-ESO-1 (5 nM) antibody plus DTPA-anti-NY-ESO-1-TAT or unconjugated anti-NY-ESO-1 antibody were added to wells coated with NY-ESO-1 protein. The principle of the assay involves competition between the non-radiolabelled constructs and the radiolabelled antibody for the binding to the NY-ESO-1 receptor. DTPA-anti-NY-ESO-1-TAT and the unconjugated anti-NY-ESO-1 antibody were shown to bind

with similar affinity to the NY-ESO-1 receptor, with IC_{50} values of 0.83 nM ± 0.079 nM and 1.00 nM ± 0.076 nM respectively (Figure 4.1). There was no statistically significant difference between these IC_{50} values (P = 0.151, extra sum of F test). This result confirms that the binding affinity of the chemically modified antibody, DTPA-anti-NY-ESO-1-TAT, has not been altered by conjugation to TAT and the metal chelator cDTPA.

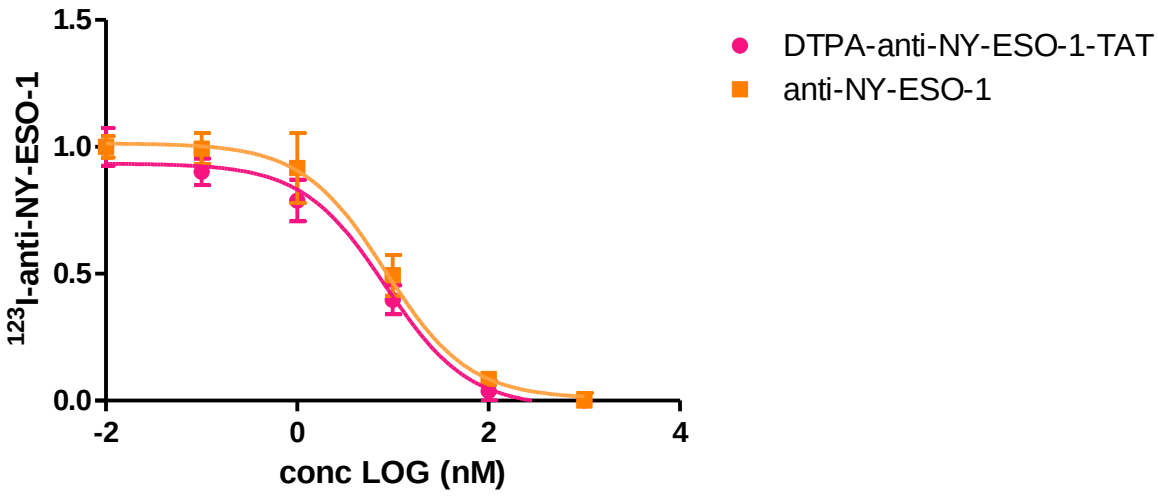

Figure 4.1. Radioimmunoassay showing the binding affinity of DTPA-anti-NY-ESO-1-TAT compared to anti-NY-ESO-1. Data represent the mean and standard deviation of triplicates from three separate experiments. Data were fitted to a variable slope competition curve model in GraphPad Prism.

4.3. Identification of a suitable cell line for in vitro assessment of anti-NY-ESO-1 RICs

A panel of different cancer cell lines including bladder, breast and melanoma lines were screened by Western blot for the expression of NY-ESO-1 protein. There was a distinct NY-ESO-1 band present in the melanoma cell lines Trombelli and SK-MEL-37 (Figure 4.2), but no NY-ESO-1 band was observed in any of the other cancer cell lines tested, including the melanoma cell line SK-MEL-23. This is consistent with published data (Zelphati and Szoka, 1996, Zassler et al., 2005).

Immunohistochemistry experiments were carried out to investigate the cellular localisation of NY-ESO-1 protein in Trombelli, SK-MEL-37 and SK-MEL-23 cells (Figure 4.3). Strong positive staining was observed in SK-MEL-37 and Trombelli cells but not in SK-MEL-23 cells, which was concordant with the results of the Western blot analyses. In SK-MEL-37 cells, the staining was evenly distributed in both cytoplasm and nucleus, whereas NY-ESO-1 protein was found predominantly in the cytoplasm of Trombelli cells. As the aim of this study was to attach a short range Auger electron-emitting isotope to the anti-NY-ESO-1 antibody, use of a cell line with nuclear expression of NY-ESO-1 was considered to be important, given that deposition of Auger electrons in the nucleus of tumour cells causes maximum damage to the DNA. SK-MEL-37 was considered the most suitable cell line for use in investigating the *in vitro* properties of the radiolabelled antibodies produced in this study, with SK-MEL-23 used as a negative control.

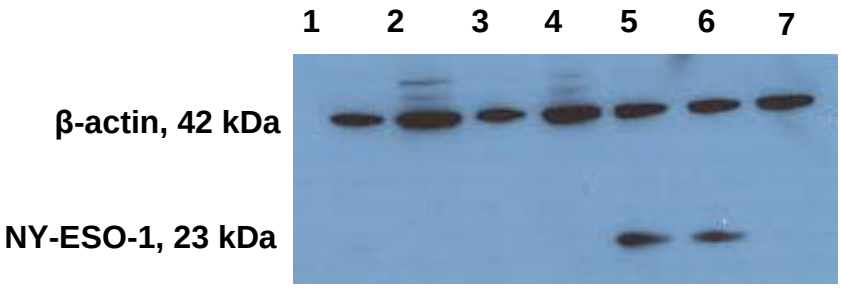

Figure 4.2. Western blot analyses analysis showing NY-ESO-1 expression in lysates (20 μg) from (1) SK-MEL-23, (2) MDA-MB-468, (3) 5637, (4) J82, (5) Trombelli, (6) SK-MEL-37 and (7) T24 cells (Lanes 1-7 respectively). β-actin was used as the control for protein loading.

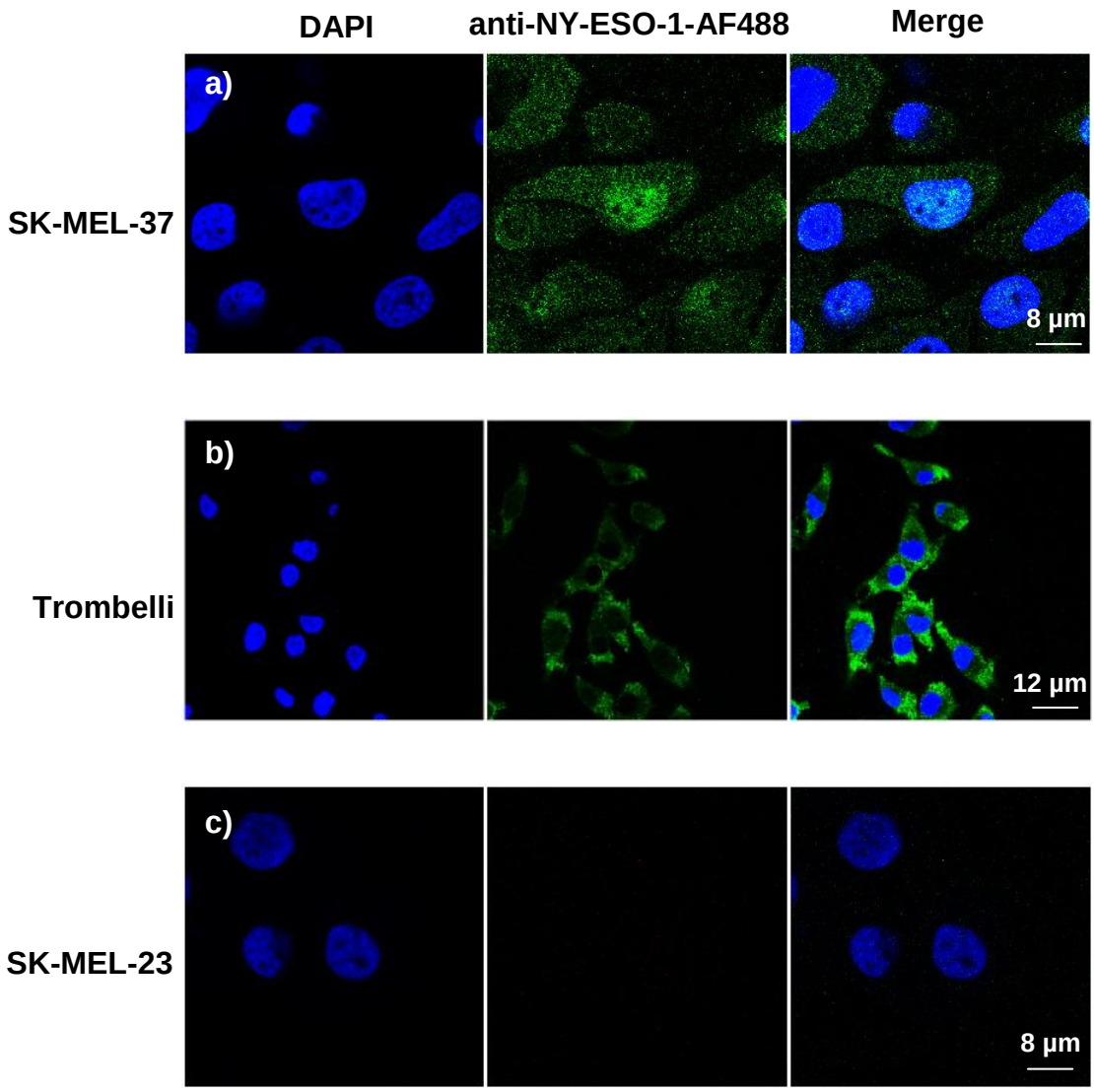
DAPI
anti-NY-ESO-1-AF488
Merge
a)
SK-MEL-37
8 µm
b)
Trombelli
12 µm
c)
SK-MEL-23
8 µm

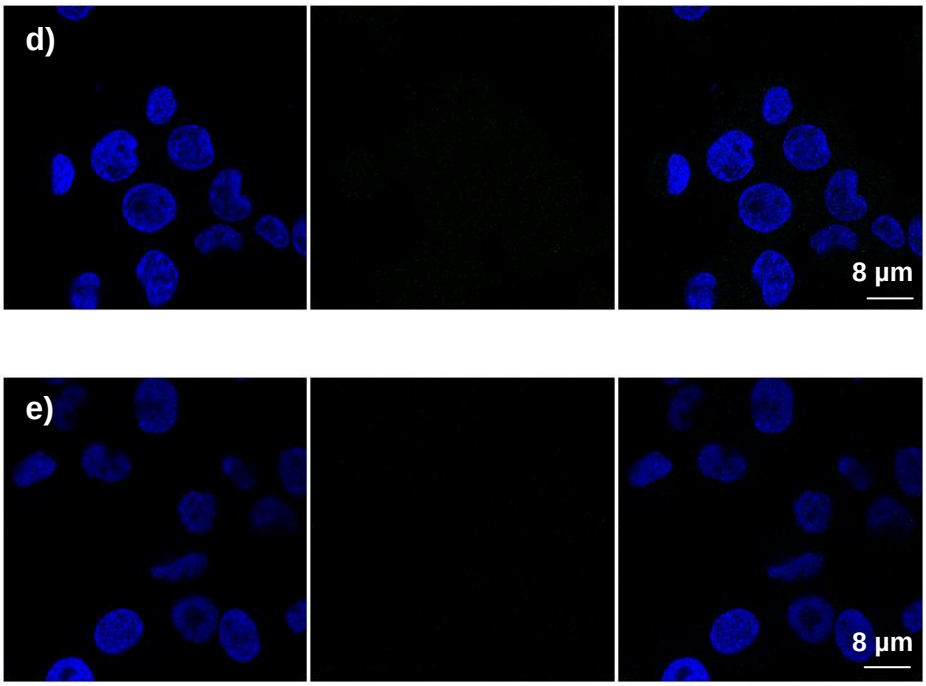

Figure 4.3. NY-ESO-1 expression in three melanoma cell lines. (a) SK-MEL-37, (b) Trombelli and(c) SK-MEL-23 cells were stained with anti-NY-ESO-1 antibody followed by AF488 conjugated secondary antibody. (d) SK-MEL-37 cells were stained with mouse IgG isotype control followed by AF488-conjugated secondary antibody or (e). AF488-conjugated secondary antibody alone All images were obtained using a confocal microscope (Zeiss).

4.4.Internalisation of RICs into SK-MEL-37 cells

The conjugation of the cell-penetrating peptide TAT to NY-ESO-1 was expected to facilitate the uptake of antibody into SK-MEL-37 cells. Confirmation that TAT conjugation was successful was demonstrated by the experiments detailed in chapter 3.

However, the percentage of ^{123}I-anti-NY-ESO-TAT internalised in SK-MEL-37 cells peaked after 1 h incubation at approximately 0.15% (0.5 nM) of the total radioimmunoconjugate administered (Figure 4.4). The percentage internalised then steadily declined over the next 3 h. Statistical analysis showed no significant difference in the percentage internalisation of the TAT-conjugated antibody compared to the unconjugated antibody ($P>0.05$, 2 way ANOVA). An experiment was conducted to investigate whether TAT alone could be taken up by SK-MEL-37 cells. The results of this experiment showed that only 0.28 % of total added ^{123}I-TAT internalised into SK-MEL-37 cells (Figure 4.5). This figure compares unfavourably with reports in the literature that internalisation of ^{123}I-mIgG-TAT by breast cancer cells reached approximately 3.5%-4.5% (28 nM - 36 nM) (Hu et al., 2006, Cornelissen et al., 2007).

It was previously reported that heparan sulfate proteoglycans on the cell surface play an important role in translocation of molecules across cell membrane by interacting with CPPs. Syndecan-4 (SDC-4), a heparan sulfate proteoglycan present on the cell surface, was shown to be associated with cationic CPPs such as TAT, suggesting that TAT acts as a ligand for SDC-4 during the translocation process [101]. In the literature, low levels of cellular uptake of TAT were observed in the K562 myelogenous leukemia cell line, which does not express heparin sulphate proteoglycans. Transfection of SDC-4 into K562 cells

significantly enhanced the uptake of TAT, which further supports an important role of heparan sulfate proteoglycans in mediating TAT internalisation [123]. It is possible that there is low expression of SDC-4 in SK-MEL-37 cells and this may explain why TAT failed to facilitate the uptake of RICs into these cells. Due to a lack of literature detailing the expression of SDC-4 in SK-MEL-37 cells, more experiments would need to be conducted to confirm this theory.

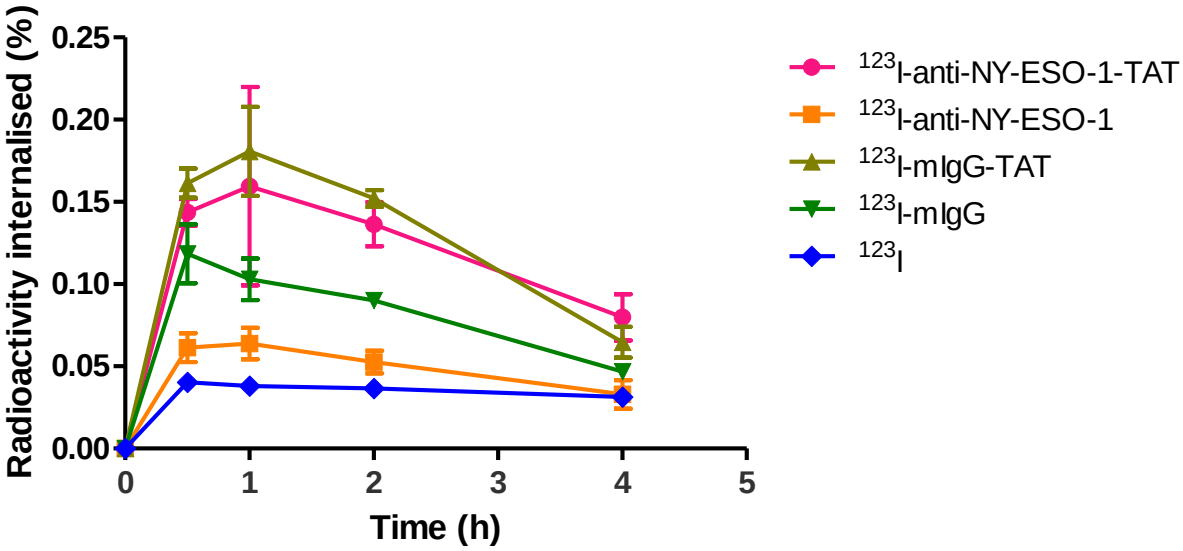

Figure 4.4. Internalisation of ^{123}I-labelled RICs in SK-MEL-37 cells. Data represent the mean and standard deviation of triplicates from three separate experiments. (P>0.05, 2 way ANOVA)

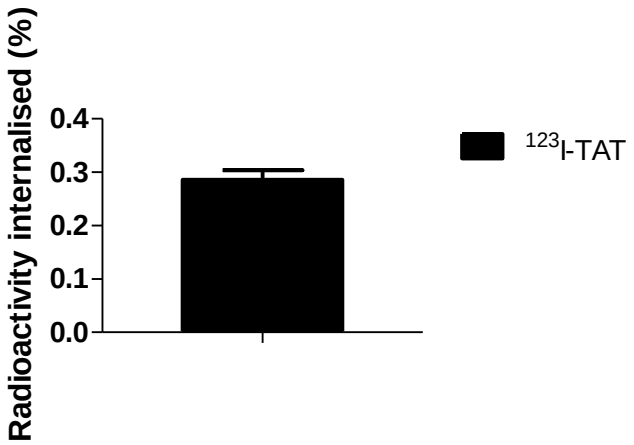

Figure 4.5. Internalisation of ^{123}I-TAT in SK-MEL-37 cells. Data represent the mean and standard deviation of triplicates from three separate experiments.

Because conjugation to TAT alone did not promote internalisation of RICs, a decision was made to transfect RICs into the cells. Transfection is a term generally used to describe the process of deliberately introducing nucleic acids into cells. For instance, delivery of small interference RNA (siRNA) to knock-down the expression of a protein to study the biological functions of proteins of interest. A common method of transfection is to mix the nucleic acids with cationic lipids to produce liposomes. It has been found that a similar mechanism can be used to deliver anti-NY-ESO-1 antibody into cells. Research revealed that chemical-based reagents designed to introduce proteins into cells are commercially available, though some of them are toxic, need to be used in serum-free conditions, and become less efficient with longer incubation times, thus limiting their use in experimental settings (Zelphati et al., 2001, Zassler et al., 2005, Dalkara et al., 2006). SAINT-PhD is a protein transfection reagent consisting of a cationic amphiphile and helper lipid, which has been shown to achieve protein delivery in a non-toxic and serum-insensitive manner (van der

Gun et al., 2007). Moreover, it has reported that a cationic lipid formulation was more effective than TAT for protein delivery (Ye et al., 2002). Therefore, the protein transfection reagent SAINT-PhD was evaluated for its ability to promote the internalisation of anti-NY-ESO-1 RICs into SK-MEL-37 cells. As shown in Figure 4.6, the internalisation of ^{123}I-labelled RICs into SK-MEL37 cells was significantly enhanced in the presence of the protein transfection reagent (PT). The percentage of ^{123}I-anti-NY-ESO-1-TAT-PT internalised into SK-MEL-37 cells after incubation for 4 h was 18.9% ± 0.8%, compared to approximately 0.15% without transfection reagent. The difference in the internalisation of the ^{123}I-anti-NY-ESO-1-TAT-PT compared to ^{123}I was statistically significant at all time points except 0 min (2 way ANOVA, $P < 0.001$).

To measure internalisation of ^{111}In-labelled RICs in SK-MEL-37 cells, the incubation time was extended to 24 h, after initial experiments indicated that internalisation of ^{111}In-labelled RICs was slower than that of ^{123}I-labelled RICs. The presence of the protein transfection reagent caused a significant increase in the percentage of the ^{111}In-labelled RICs taken up by SK-MEL-37 cells (Figure 4.7). However the percentage of the ^{111}In-labelled RICs internalised into cells was significantly lower than that of the ^{123}I-labelled RICs. After 24 h incubation, 1.47% ± 0.1% of the total amount of ^{111}In-DTPA-anti-NY-ESO-1-TAT-PT was internalised, compared to 18.9% for ^{123}I-DTPA-anti-NY-ESO-1-TAT-PT. Possible reasons for this difference in internalisation are discussed below.

As shown in Fig 1.8, the penetration of liposomes into cells involves a neutralisation reaction between the cationic lipids of the liposome and anionic

lipids of the cell membrane which allows penetration of the lipid bilayer and release of the liposomal contents into the cytoplasm. cDTPA, which was used to conjugate ^{111}In to antibody constructs in this study, is a polyamino carboxylic acid consisting of a diethylenetriamine backbone with five carboxymethyl groups, and thus has a high affinity for metal cations. DTPA has the potential to form up to eight coordination bonds due to the presence of three amine centres and five carboxyl groups. However, it typically forms less than eight bonds with a transition metal, so after chelating the indium, the remaining negatively charged groups could neutralise the cationic lipids of the liposomes (Fomenko et al., 1973). This would have a detrimental effect on the fusion of the liposome with the cell membrane and subsequent release of the liposomal contents. This could explain why the percentage of ^{111}In-labelled RICs internalised in SK-MEL-37 cells is substantially lower than that of the ^{123}I-labelled RICs.

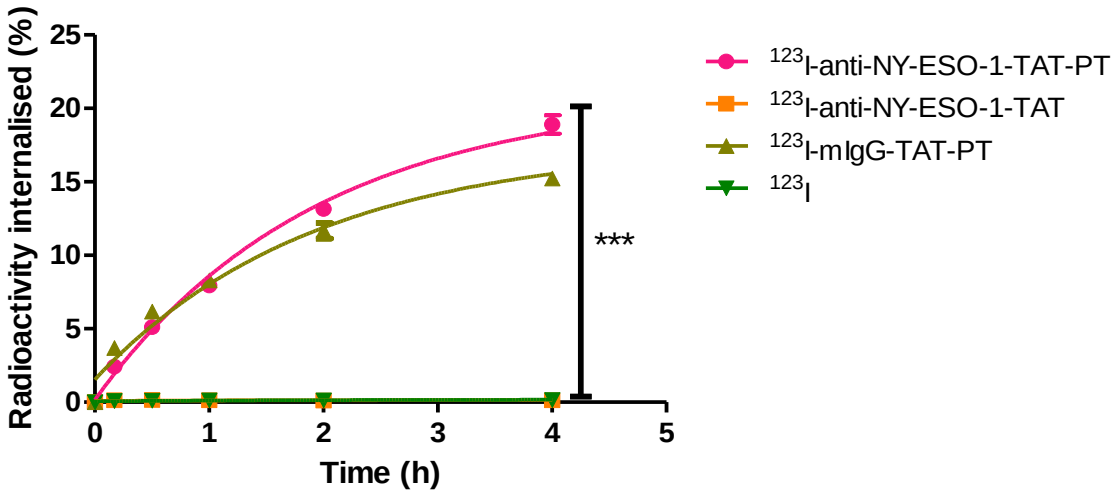

Figure 4.6. Internalisation of ^{123}I-labelled RICs in SK-MEL-37 cells. Data represent the mean and standard deviation of triplicates from three separate experiments.. Data were fitted to a single phase exponential association model. * indicates a statistically significant difference (P<0.001, 2 way ANOVA) between the percentage of ^{123}I-anti-NY-ESO-1-TAT-PT internalised compared to ^{123}I .**

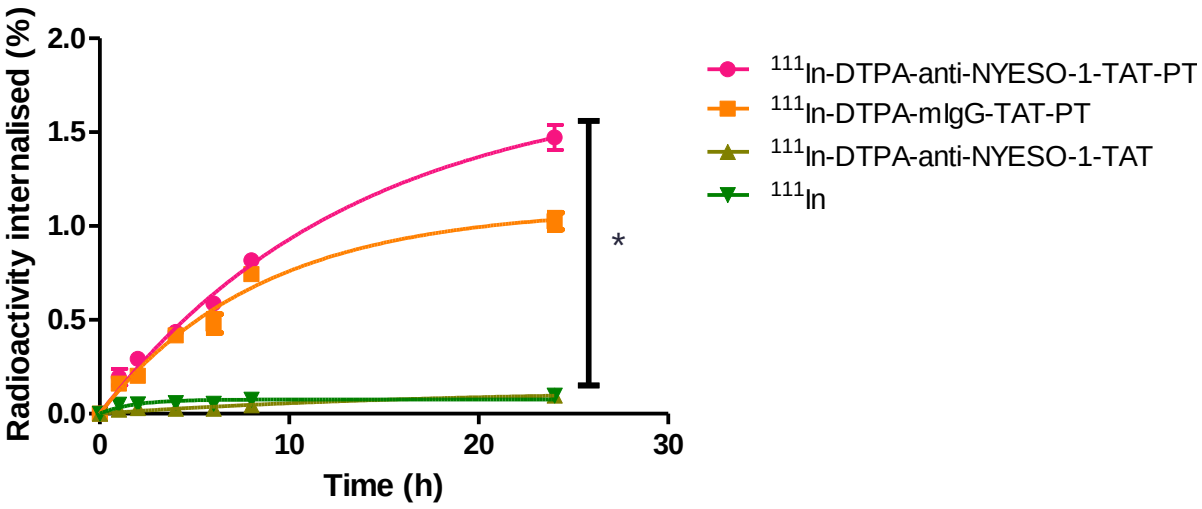

Figure 4.7. Internalisation of ^{111}In-labelled RICs in SK-MEL-37 cells. Data represent the mean and standard deviation of triplicates from three separate experiments. Data were fitted to a single phase exponential association model. * indicates a statistically significant difference (P<0.05, 2 way ANOVA) between the percentage of ^{111}In-DTPA-anti-NY-ESO-1-TAT-PT internalised compared to ^{111}In .

4.5. Internalisation of RIC into subcellular compartments of SK-MEL-37 cells.

Auger electrons have a short range and it is therefore important that they are localised in close proximity to DNA to exert maximum cytotoxic effect. Therefore, the percentage of ^{123}I- and ^{111}In-labelled anti-NY-ESO-1-TAT-PT and anti-NY-ESO-1-PT that internalised into the cytoplasmic and nuclear fractions of SK-MEL-37 cells was determined. The percentage of RIC in the cytoplasmic and nuclear fractions is expressed relative to the total amount of RIC added (Figures 4.8a, b and 4.9a, b). The percentage of RIC in the cytoplasmic and nuclear

fractions was then calculated relative to the total amount of RIC internalised, and these data are shown in Figures 4.8c, d and 4.9c, d.

When the cells were exposed to ^{123}I-labelled RICs, there was a higher percentage of the non-TAT conjugated construct in the cytoplasm compared to the TAT-conjugated construct (7.05% ± 1.8% v 2.96% ± 0.4%), as shown in Figure 4.8a. However, the nuclear uptake of the TAT-conjugated construct was higher than that of the non-TAT conjugated construct (9.08% ± 1.1% v 5.36% ± 0.5%), as shown in Figure 4.8b. Expressing the data as a percentage of total internalised activity showed that 76% of internalised ^{123}I-anti-NY-ESO-1-TAT-PT accumulates in the nucleus compared to 42% of ^{123}I-anti-NY-ESO-1–PT (Figures 4.8c, d). The difference in nuclear uptake between the two RICs was statistically significant (2 way ANOVA, P <0.001), and indicates that the presence of TAT enhances nuclear localisation of the RICs.

When cells were treated with ^{111}I-labelled RICs, a similar pattern of RIC distribution was observed. Again there was a higher percentage of the non-TAT conjugated construct in the cytoplasm compared to the TAT-conjugated construct (0.58% ± 0.09% v 0.34% ± 0.3%), as shown in Fig. 4.9a. Again, the nuclear uptake of the TAT-conjugated construct was higher than that of the non-TAT conjugated construct (0.77% ± 0.05% v 0.30% ± 0.01%), as shown in Fig. 4.9b. Expressing the data as a percentage of total internalised activity showed that 69% of internalised ^{111}In-DTPA-anti-NY-ESO-1-TAT-PT accumulates in the nucleus compared to 39% of ^{111}In-DTPA-anti-NY-ESO-1–PT (Figure 4.9c, d). The difference in nuclear uptake between the two RICs was statistically significant (2 way ANOVA, P <0.001).

a)

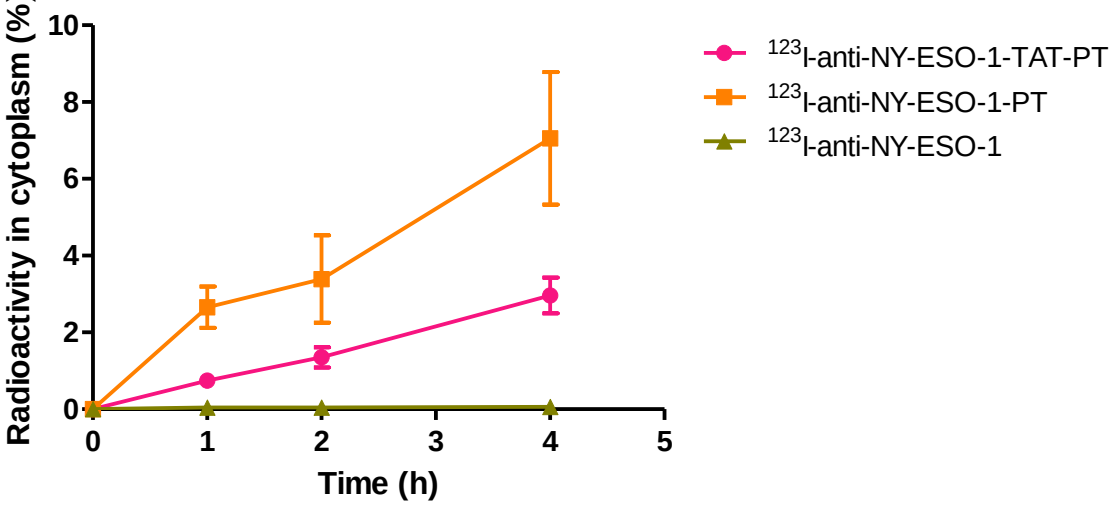
Radioactivity in cytoplasm (%)
10
8
6
4
2
0
0
1
2
3
4
5
Time (h)
123I-anti-NY-ESO-1-TAT-PT
123I-anti-NY-ESO-1-PT
123I-anti-NY-ESO-1

b)

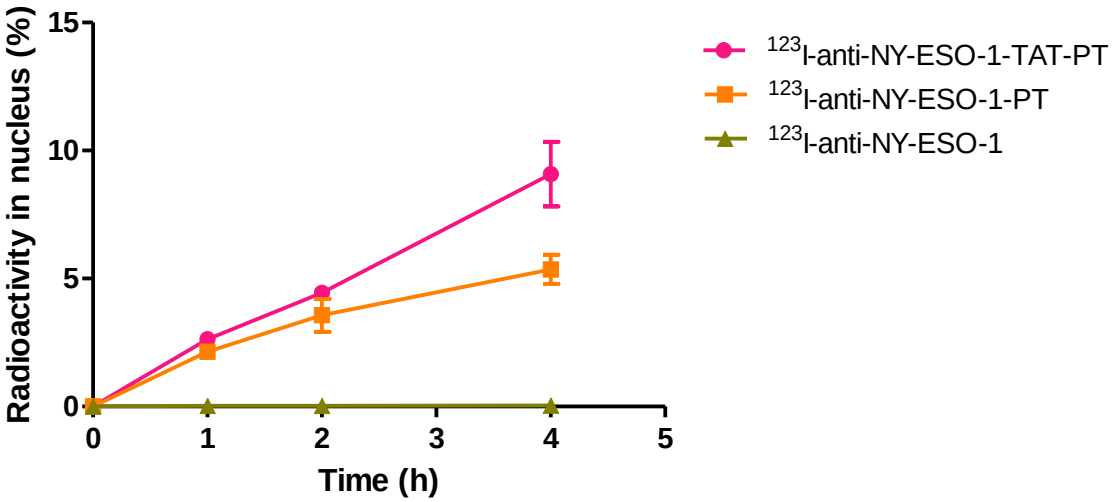
Radioactivity in nucleus (%)
15
10
5
0
0
1
2
3
4
5
Time (h)
123I-anti-NY-ESO-1-TAT-PT
123I-anti-NY-ESO-1-PT
123I-anti-NY-ESO-1

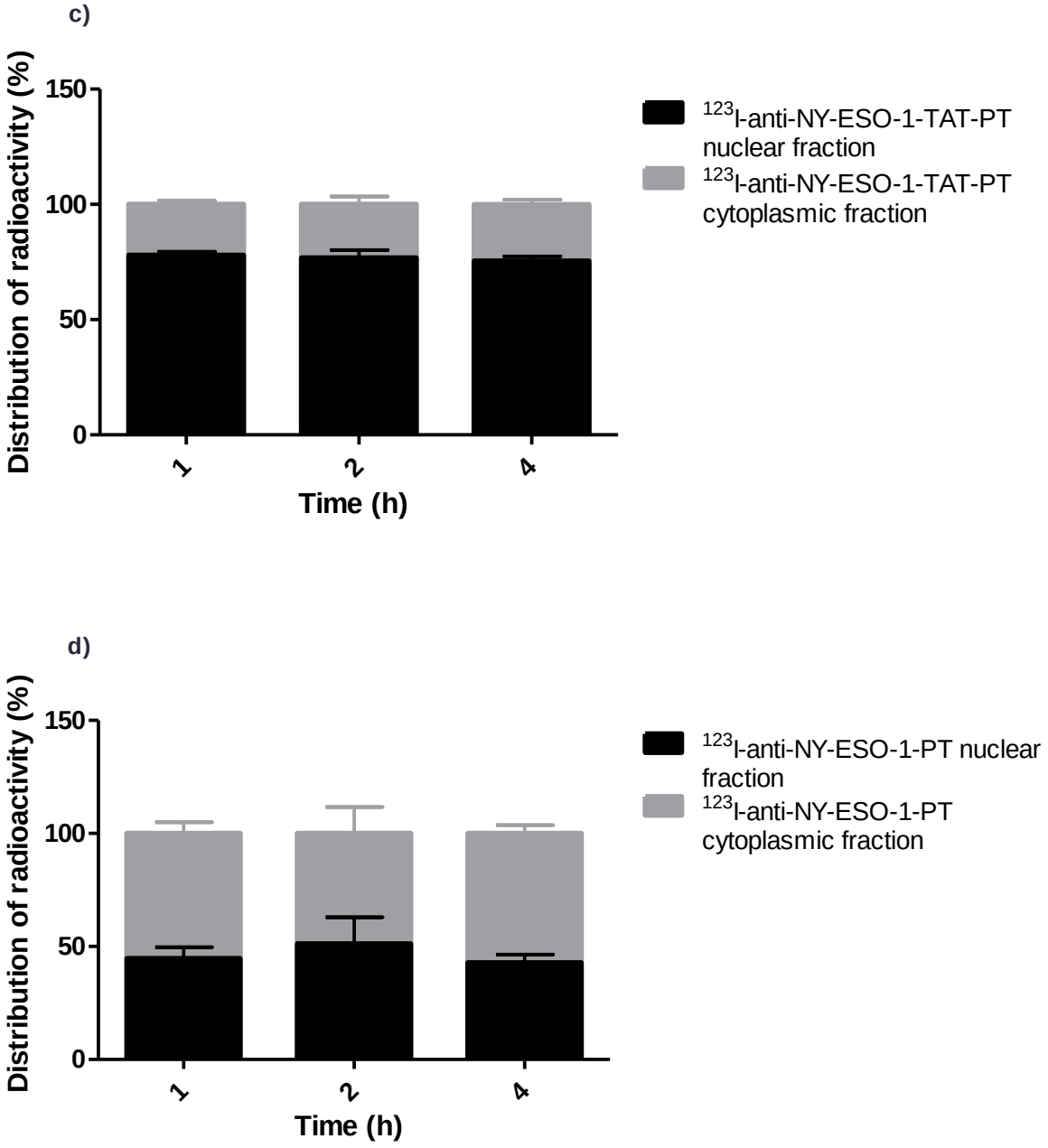

Figure 4.8. Internalisation of ^{123}I-labelled RICs into (a) the cytoplasm and(b) nucleus of SK-MEL-37 cells. The proportion of the total internalised fraction of ^{123}I-anti-NY-ESO-1-TAT-PT and ^{123}I-anti-NY-ESO-1-PT present in the cytoplasm and nucleus of SK-MEL-37 cells is shown in (c) and (d) respectively. Data represent the mean and standard deviation of triplicates from two separate experiments. (P <0.001, 2 way ANOVA).

a)

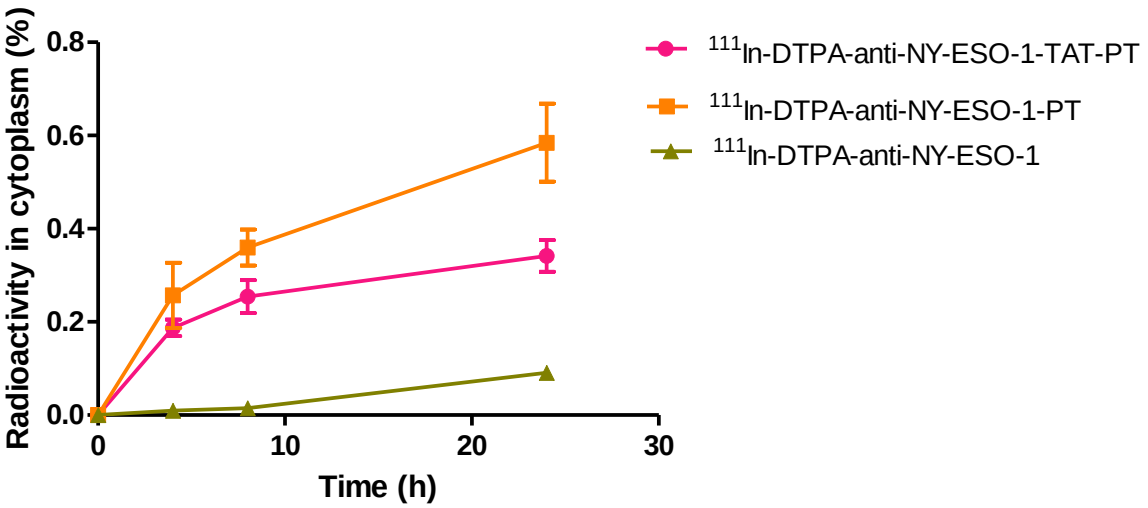
Radioactivity in cytoplasm (%)
0.8
0.6
0.4
0.2
0.0
0
10
20
30
Time (h)
111In-DTPA-anti-NY-ESO-1-TAT-PT
111In-DTPA-anti-NY-ESO-1-PT
111In-DTPA-anti-NY-ESO-1

b)

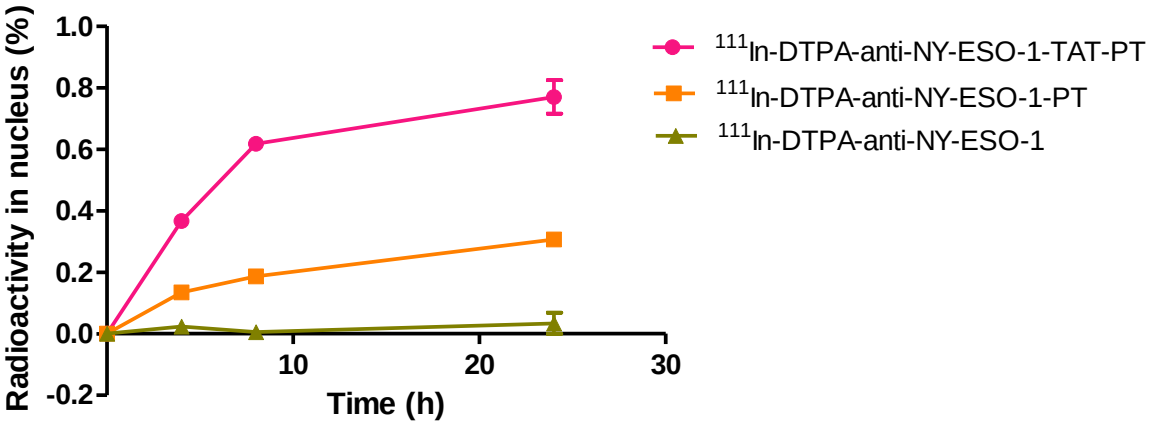
Radioactivity in nucleus (%)
1.0
0.8
0.6
0.4
0.2
0.0
-0.2
10
20
30
Time (h)
111In-DTPA-anti-NY-ESO-1-TAT-PT
111In-DTPA-anti-NY-ESO-1-PT
111In-DTPA-anti-NY-ESO-1

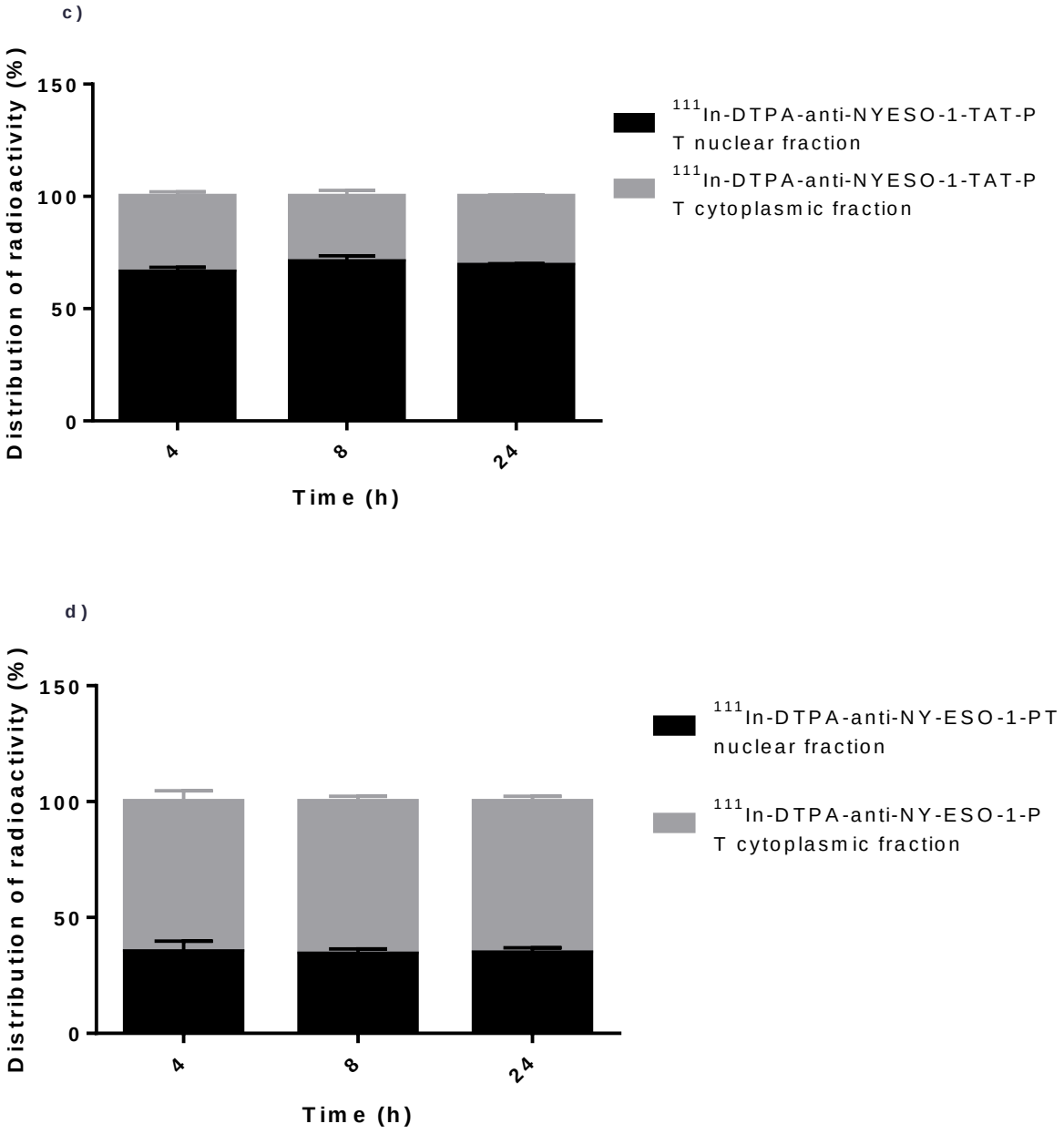

Figure 4.9. Internalisation of ^{111}In-labelled RICs into (a) the cytoplasm and(b) nucleus of SK-MEL-37 cells. The proportion of the total internalised fraction of ^{111}In-DTPA-anti-NY-ESO-1-TAT-PT and ^{111}In-DTPA-anti-NY-ESO-1-PT present in the cytoplasm and nucleus of SK-MEL-37 cells is illustrated in (c) and (d) respectively. Data represent the mean and standard deviation of triplicates from two separate experiments. (P <0.001, 2 way ANOVA).

4.6. Internalisation of RICs demonstrated using immunocytochemistry

SK-MEL-37 cells were exposed to DTPA-anti-NY-ESO-1-TAT-PT and DTPA-anti-NY-ESO-1-TAT for 24 h, and then fixed and stained as described in the Methods section. To detect the DTPA-anti-NY-ESO-1-TAT-PT construct, an anti-mouse IgG secondary antibody conjugated to AF488 was used. To demonstrate co-localisation with endogenous NY-ESO-1 expression, treated cells were also stained with rabbit anti-NY-ESO-1 polyclonal primary antibody followed by an anti-rabbit secondary antibody conjugated to AF555.

SK-MEL-37 cells exposed to DTPA-anti-NY-ESO-1-TAT-PT showed cytoplasmic and nuclear staining (Figure 4.10), indicating that the construct was successfully internalised. This result is consistent with data from the internalisation assay (Figures 4.6 and 4.7). The small areas of intense green staining, indicated by arrows in Figure 4.10, could represent DTPA-anti-NY-ESO-1-TAT-PT associated with liposomes that had not yet crossed the cell membrane. However, it was difficult to determine whether staining for DTPA-anti-NY-ESO-1-TAT-PT co-localised with staining for endogenous NY-ESO-1 since NY-ESO-1 staining was observed homogenously throughout the nucleus. No fluorescence was observed in cells treated with DTPA-anti-NY-ESO-1-TAT, indicating that this construct was not internalised without the protein transfection reagent.

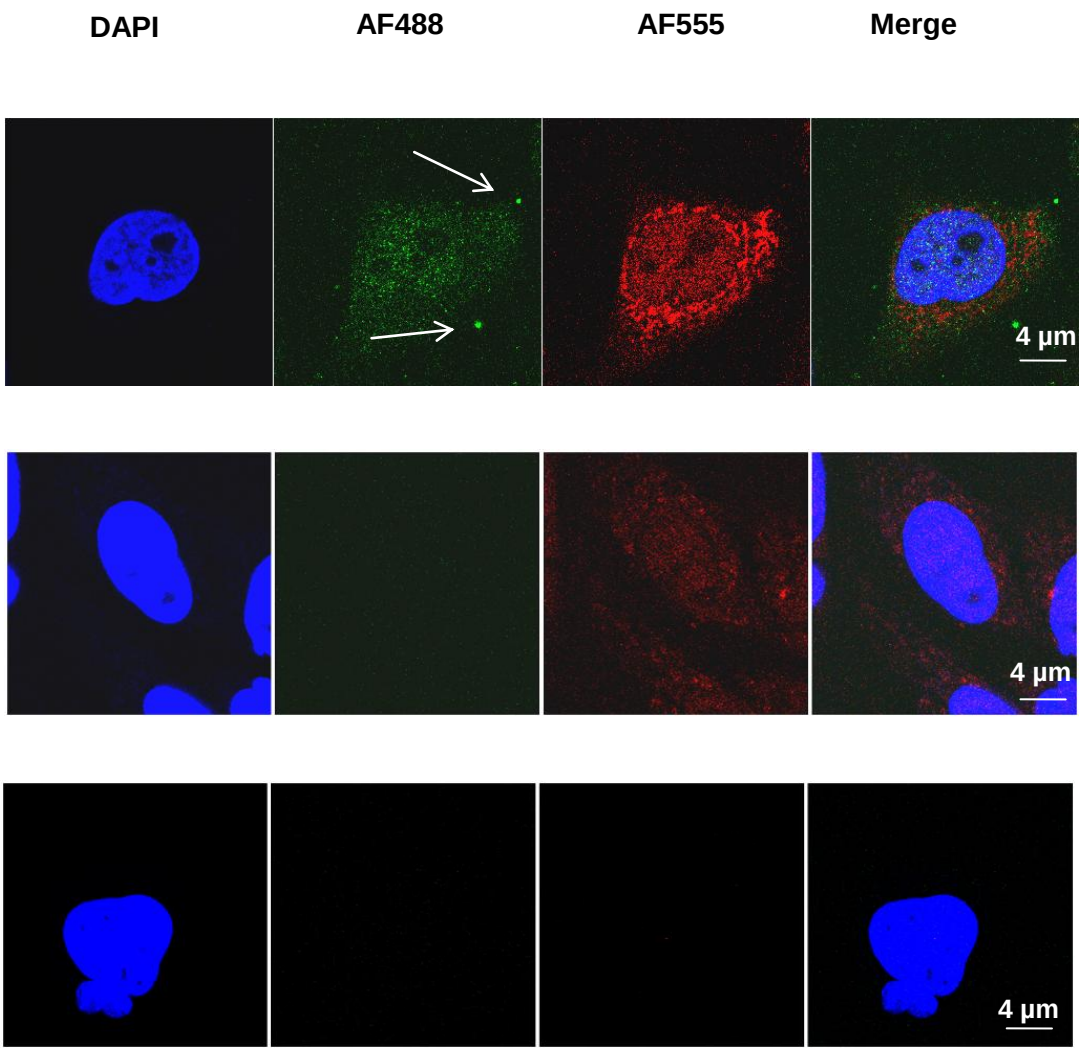

Figure 4.10. Confocal microscopy demonstrating the uptake of DTPA-anti-NY-ESO-1-TAT-PT in SK-MEL-37 cells. SK-MEL-37 cells were incubated with DTPA-anti-NY-ESO-1-TAT-PT (top row), DTPA-anti-NY-ESO-1-TAT (middle row), or no treatment (bottom row) for 24 h before fixing and staining cells. Treated cells were stained with AF488-conjugated anti-mouse secondary antibody (column 2) to detect internalised immunoconjugates. Treated cells were also stained with rabbit anti-NY-ESO-1 followed by AF555-conjugated anti-rabbit secondary antibody (column 3) to detect endogenous NY-ESO-1. The bottom row represents untreated cells stained with secondary antibodies alone.

4.7.The retention of RIC in SK-MEL-23 and SK-MEL-37 melanoma cell lines

The retention of ^{111}In- and ^{123}I-labelled anti-NY-ESO-1-TAT-PT and anti-mIgG-TAT-PT in SK-MEL-37 and SK-MEL-23 cells was investigated. It was predicted that NY-ESO-1-specific RICs would be retained in the NY-ESO-1 expressing SK-MEL-37 cell line.

The percentage of ^{111}In-DTPA-anti-NY-ESO-1-TAT-PT retained in SK-MEL-37 cells decreased gradually over 48 h compared to the ^{111}In-DTPA-mIgG-TAT-PT, which showed a significant decline during the first 10 h following incubation, before reaching a plateau (Figure 4.11). The rate of efflux of ^{111}In-DTPA-mIgG-TAT-PT ($T_{1/2}$: 4.8 h) was 8-fold faster than ^{111}In-DTPA-anti-NY-ESO-1-TAT-PT ($T_{1/2}$: 43.4 h), which was a statistically significant difference (P = 0.0008, sum of square F test). In contrast, in the NY-ESO-1 negative cell line SK-MEL-23, there was no statistically significant difference between the rate of efflux of both RICs ($T_{1/2}$: 3.4 h v 3.2 h for ^{111}In-DTPA-anti-NY-ESO-1-TAT-PT and ^{111}In-DTPA-mIgG-TAT-PT, respectively; P = 0.85, sum of square F test).

A similar result was also observed for ^{123}I-labelled RICs (Figure 4.12). The rate of efflux of the ^{123}I-DTPA-mIgG-TAT-PT ($T_{1/2}$: 2.6 h) was 2.5-fold faster than ^{123}I-DTPA-anti-NY-ESO-1-TAT-PT ($T_{1/2}$: 6.8 h), which was a statistically significant difference (P = 0.04, sum of square F test). In contrast, in the NY-ESO-1 negative cell line, SK-MEL-23, there was no statistically significant difference between the rate of efflux of the RICs ($T_{1/2}$: 10.8 h v 18.0 h for ^{111}In-DTPA-anti-NY-ESO-1-TAT-PT and ^{111}In-DTPA-mIgG-TAT-PT, respectivel; P = 0.06, sum of square F test).

In a separate experiment in SK-MEL-37 cells, there was no significant difference in the rate of efflux of the non-TAT conjugated antigen specific probe, ^{123}I-anti-NY-ESO-PT, compared to the non-TAT conjugated control probe, ^{123}I-mIgG-PT (P = 0.18, sum of square F test), as shown in Figure 4.13. This suggests that the presence of TAT influences the retention of the antigen specific probe. This is supported by the finding from Rayne *et al.* that TAT could accumulate at the plasma membrane through its specific interaction with phosphatidylinositol-4,5-bisphosphate ($PI(4,5)P_2$). This interaction was governed by specific motifs (residue 49-51) of the TAT basic domain that recognised the $PI(4,5)P_2$ molecules, and was stabilised by membrane insertion of the TAT tryptophan side chain (Rayne et al., 2010). The TAT peptide sequence used in this study contained the key residues for binding to $PI(4,5)P_2$ molecules (G**RKK**RRQRRRPPQGYG, where bold letters indicate residue 49-51). $PI(4,5)P_2$ is a phospholipid that is localised on the cytoplasmic side of the cell membrane, and acts as a mediator to recruit signalling molecules which initiate many cell activities such as phagocytosis, endocytosis, exocytosis, cell adhesion and cell migration (De Matteis and Godi, 2004, Di Paolo and De Camilli, 2006). Therefore, it is possible that TAT-conjugated non-antigen specific RICs could be excluded from the melanoma cell lines via binding of TAT to $PI(4,5)P_2$ molecules, whereas the TAT-conjugated antigen specific RICs would be retained via the binding of RICs to NY-ESO-1 protein expressed in the SK-MEL-37 cells.

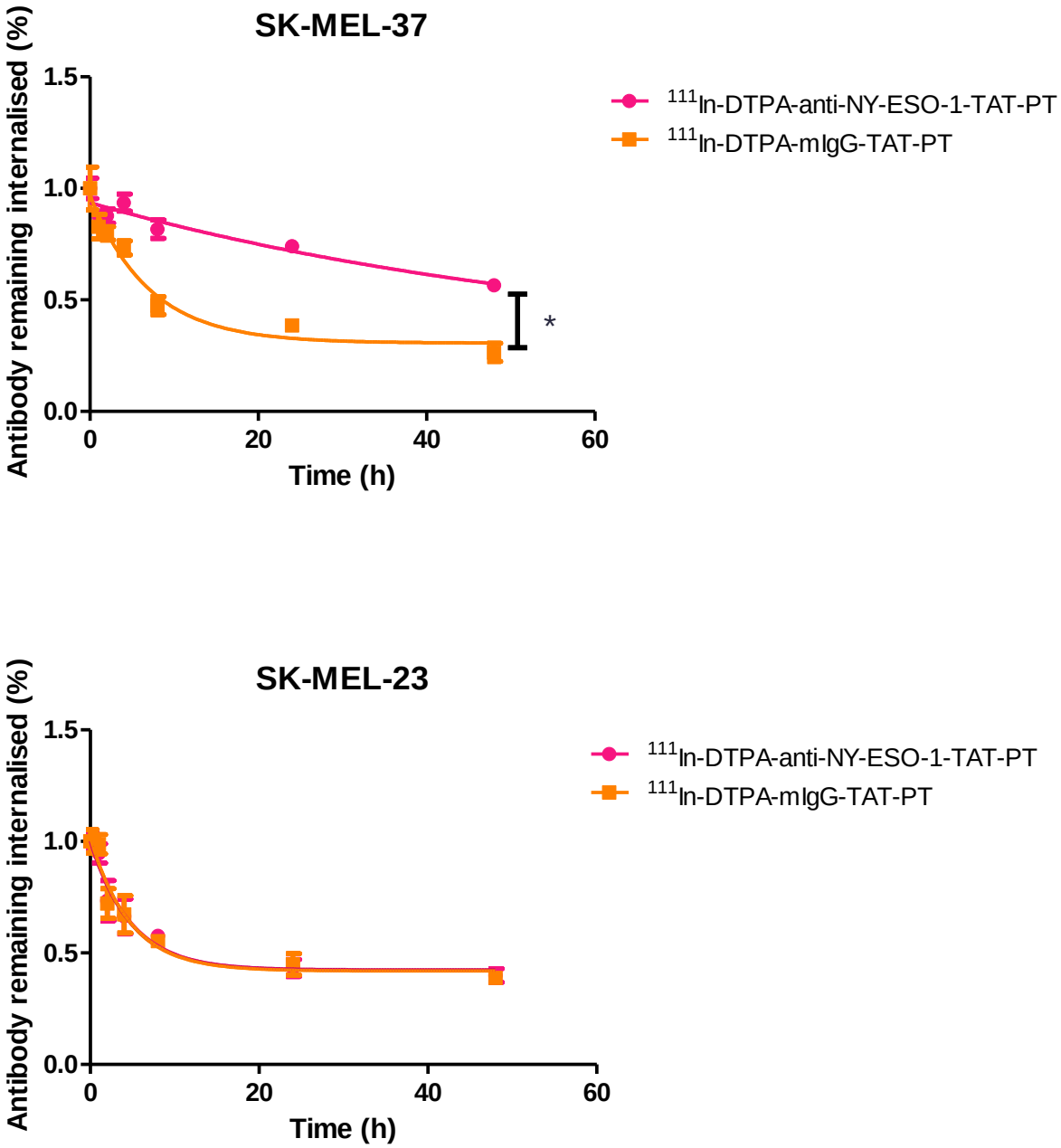

Figure 4.11. The retention of ^{111}In-labelled RICs in SK-MEL-37 and SK-MEL-23 cells. Data represent the mean and standard deviation of triplicates from two separate experiments. Data was fitted to a one phase exponential dissociation model.

*** represents a statistically significant difference (P<0.05, sum of square F test) between retention half-life of antigen specific RIC compared to control RIC**

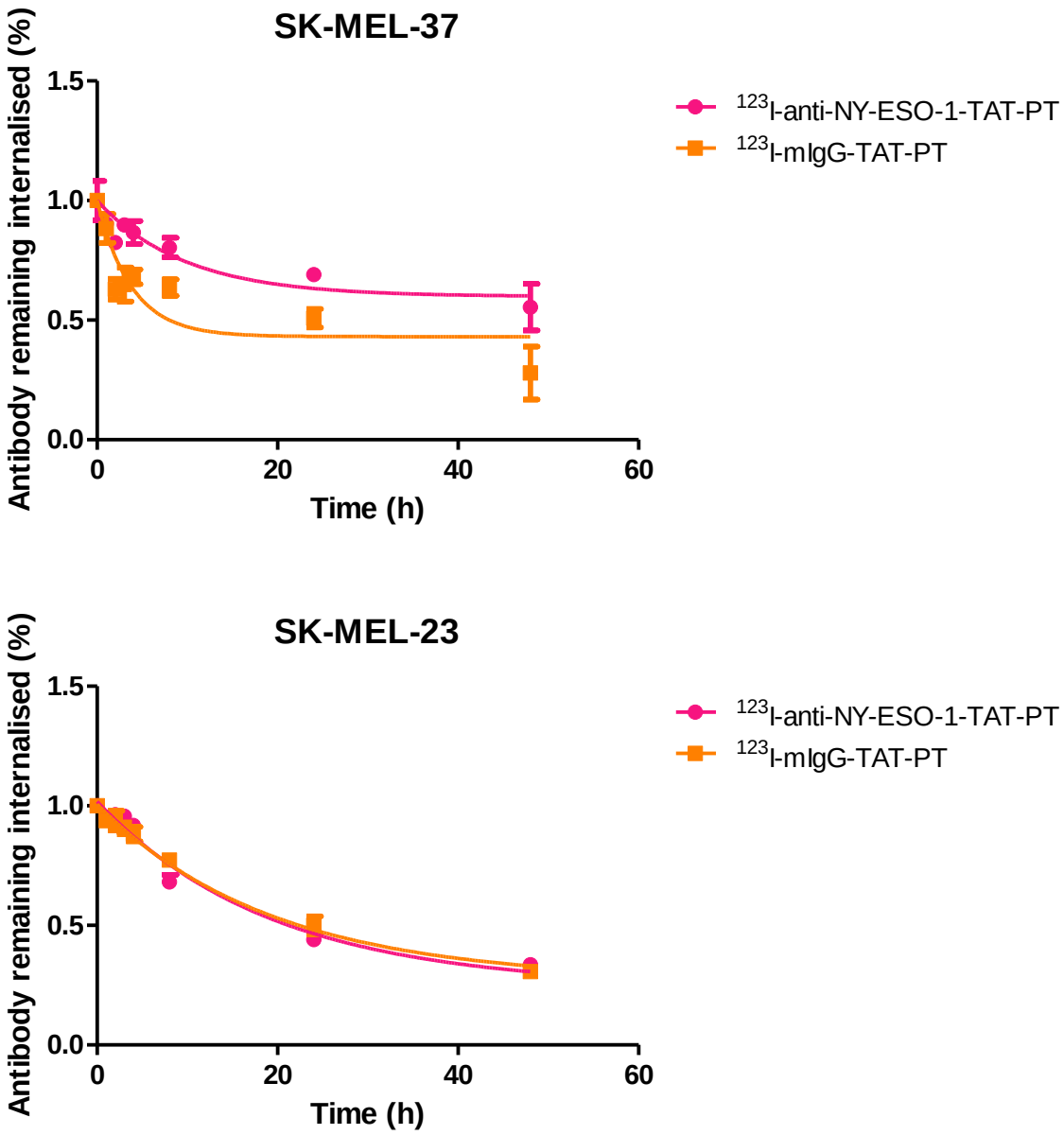

Figure 4.12. The retention of ^{123}I labelled RICs in SK-MEL-37 and SK-MEL-23 cells. Data represent the mean and standard deviation of triplicates from two separate experiments. Data was fitted to one phase exponential dissociation model.

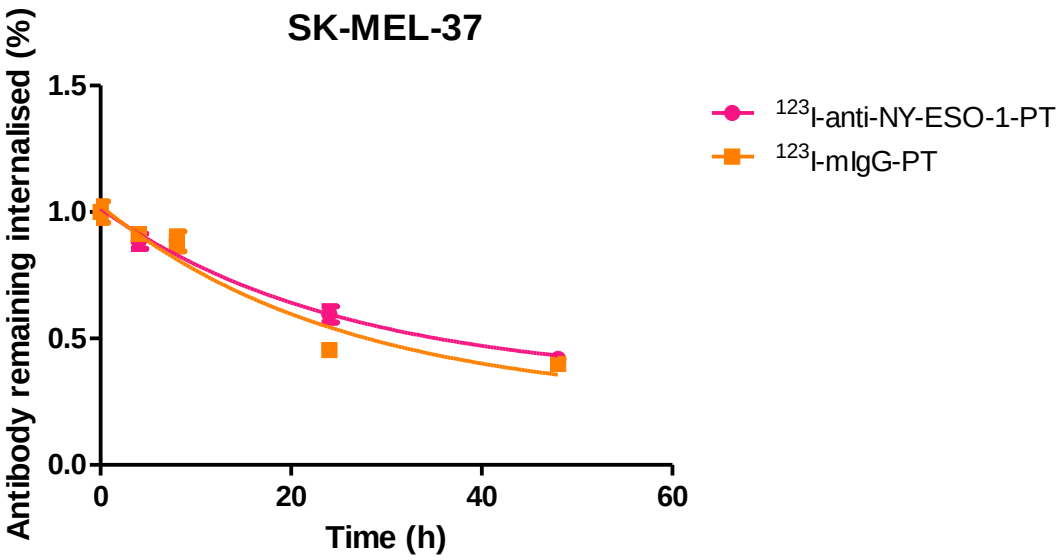

Figure 4.13. The retention of ^{123}I-labelled non-TAT conjugated RICs in SK-MEL-37 cells. Data represent the mean and standard deviation of triplicates from two separate experiments.

4.8.Cell viability following exposure to RIC

Cell viability was measured using a WST-1 (Water soluble Tetrazolium salts) assay. This assay is a quicker alternative to the commonly used MTT assay, due to the lack of a solubilisation step (Ngamwongsatit et al., 2008). The WST-1 reagent is reduced by cellular dehydrogenases in the presence of an intermediate electron acceptor, such as mPMS (1-methoxy-5-methyl-phenazinium methyl sulfate), forming formazans, the measurement of which can be used as an indirect indicator of the level of cell metabolism (Yin et al., 2013). Unlike the MTT assay, in which formazans are precipitated inside cells, reduction of WST-1 occurs outside the cells via cell membrane electron transport, thus reducing the cytotoxicity of the dyes (Berridge et al., 2005).

The percentage viability of SK-MEL-37 cells after incubation with increasing concentrations (0.005 nM to 500 nM) of ^{111}In-labelled and ^{123}I-labelled RICs was measured, and the results are illustrated in Figures 4.14 and 4.15. The percentage cell viability showed a significant reduction after treatment with increasing concentrations of the antigen specific probes, ^{111}In-DTPA-anti-NY-ESO-1-TAT-PT and ^{123}I-anti-NY-ESO-TAT-PT. At the highest RIC concentration (500 nM), percentage cell viability was reduced to 9.9% and 8.9% after treatment with ^{111}In-DTPA-anti-NY-ESO-1-TAT-PT and ^{123}I-anti-NY-ESO-TAT-PT, respectively ($P < 0.001$, 2 way ANOVA, compared to untreated cells). In contrast, exposure to non-radiolabelled immunoconjugates did not affect cell viability. The inhibitory effect on cell viability was observed at lower concentrations of ^{123}I-anti-NY-ESO-TAT-PT (from 5 nM) and was of greater magnitude at the 50 nM concentration when compared to ^{111}In-DTPA-anti-NY-ESO-1-TAT-PT (75% viability v 24.2% viability at 50 nM for ^{111}In-DTPA-anti-NY-ESO-1-TAT-PT and ^{123}I-anti-NY-

ESO-TAT-PT, respectively). A significant difference between these figures was demonstrated using 2 way ANOVA, $P < 0.001$). Therefore, it appears that the ^{123}I-anti-NY-ESO-TAT-PT is more potent in terms of cytotoxic effect than ^{111}In-DTPA-anti-NY-ESO-1-TAT-PT. There was also a significant reduction in cell viability following exposure to the highest concentration (500 nM) of the non-specific isotype control probes, ^{111}In-DTPA-mIgG-TAT-PT and ^{123}I-mIgG-TAT-PT. This suggests that high amount of radioactivity causes some non-specific cytotoxicity.

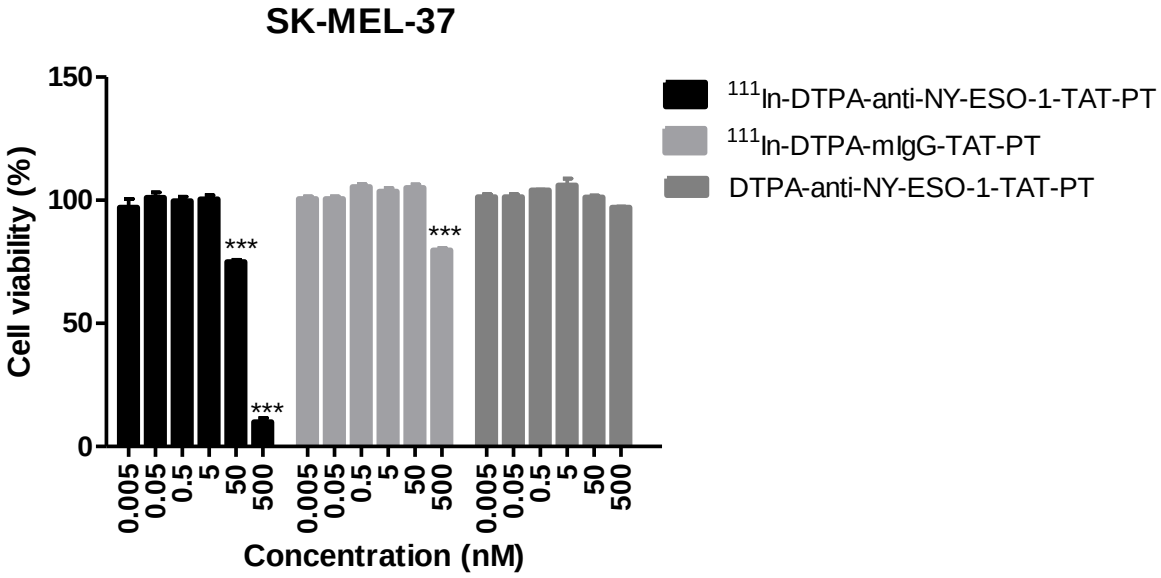

Figure 4.14. Viability of SK-MEL-37 cells following exposure to ^{111}In-labelled RICs. Data represent the mean and standard deviation of triplicates from three separate experiments.

***** indicates a statistically significant ($P < 0.001$, 2 way ANOVA) difference in cell viability compared to untreated control.**

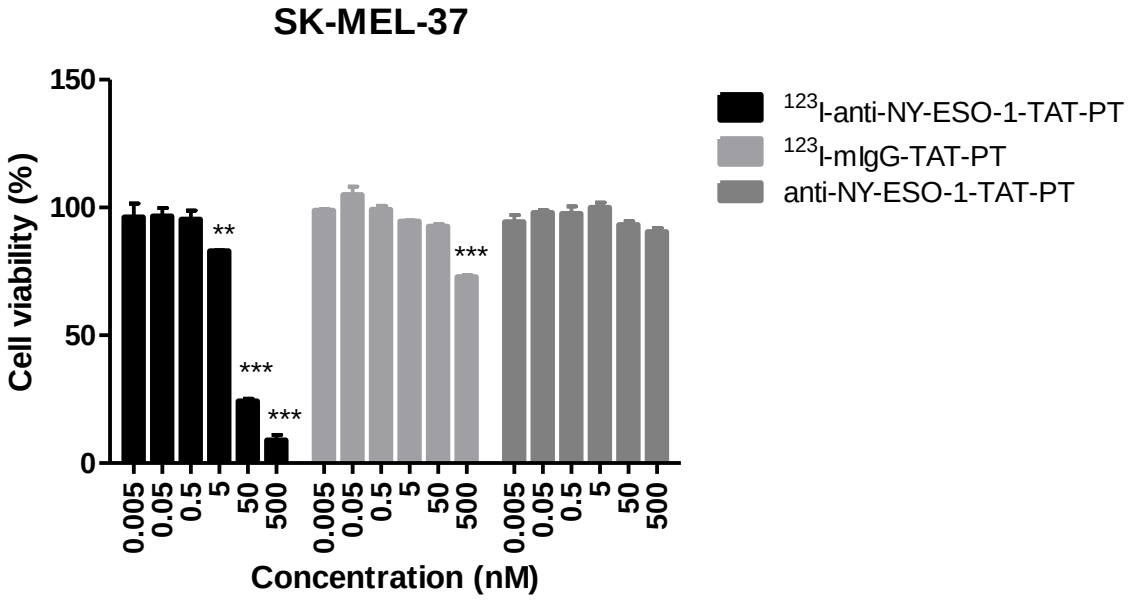

Figure 4.15. Viability of SK-MEL-37 cells following exposure to ^{123}I-labelled RICs. Data represent the mean and standard deviation of triplicates from three separate experiments.
**** and *** indicate a statistically significant (*P* < 0.01 and *P* < 0.001, 2 way ANOVA) difference in cell viability compared to untreated control.**

4.9. The effect of RICs on clonogenic survival of SK-MEL-37 and SK-MEL-23 cells

A clonogenic assay is an *in vitro* cell survival assay that measures the ability of single cells to form colonies. This type of assay is frequently used in cancer research to study the effect of cytotoxic agents, such as drugs or ionising radiation, on the survival and proliferation of cells (Franken et al., 2006).

The clonogenic survival of SK-MEL-37 cells after exposure to ^{111}In-labelled and ^{123}I-labelled RICs, as well as appropriate controls, is illustrated in Figures 4.16 and 4.17. Data is normalised to clonogenic survival in untreated cells, which have a survival fraction (SF) of 1. A statistically significant reduction in clonogenic survival of SK-MEL-37 cells was observed following treatment with a single concentration of ^{111}In-DTPA-anti-NY-ESO-1-TAT-PT and ^{123}I-anti-NY-ESO-1-TAT-PT. The SF was reduced to 0.17 and 0.1 respectively (statistical significance

from untreated cells demonstrated for both agents using 1 way ANOVA, *P* <n0.001). In contrast, there was no reduction in clonogenic survival following treatment with the control probes; including the non-radiolabelled antigen specific probes, the radiolabelled antigen-specific probes that were not conjugated to the protein transfection reagent, and the radiolabelled non-specific mouse IgG probes.

These clonogenic assay results indicate that both antigen specific probes ^{111}In-DTPA-anti-NY-ESO-1-TAT-PT and ^{123}I-anti-NY-ESO-1-TAT-PT exert a cytotoxic effect on SK-MEL-37 cells, which correlates with the WST-1 assay data. No reduction in SF was observed in SK-MEL-37 cells treated with protein transfection (PT) reagent alone, indicating that the concentration of PT reagent used in this study was not cytotoxic to SK-MEL-37 cells. The lack of cytotoxicity observed with the non-radiolabelled immunoconjugates DTPA-anti-NY-ESO-1-TAT-PT and anti-NY-ESO-1-TAT-PT correlates with the WST-1 assay data, and confirms that the cytotoxic effect of the RICs is exerted by the Auger electron emitters, ^{111}In and ^{123}I. The lack of cytotoxicity observed with the RICs which were not conjugated to PT confirms that the PT reagent was necessary for internalisation of the RICs.

The clonogenic survival of SK-MEL-37 cells after exposure to increasing specific activities (0.2 MBq/μg – 3 MBq/μg) and molar concentrations (16.8 – 500 nM) of ^{111}In-DTPA-anti-NY-ESO-1-TAT-PT is illustrated in Figures 4.18 and 4.19. Figure 4.18 shows that an activity dependent reduction in clonogenic survival was observed following treatment with ^{111}In-DTPA-anti-NY-ESO-1-TAT-PT. This effect was statistically significant compared to untreated cells at specific activities of 0.5 Mq/μg and above ($P < 0.001$, 1 way ANOVA). In contrast, equivalent

specific activities of free indium did not significantly reduce clonogenic survival, confirming that the indium must be internalised to exert a cytotoxic effect.

Figure 4.19 shows that a concentration dependent reduction in clonogenic survival was observed following treatment with ^{111}In-DTPA-anti-NY-ESO-1-TAT-PT. This effect was statistically significant compared to untreated cells at concentrations of 125 nM and above. The control probe ^{111}In-DTPA-mIgG-1-TAT-PT caused a reduction in clonogenic survival at the highest concentration tested i.e. 500 nM ($P<0.05$, 1 way ANOVA). This is consistent with the data from the WST-1 cell viability assay (Figure 4.14), and suggests that in a clinical setting the concentration of RIC would have to be adjusted so as to achieve cytotoxicity of the tumour cells without damaging surrounding tissue.

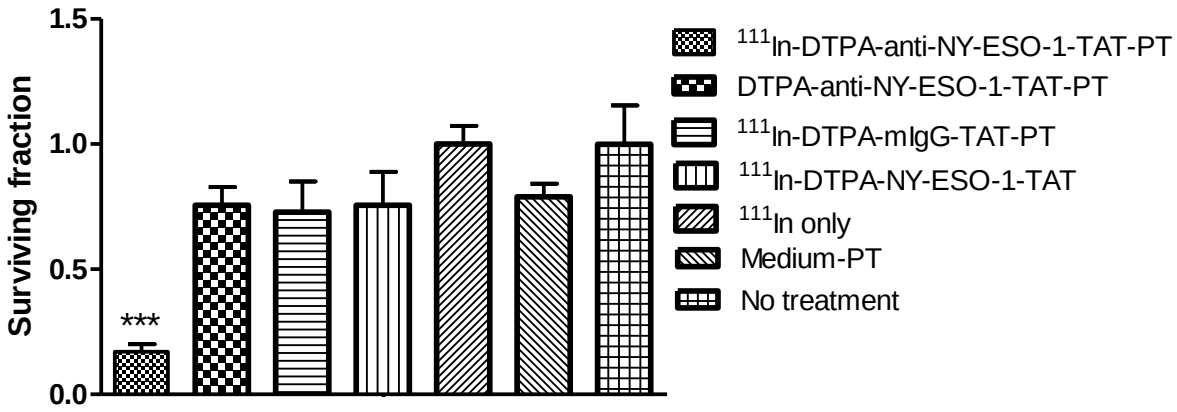

Figure 4.16. Clonogenic survival of SK-MEL-37 cells after exposure to ^{111}In-labelled RICs and appropriate controls. Data represent the mean and standard deviation of triplicates from three separate experiments.
***** indicates a statistically significant reduction (*P* < 0.001, 1 way ANOVA) in survival fraction compared to untreated cells.**

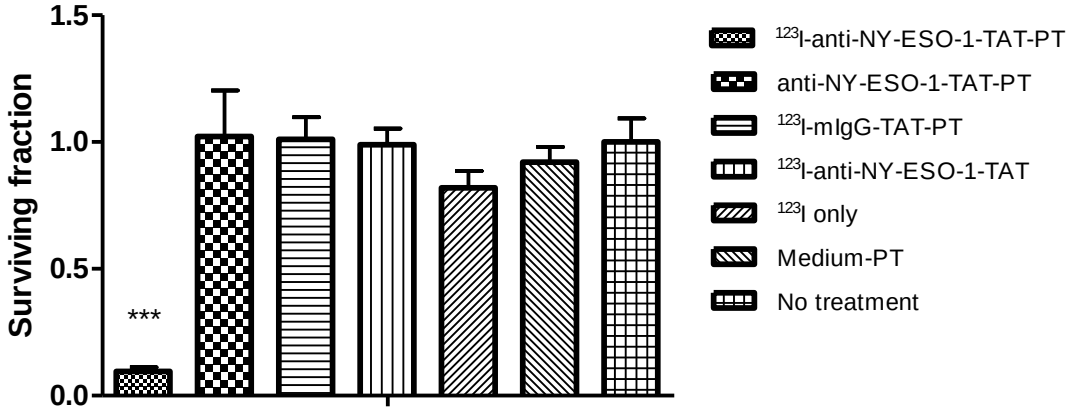

Figure 4.17. Clonogenic survival of SK-MEL-37 cells after exposure to ^{123}I-labelled RICs and appropriate controls. Data represent the mean and standard deviation of triplicates from three separate experiments.
***** indicates a statistically significant reduction (*P* < 0.001, 1 way ANOVA) in survival fraction compared to untreated cells.**

a)

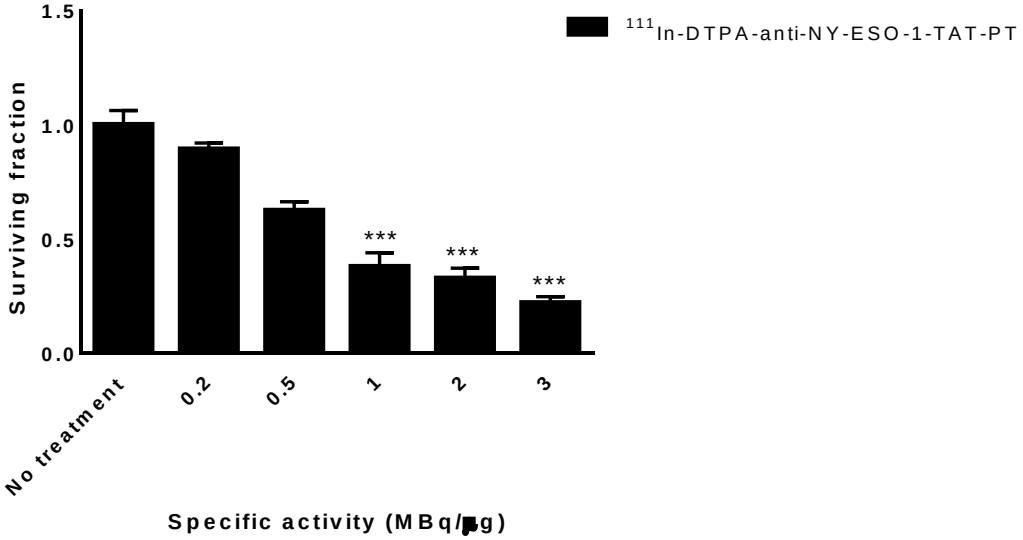
1.5
1.0
0.5
0.0
Surviving fraction
111In-DTPA-anti-NY-ESO-1-TAT-PT
***
***
***
No treatment
0.2
0.5
1
2
3
Specific activity (MBq/µg)

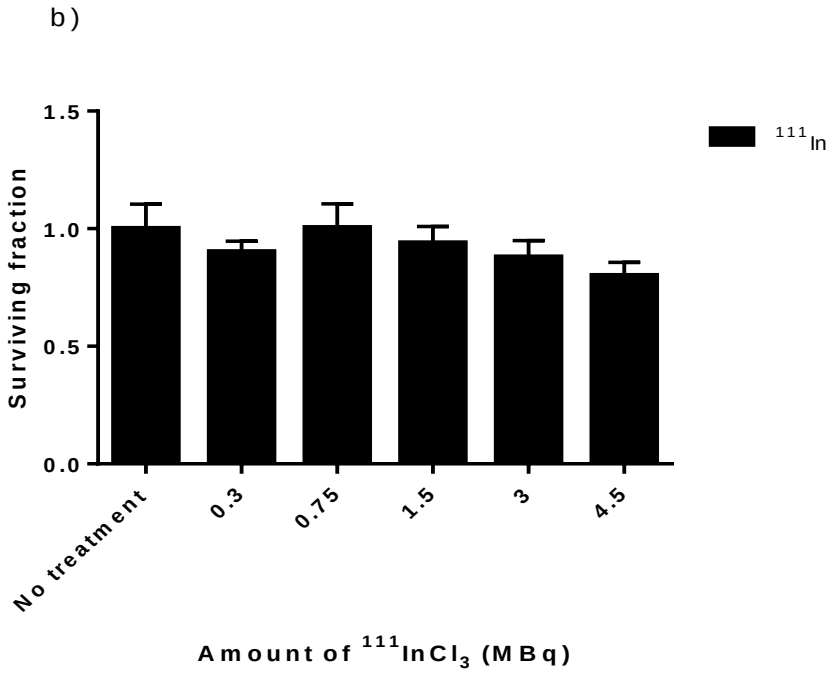

Figure 4.18. Clonogenic survival of SK-MEL-37 cells after exposure to ^{111}In-DTPA-anti-NY-ESO-1-TAT-PT of increasing specific activity. Data represent the mean and standard deviation of triplicates from two separate experiments. a) represents treatment of cells with ^{111}In-DTPA-anti-NY-ESO-1-TAT-PT, and b) represents treatment of cells with an equivalent amount of free ^{111}In.
***** indicates a statistically significant reduction ($P < 0.001$, 1 way ANOVA) in survival fraction compared to untreated cells.**

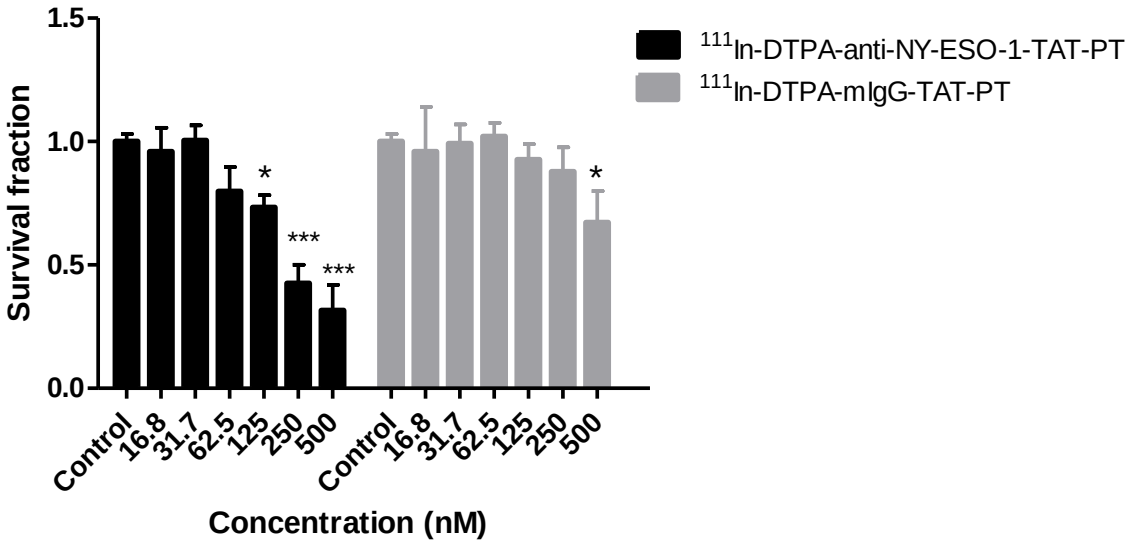

Figure 4.19. Clonogenic survival of SK-MEL-37 cells after exposure to increasing concentrations of ^{111}In-DTPA-anti-NY-ESO-1-TAT-PT and ^{111}In-DTPA-mIgG-TAT-PT (specific activity 1 MBq/µg). Data represent the mean and standard deviation of triplicates from two separate experiments.
*** and *** indicate a statistically significant reduction ($P < 0.05$ and $P < 0.001$, 1 way ANOVA) in survival fraction compared to untreated cells.**

The clonogenic survival of the NY-ESO-1 negative cell line, SK-MEL-23, after exposure to ^{111}In-labelled RICs, as well as appropriate controls, is illustrated in Figure 4.20. There was no significant reduction in clonogenic survival with any of the agents tested ($P > 0.05$, 1 way ANOVA). The lack of cytotoxic effect of the antigen specific RIC, ^{111}In-DTPA-anti-NY-ESO-1-TAT-PT, is consistent with data from the retention assay (Figure 4.11), which showed a lack of retention of this probe in SK-MEL-23 cells. These results confirm that the cytotoxic effect of this probe is exerted only in cells that express the NY-ESO-1 antigen, which suggests that toxicity to surrounding tissues would be minimal if this agent were to be utilised in a cancer treatment regimen.

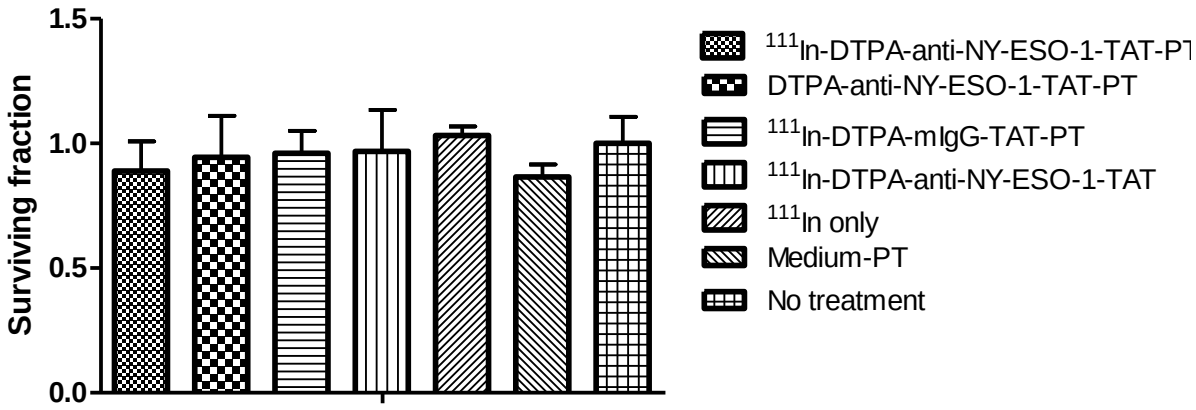

Figure 4.20. Clonogenic survival of SK-MEL-23 cells after exposure to ^{111}In-labelled RICs and appropriate controls. Data represent the mean and standard deviation of triplicates from three separate experiments.

4.10. Effect of ^{111}In-labelled RICs on clonogenic survival of SK-MEL-37 cells following knock down of NY-ESO-1 protein by siRNA

RNA interference (RNAi) refers to the process of silencing gene expression that occurs in response to the introduction of double-stranded RNA (dsRNA) into cells, which leads to initiation of degradation of cytoplasmic mRNAs containing the same sequence as the dsRNA trigger (Fire et al., 1998). Initially, RNA interference was achieved using long dsRNAs, but these long dsRNAs were not successful due to activation of an anti-viral interferon response which led to cell death (Stark et al., 1998). Intensive research on mechanisms of RNA interference revealed that long dsRNA introduced into cells can be cleaved by the RNAse-III class endoribonuclease Dicer to form 21-mer to 28-mer nucleotide small interfering molecules (siRNA) (Hammond et al., 2000, Zamore et al., 2000). Research using siRNA molecules to silence individual genes has shed light on the biological function of proteins and their role in different cellular activities.

The results of clonogenic assays showed that a cytotoxic effect of the antigen specific RIC was observed in the NY-ESO-1 expressing cell line SK-MEL-37, but not the NY-ESO-1 negative cell line SK-MEL-23 (Figures 4.16 – 4.20). The siRNA gene knock-down experiments were carried out to provide additional confirmation of the necessity for cells to express the NY-ESO-1 antigen for the cytotoxic effect of this RIC to be exerted. Synthetic Dicer-substrate 27-mer siRNAs optimised for Dicer processing were used, as they have been demonstrated to have greater potency and efficacy in gene silencing compared to the traditional 21-mer siRNAs (Kim et al., 2004).

A Western blot confirmed successful knock-down of the NY-ESO-1 protein in SK-MEL-37 cells after a 6 h incubation with 3 different siRNA molecules (Figure

4.21). The combination of the 3 siRNAs was more effective at knocking down NY-ESO-1 protein expression when compared to incubation with the individual siRNA molecules alone.

Figure 4.22 shows the effect of siRNA incubation on the clonogenic survival of SK-MEL-37 cells following treatment with ^{111}In-RICs. The cytotoxic effect of ^{111}In-DTPA-anti-NY-ESO-1-TAT-PT was partially reversed by the presence of the siRNA, and this effect was statistically significant (survival fraction of 0.07 v 0.37 in the absence and presence of siRNA respectively, $P > 0.05$, 1 way ANOVA). A full reversal of the cytotoxic effect of the antigen specific RIC was not observed in the presence of the mixture of three sets siRNA even though Fig 4.21 showed the complete knock-down of the NY-ESO-1. It was possibly due to the fact that the anti-NY-ESO-1 antibody could be binding to the LAGE-1 CT antigen, which is highly homologous to NY-ESO-1 (Zou, 2006). The LAGE-1 gene yields two mRNA transcripts, termed LAGE-1a and LAGE-1b. LAGE-1a and NY-ESO-1 are highly homologous with 84% shared identity at the protein level, while LAGE1b shares 76.6% homology with NY-ESO-1 in its N-terminal portion but differs in its C-terminal portion. The anti-NY-ESO-1 antibody (clone E978) used in this study was generated against full length NY-ESO-1 (180 amino acids) and was shown to bind to the NY-ESO-$1_{73\text{-}90}$ epitope (Jungbluth et al., 2001b). It was previously reported that anti-NY-ESO-1 antibody E978 showed a positive signal in immunostaining experiments in melanoma that typed negative for NY-ESO-1 and positive for LAGE-1, suggesting the possibility of cross-reaction of anti-NY-ESO-1 antibody to LAGE-1 (Vaughan et al., 2004).

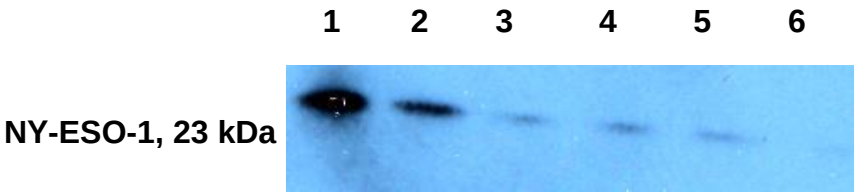

Figure 4.21. Western blot analysis to show the effect of incubation with PBS (Lane 1), scrambled siRNA (Lane 2), siRNA 1 (Lane 3), siRNA 2 (Lane 4), siRNA 3 (Lane 5) and a mixture of the 3 siRNAs (Lane 6) on NY-ESO-1 protein expression in SK-MEL-37 cells (bottom panel). β-actin was used as the loading control to ensure same concentration of protein (20 μg) was loaded onto each well.

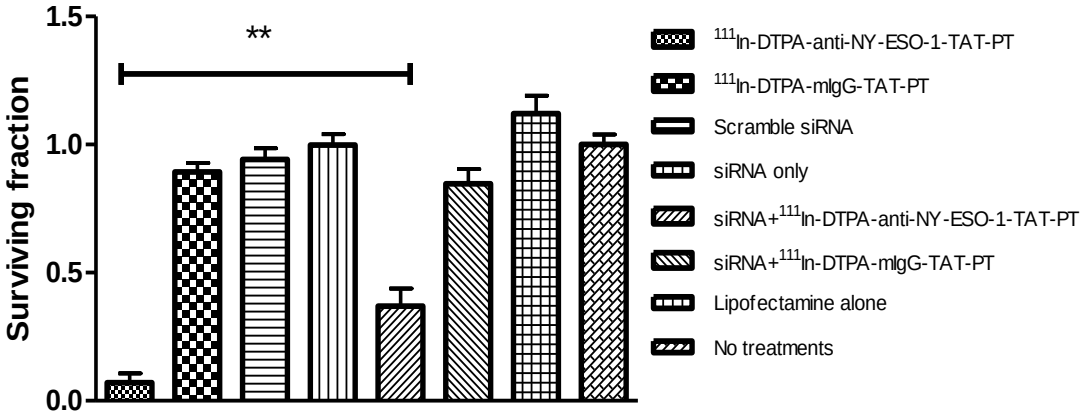

Figure 4.22. Clonogenic survival of SK-MEL-37 cells after exposure to ^{111}In-labelled RICs in the absence and presence of mixtures of three siRNA. Data represent the mean and standard deviation of triplicates from two separate experiments.
**** represents a statistically significant difference ($P < 0.01$, 1 way ANOVA) in survival fraction after ^{111}In-DTPA-anti-NY-ESO-1-TAT-PT treatment in the absence and presence of NY-ESO-1 siRNA.**

4.11. Effect of ^{111}In-DTPA-anti-NY-ESO-1-TAT-PT on γH2AX foci formation in SK-MEL-37 cells

The phosphorylation of Histone H2AX at serine 139, forming γH2AX, occurs in response to DNA double-strand breaks. Immediately after DSB formation, multiple γH2AX molecules accumulate at the site of the damaged DNA, forming a focus for the recruitment of proteins involved in DNA repair and chromatin remodelling (Rogakou et al., 1999, Banáth. and Olive, 2003, Bonner et al., 2008). Therefore, staining for γH2AX using a specific antibody can be used as a marker for DNA DSB.

In general, basal γH2AX expression is high in cancers compared with normal cells due to genomic instability (Martin and Bonner, 2006). In this study, the basal number of γH2AX foci in untreated SK-MEL-37 cells was approximately 10 foci/cell. Hence, during data analysis the number of foci was normalised to basal level in order to allow the effect of treatment with the RICs to be clearly appreciated.

Figures 4.23 and 4.24 illustrate the effect of increasing specific activities and molar concentrations of ^{111}In-labelled RICs on the formation of γH2AX foci in SK-MEL-37 cells. Figure 4.23 shows that an activity dependent increase in γH2AX foci formation was observed following treatment with ^{111}In-DTPA-anti-NY-ESO-1-TAT-PT. This effect was statistically significant compared to untreated cells at specific activities of 1.5 Mq/μg and 3 Mq/μg ($P < 0.001$, 2 way ANOVA). The 3 MBq/μg dose of RIC induced an increase in γH2AX foci comparable to that of the positive control (4 Gy external irradiation). Incubation with the non-specific control, ^{111}In-DTPA-mIgG-TAT-PT, also caused a

significant increase in γH2AX foci formation at the 3 MBq/μg dose ($P < 0.01$, 2 way ANOVA), though the number of foci was substantially lower than that observed with the equivalent dose of antigen specific RIC.

Figure 4.24 shows that a concentration dependent increase in γH2AX foci formation was observed following treatment with ^{111}In-DTPA-anti-NY-ESO-1-TAT-PT. This effect was statistically significant compared to untreated cells at the 200 nM and 400 nM concentrations ($P < 0.01$ and $P < 0.001$ respectively, 2 way ANOVA). However the number of foci did not reach the positive control level. The non-specific control probe ^{111}In-DTPA-mIgG-TAT-PT showed no significant increase in γH2AX foci formation in SK-MEL-37 cells. The results from these experiments correlate with those obtained in the clonogenic survival assays, and suggest that the cytotoxic effect of the antigen specific RIC is mediated via DNA damage.

The rate of γH2AX foci formation and DNA repair can be roughly evaluated by conducting this experiment with 6 different time points ranging from 0 h up to 24 h. However, the basal level of γH2AX foci for SK-MEL-37 was high due to genome instability (discussed in chapter 6), the change in γH2AX foci formation at each time point may not be able to be observed clearly.

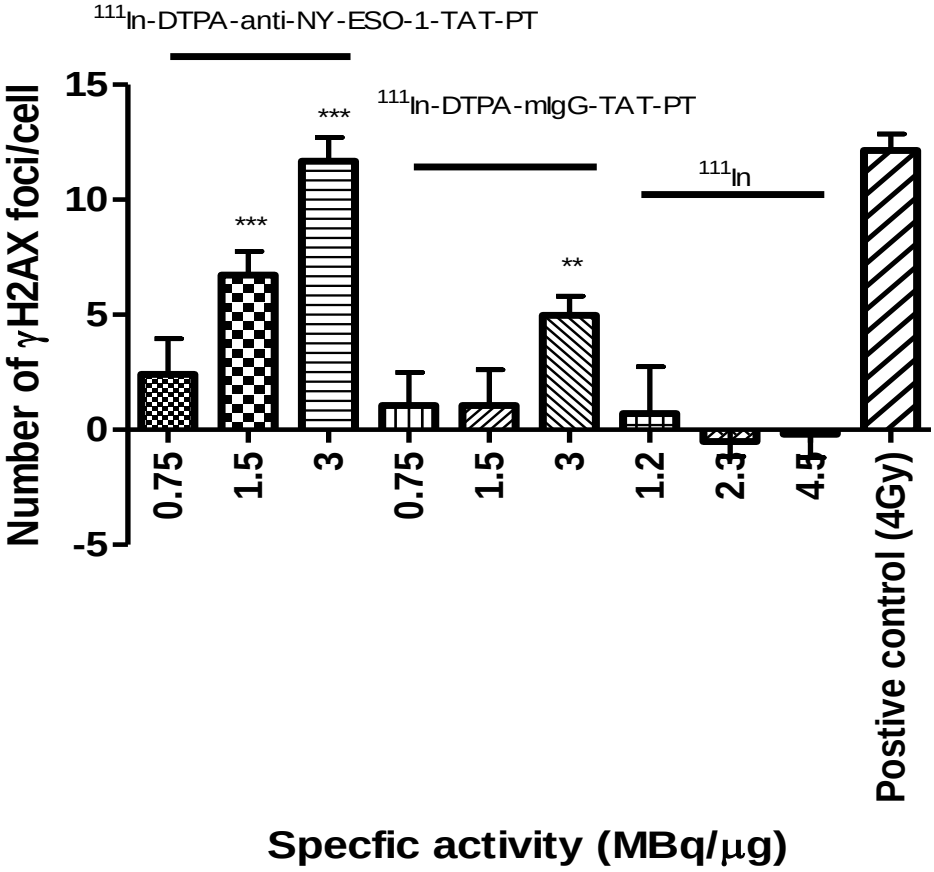

Figure 4.23. Quantification of γH2AX foci in SK-MEL-37 cells following treatment with ^{111}In-labelled RICs of increasing specific activity. Cells exposed to γ-irradiation (4 Gy) were used as a positive control for DNA damage. The γH2AX foci per cell were quantified using the INCell analyser software (GE Healthcare, Pittsburgh, PA) and normalised to untreated controls. Data represent the mean and standard deviation of triplicates from two separate experiments.

**** and *** indicates a statistically significant increase (*P* < 0.01 and *P* < 0.001, 2 way ANOVA) in number of foci/cell compared to untreated controls.**

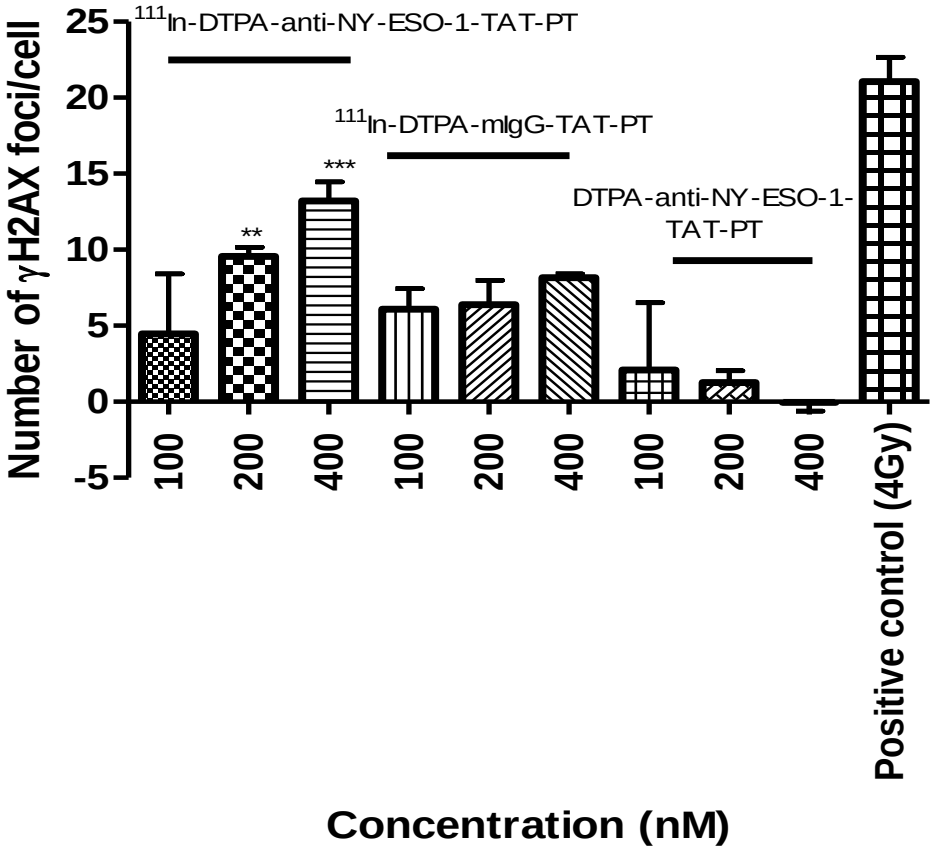

Figure 4.24. Quantification of γH2AX foci in SK-MEL-37 cells following treatment with increasing concentrations of ^{111}In-labelled RICs. Cells exposed to γ-irradiation (4 Gy) were used as a positive control for DNA damage. The γH2AX foci per cell were quantified using the INCell analyser software (GE Healthcare, Pittsburgh, PA) and normalised to untreated controls. Data represent the mean and standard deviation of triplicate samples from two separate experiments.

**** and *** indicates a statistically significant increase (P<0.01 and P<0.001, 2 way ANOVA) in number of foci/cell compared to untreated controls.**

Chapter 5

In Vivo Studies of NY-ESO-1 Targeting Radiopharmaceuticals: Results and Discussion

Chapter 5: *In Vivo* Studies of NY-ESO-1 Targeting Radiopharmaceuticals: Results and Discussion

5.1.Introduction

The previous chapter focused on studying the effects of the ^{123}I- and ^{111}In-labelled radioimmunoconjugates (RIC) in cultured cells *in vitro*. This chapter describes the biodistribution of the ^{111}In-labelled RICs in mice bearing NY-ESO-1 expressing xenografts, to demonstrate and quantify the accumulation of the RICs in tumours *in vivo*.

The ability to target radionuclides to tumours through the use of highly selective monoclonal antibodies suggests that toxicity to the surrounding healthy tissue should be reduced, conferring an advantage over conventional radiotherapy. However, being a systemic treatment, it is possible that the radiolabelled antibody could exert a bystander or crossfire effect, which could potentially affect adjacent cells even if they lack the specific tumour-associated antigen or receptor. It is therefore important to evaluate the distribution of a novel radiotherapeutic in an *viv*o experimental model to gain insight into the precision of tumour targeting. The Balb/c nude strain of mice was chosen for use in this study, because these mice possess a dysfunctional thymus, which reduces the chance of tumour xenografts being rejected by the immune system. Furthermore, Kawashima *et al* demonstrated that SK-MEL-37 cells could form xenografts in this strain of mice (Kawashima et al., 1993).

Two techniques were used to provide data on the biodistribution of RICs in the xenograft model – nano Single Photon Emission Computerised Tomography

(nanoSPECT) and direct measurement of radioactivity in organs. The nanoSPECT works via the same principle as clinical SPECT (discussed in the Introduction), but is designed for use with small animals in a preclinical setting. Images illustrating the location of the radioactivity in the animal were generated by the nanoSPECT scans. These images were uploaded to an analysis software programme, to quantify radioactive signal in specific organs. The nanoSPECT scans were carried out with simultaneous x-ray Computerised Tomography (CT) scans to generate anatomical information to aid organ identification. The second technique of direct measurement simply involved removal of organs at the end of the study period, and quantification of the radioactive signal by counting in a Gamma counter. ^{111}In-labelled RICs were used in the *in vivo* experiments, because the longer decay half-life of ^{111}In compared to ^{123}I meant that SPECT scans could be carried out up to 72 h after dosing.

5.2. Immunohistochemical analysis of NY-ESO-1 antigen expression in SK-MEL-37 and SK-MEL-23 xenografts

Although *in vitro* analysis showed positive staining for NY-ESO-1 protein in SK-MEL-37 cells, it was necessary to confirm expression in SK-MEL-37 xenografts before performing imaging experiments with the RICs, because of the possibility that cellular characteristics could be altered in a complex three dimensional multi-cellular microenvironment (Jacks and Weinberg, 2002). Immunohistochemical analysis confirmed the presence of NY-ESO-1 protein in SK-MEL-37 xenografts (Figure 5.1). Strong positive nuclear immunostaining was observed in a proportion of the NY-ESO-1 expressing cells, indicated by white arrows. However the immnostaining was evenly distributed in both cytoplasm and nucleus in the majority of the cell population, which was in accordance with the results illustrated in Chapter 4. NY-ESO-1 staining was not observed in cells incubated with isotype control primary antibody or with the fluorophore-labelled secondary antibody alone, indicating that the positive staining was not due to non-specific binding of the Fc portion of the primary antibody, or non-specific binding of the secondary antibody.

Figure 5.2 shows that NY-ESO-1 staining was not observed in the SK-MEL-23 xenografts incubated with anti-NY-ESO-1 antibody, isotype control or secondary antibody alone. These results confirm that SK-MEL-23 xenografts do not express NY-ESO-1, which was in accordance with the results illustrated in Chapter 4.

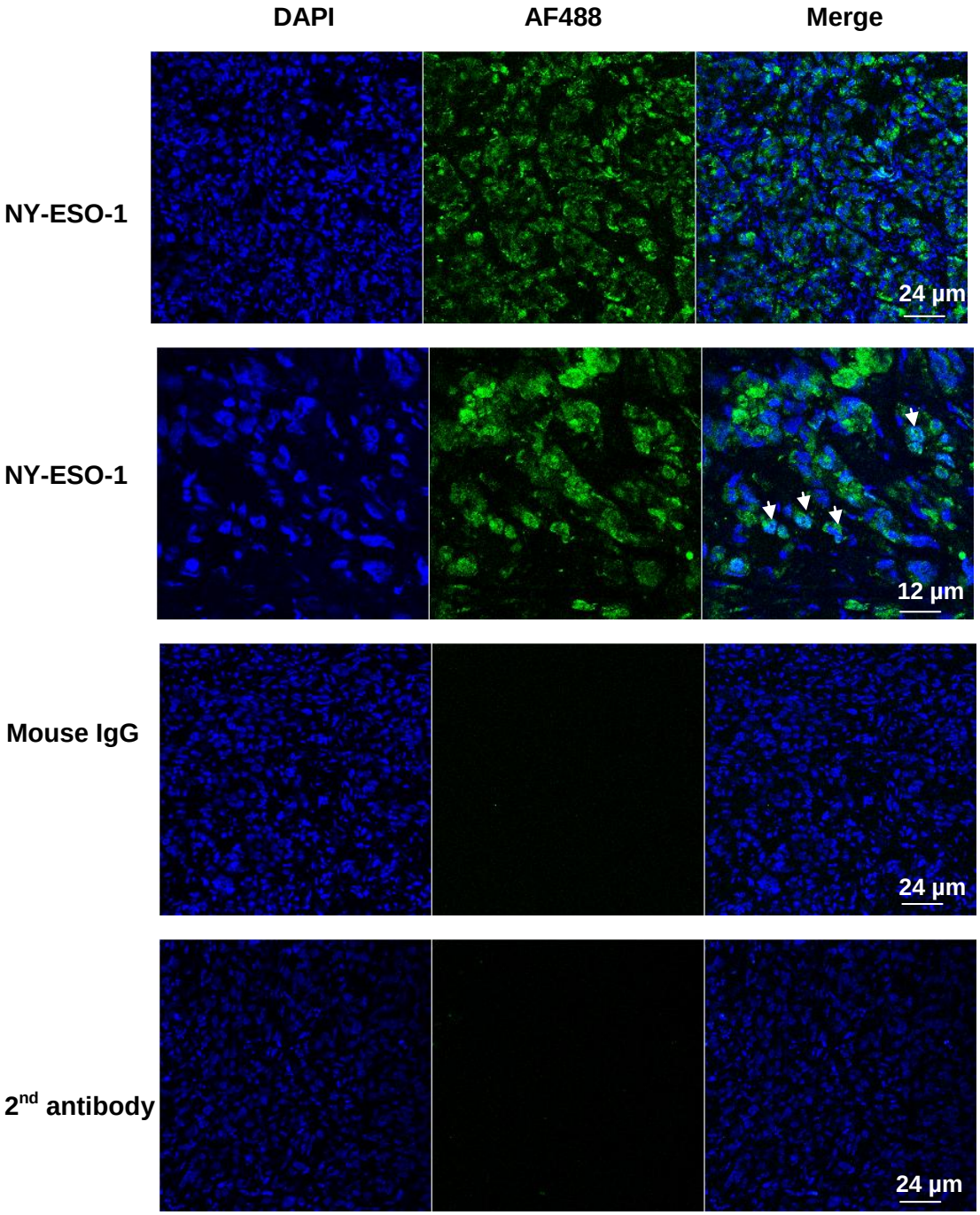

Figure 5.1. Immunohistochemical analysis demonstrating the expression of endogenous NY-ESO-1 protein in SK-MEL-37 xenografts. Tumour was removed from the mouse 72 h p.i. of RIC and frozen in OCT. Tumour sections were cut using a cryostat and stained using a primary antibody against NY-ESO-1 (top and second panels) or a mouse IgG isotype control (third panel), followed by an AF488-labelled rabbit anti-mouse IgG secondary antibody. The fourth panel represents staining with the secondary antibody alone. All images were taken using a confocal microscope (Zeiss). The images above are representative of the tumours harvested from three individual mice.

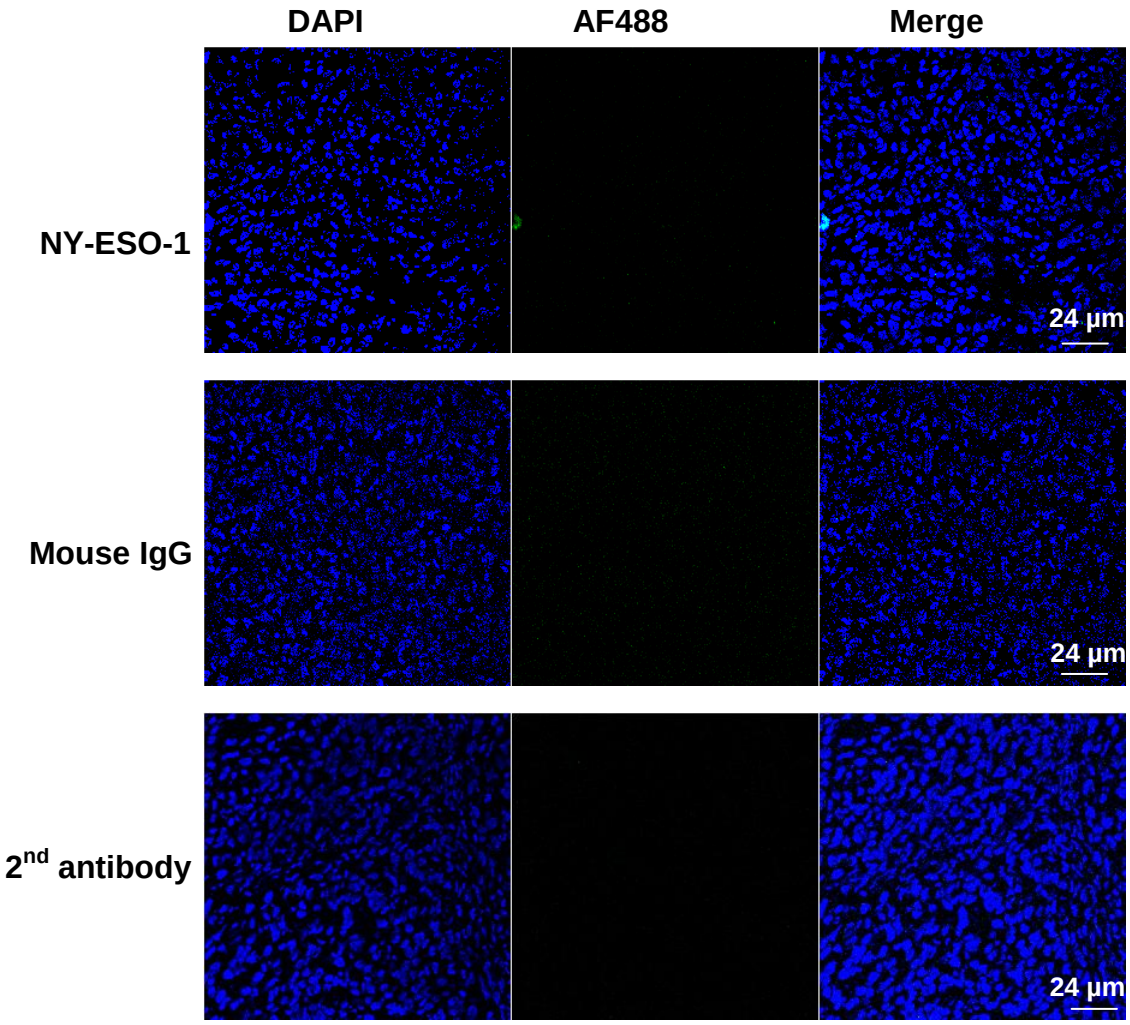

Figure 5.2. Immunohistochemical analysis of endogenous NY-ESO-1 protein expression in SK-MEL-23 xenografts. Tumour was removed from the mouse 72 h p.i. of RICand frozen in OCT. Tumour sections were cut using a cryostat and stained using a primary antibody against NY-ESO-1 (top panel) or a mouse IgG isotype control (middle panel), followed by an AF488-labelled rabbit anti-mouse IgG secondary antibody. The bottom panel represents staining with the secondary antibody alone. All images were taken using a confocal microscope (Zeiss). The images above are representative of the tumours harvested from three individual mice.

5.3. Biodistribution of ^{111}In-DTPA-anti-NY-ESO-1-TAT-PT in BALB/c nude mice

NY-ESO-1 is expressed in the testis as well as in a range of different tumour tissues (Jungbluth et al., 2001b). Therefore, the objective of this experiment was to investigate the distribution of the ^{111}In-DTPA-anti-NY-ESO-1-TAT-PT in the organs of non-tumour bearing Balb/c nude mice, with particular focus on the testes. Mice were scanned using the nanoSPECT/CT at 24 h, 48 h, and 72 h following intravenous injection of ^{111}In-DTPA-anti-NY-ESO-1-TAT-PT and control probe ^{111}In-DTPA-mIgG-TAT-PT (Figure 5.3).

Analysis of the SPECT images was performed by quantification of regions of interest (ROI) at each time point post-injection. The analysis showed that the image intensity of ^{111}In-DTPA-anti-NY-ESO-1-TAT-PT and ^{111}In-DTPA-mIgG-TAT-PT was relatively high in liver, kidney and spleen compared with other organs (Figure 5.4), indicating that both RICs accumulate in these organs. Both RICs were retained in these organs at 72 h, indicating the slow blood clearance typical of whole antibody-based compounds.

Following the acquisition of SPECT/CT images at 72 h post-injection, mice were euthanized and the organs removed. The radioactivity in the organs was measured using a Gamma counter (Figure 5.5). The results from this study confirm that ^{111}In-DTPA-anti-NY-ESO-1-TAT-PT accumulated primarily in the liver and spleen. Importantly, very low uptake of ^{111}In-DTPA-anti-NY-ESO-1-TAT-PT was observed in the testis. This suggests the possibility that the blood testis barrier, often described as Sertoli cell-Sertoli cell tight junction, restricted the passage of the RICs into the testis, despite conjugation to protein transfection reagent and TAT (Mital et al., 2011).

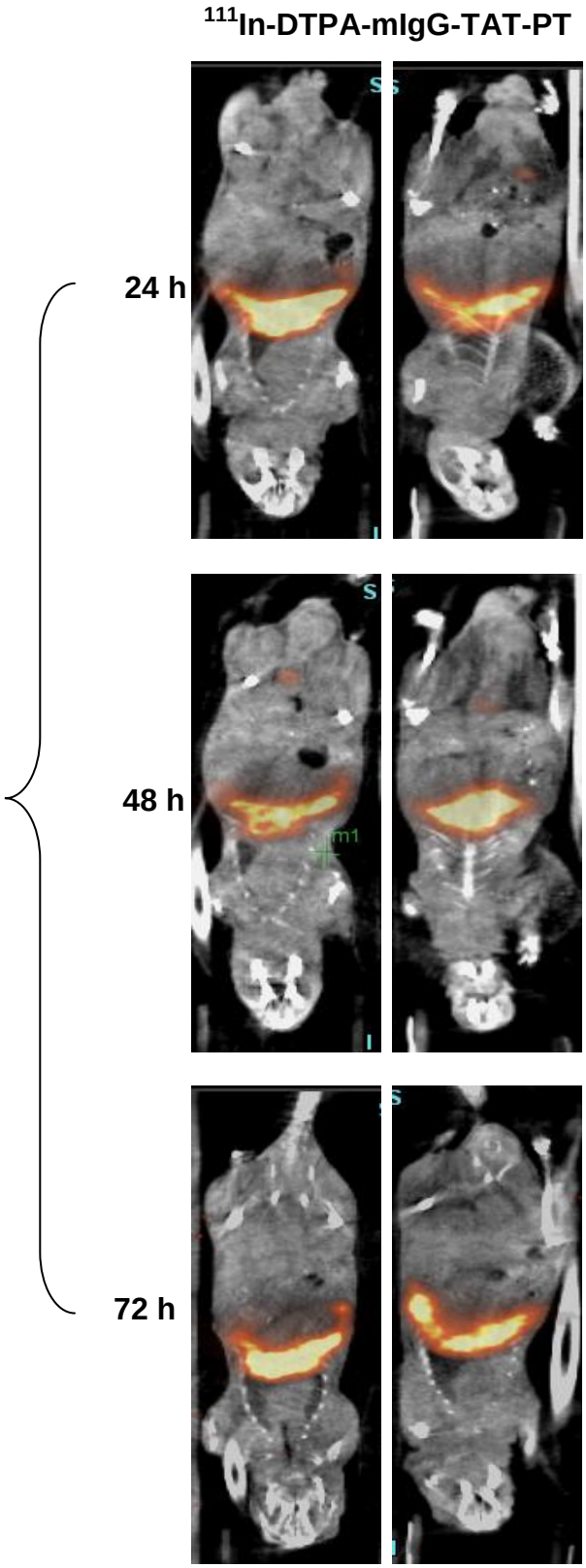
^{111}In-DTPA-mIgG-TAT-PT
24 h
48 h
72 h

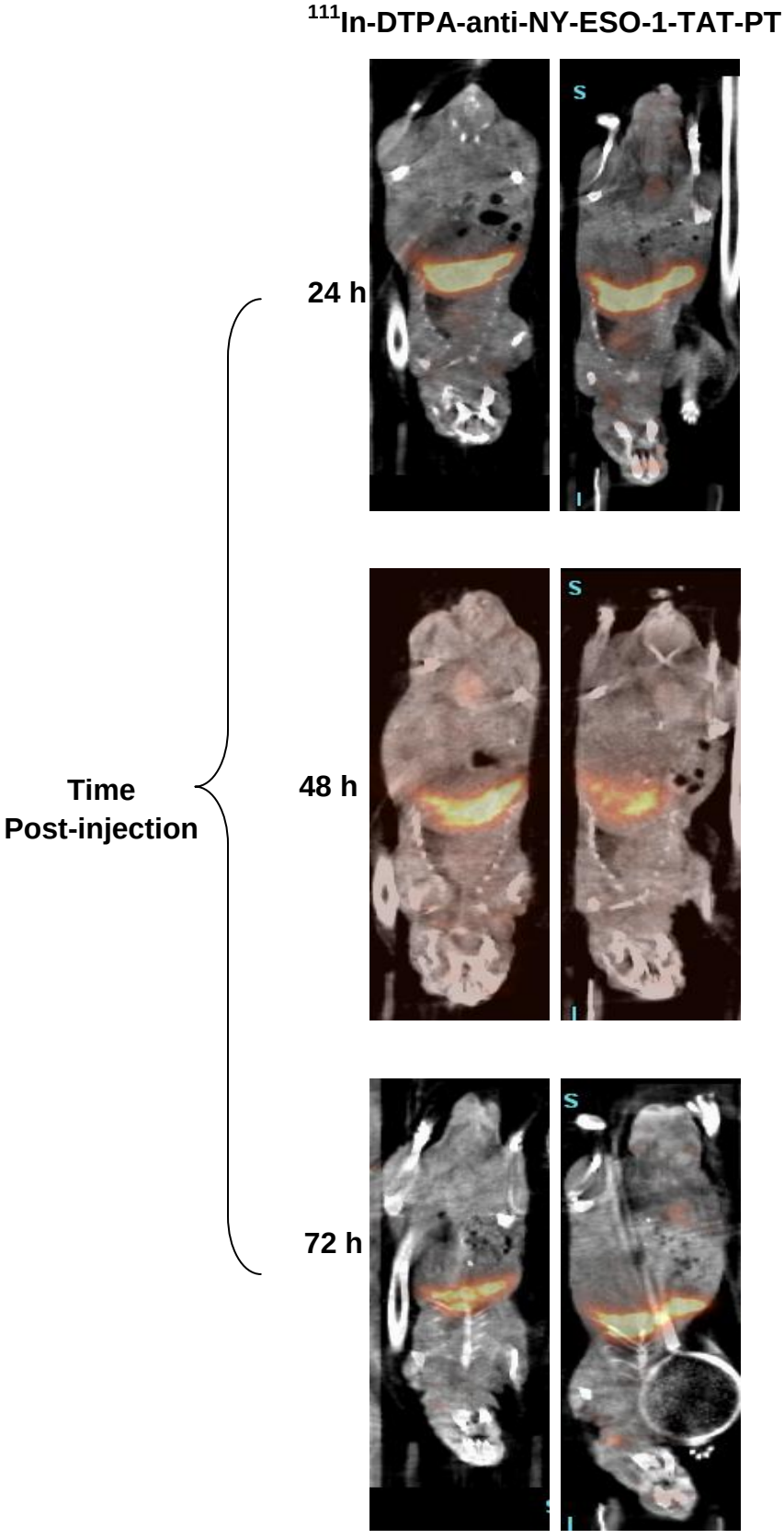

Figure 5.3. The intensity projection SPECT/CT images obtained at 24 h, 48 h and 72 h after tail vein injection of ^{111}In-DTPA-anti-NY-ESO-1-TAT-PT (10 µg, 0.5 MBq /µg), and control probe, ^{111}In-DTPA-mIgG-TAT-PT (10 µg, 0.5 MBq /µg) in Balb/c nude mice. Two mice were used per treatment group. All images at each time are normalised to optimise display using Inveon Research Workspace (Siemens, Erlangen, Germany).

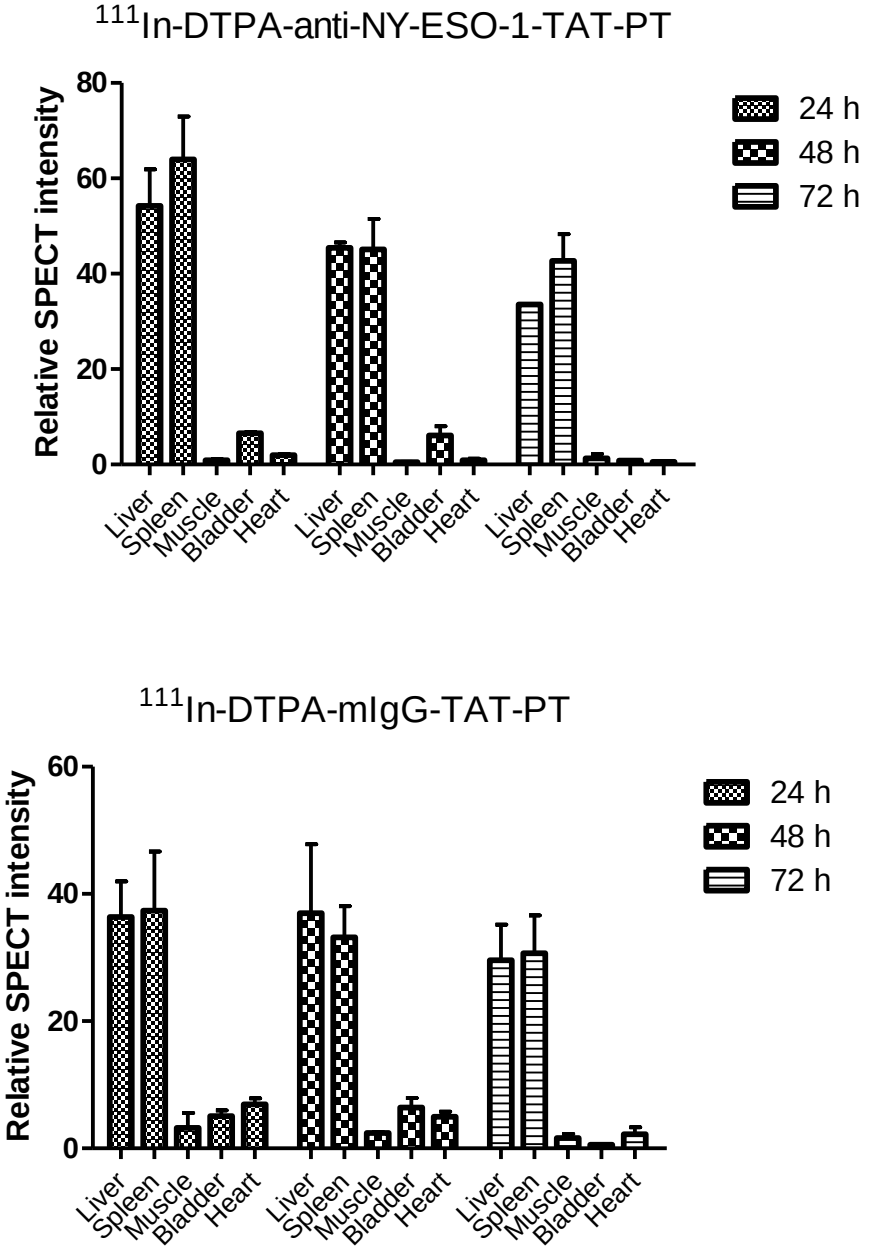

Figure 5.4. Biodistribution of ^{111}In-DTPA-anti-NY-ESO-1-TAT-PT and control probe, ^{111}In-DTPA-mIgG-TAT-PT, in Balb/c nude mice, calculated from SPECT image analysis. The SPECT intensity was calculated by quantification of regions of interest using Inveon Research Workspace software (Siemens, Erlangen, Germany). The relative SPECT intensity was normalised to the amount of radioactivity administered. The bar chart shows mean and standard deviation of data from two mice per treatment group.

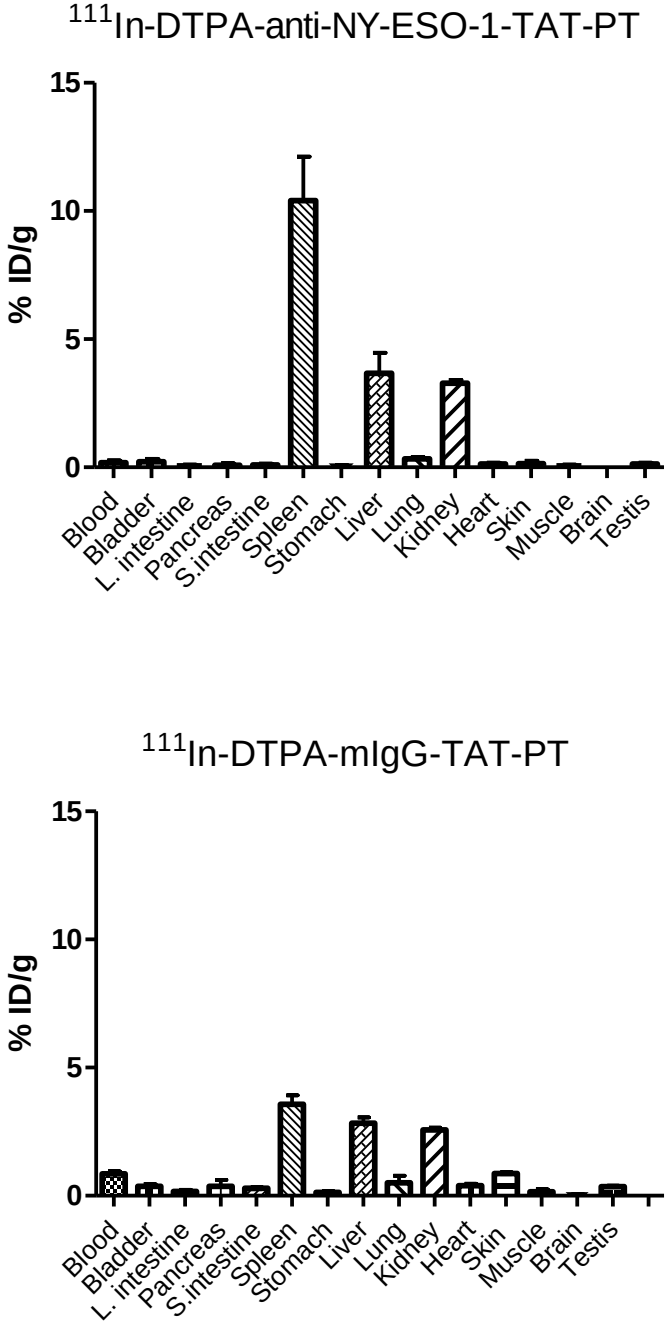

Figure 5.5. Biodistribution of ^{111}In-DTPA-anti-NY-ESO-1-TAT-PT and control probe ^{111}In-DTPA-mIgG-TAT-PT in Balb/c nude mice, calculated by quantification of radioactivity in the organs. Mice were euthanised 72 h after injection of RICs, and the organs removed. Radioactivity in the organs was quantified using a gamma counter and results expressed as % of injected dose per gram (% ID/g). The bar charts show mean and standard deviation of data from two mice per treatment group. ID/g refers to injected dose per gram weight of animal.

5.4. Biodistribution of ^{111}In-DTPA-anti-NY-ESO-1-TAT-PT in BALB/c nude mice bearing NY-ESO-1 negative xenografts

The objective of this experiment was to investigate whether accumulation of ^{111}In-DTPA-anti-NY-ESO-1-TAT-PT would occur in a NY-ESO-1 negative xenograft. To generate NY-ESO-1 negative xenografts, SK-MEL-23 cells were injected subcutaneously into the right flank of BALB/c nude mice. Mice were scanned using the nanoSPECT/CT at 24 h, 48 h, and 72 h following intravenous injection of ^{111}In-DTPA-anti-NY-ESO-1-TAT-PT and control probe, ^{111}In-DTPA-mIgG-TAT-PT (Figure 5.6).

Analysis of the SPECT images was performed by quantification of ROI at each time point post-injection. Consistent with the results highlighted in Section 5.3, the SPECT signal for both RICs was relatively high in liver and spleen (Figure 5.7). Tumour signal was relatively low for both RICs, indicating that they do not accumulate non-specifically in tumour tissue.

Following the acquisition of SPECT/CT images at 72 h post-injection, mice were euthanized and the organs removed. The radioactivity in the organs was measured using a gamma counter (Figure 5.8). The results from this study confirm that the RICs accumulated primarily in the liver and spleen. The data also confirm the relatively low accumulation of the RICs in tumour tissue. One unexpected observation was that there appeared to be higher uptake of the RICs in skin compared to the data obtained in non-tumour bearing mice.

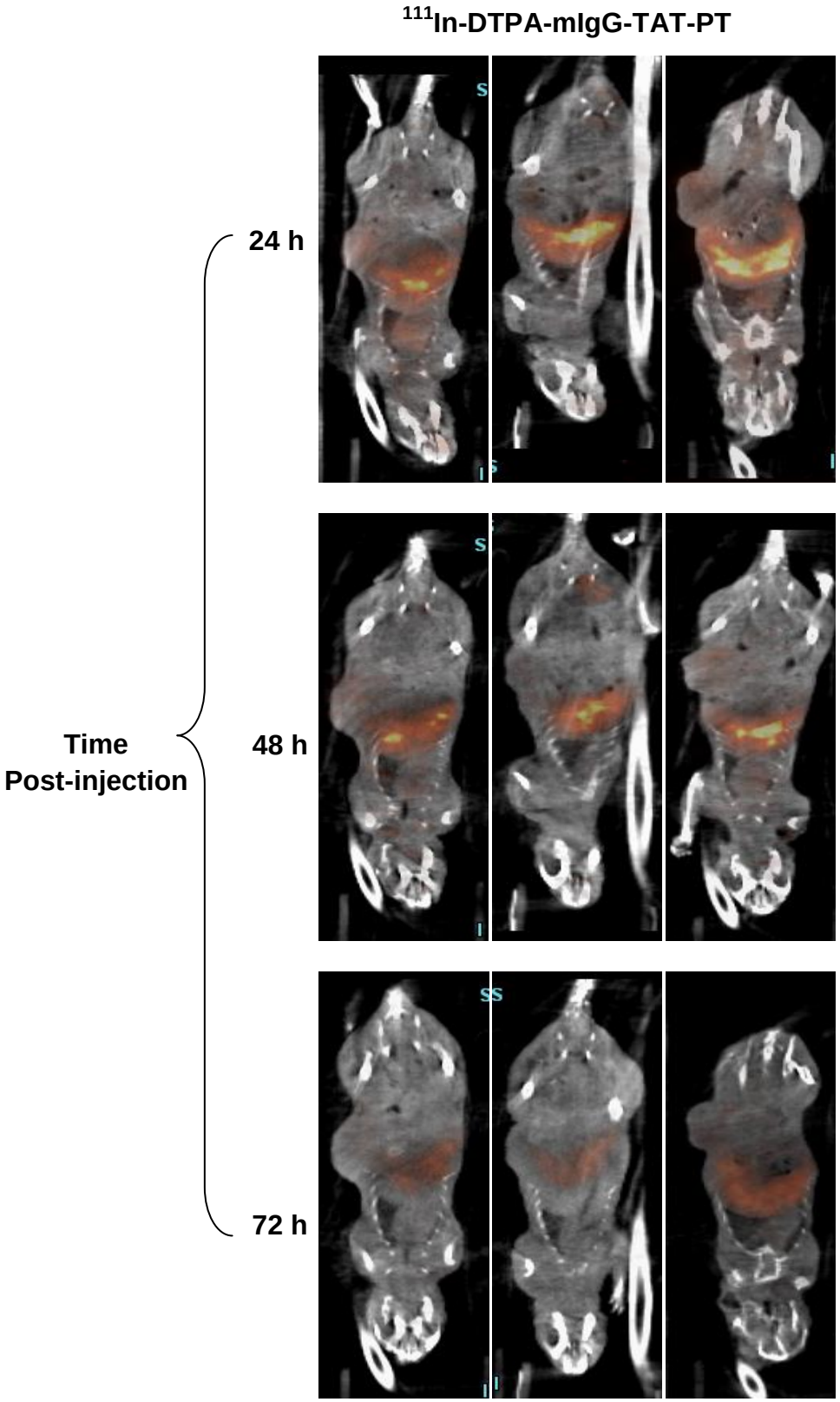
^{111}In-DTPA-mIgG-TAT-PT
Time Post-injection
24 h
48 h
72 h

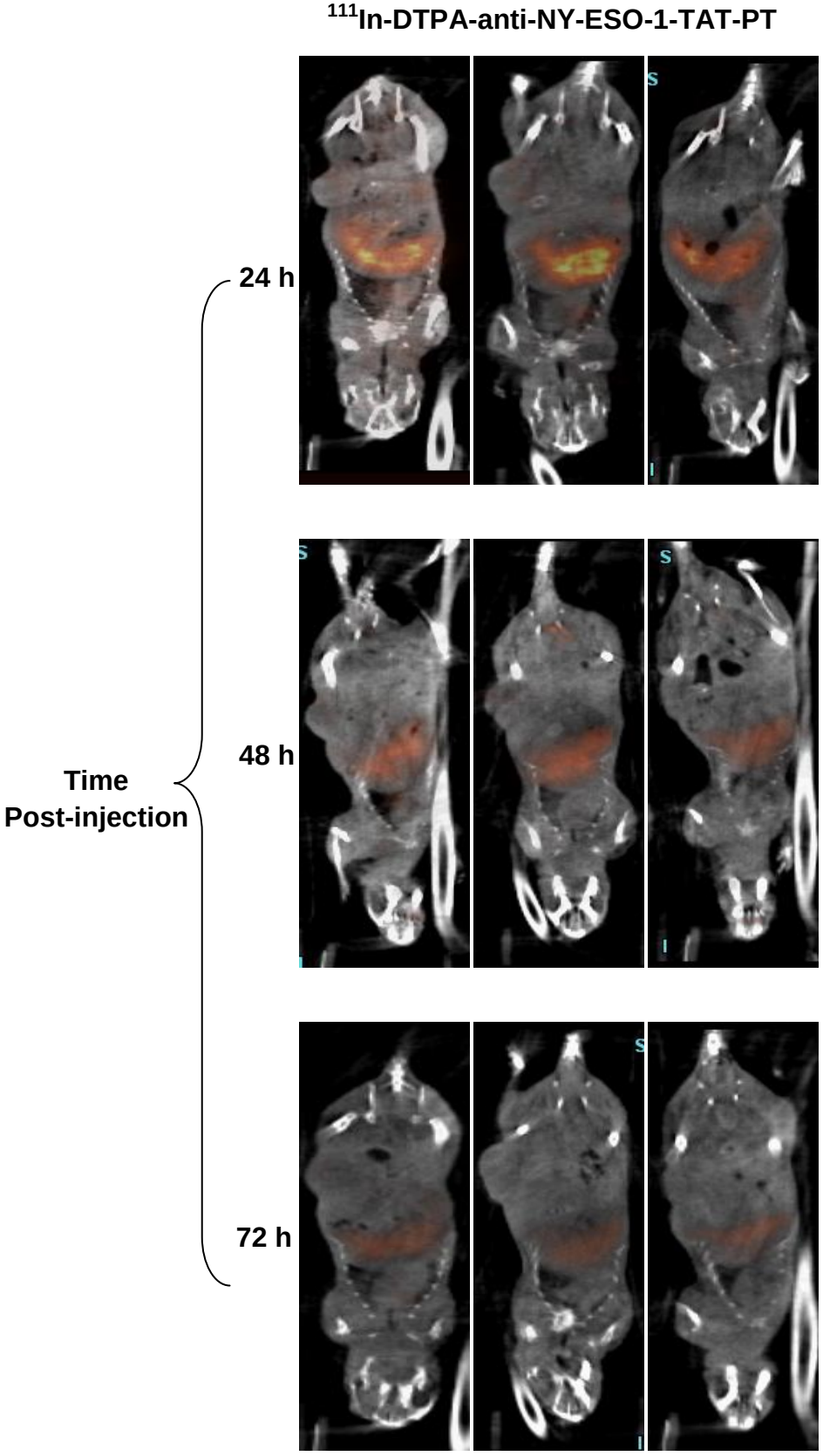

Figure 5.6: The intensity projection SPECT/CT images obtained at 24 h, 48 h and 72 h after tail vein injection ^{111}In-DTPA-anti-NY-ESO-1-TAT-PT (10 µg, 0.5 MBq / µg), and control probe ^{111}In-DTPA-mIgG-TAT-PT (10 µg, 0.5 MBq / µg) in Balb/c nude mice bearing NY-ESO-1 negative xenografts.. 3 mice were used per treatment group. All images at each time are normalised to optimise display using Inveon Research Workspace (Siemens, Erlangen, Germany).

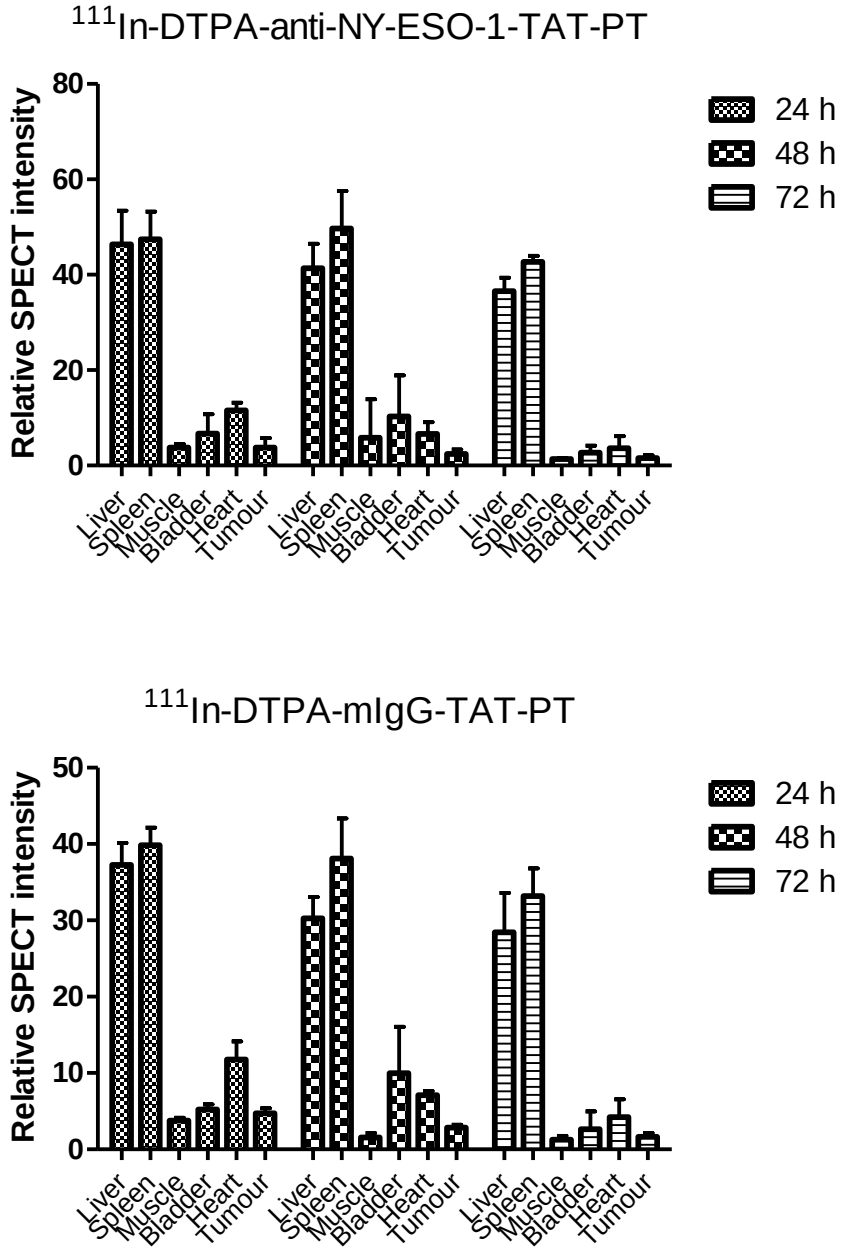

Figure 5.7: Biodistribution of ^{111}In-DTPA-anti-NY-ESO-1-TAT-PT and control probe ^{111}In-DTPA-mIgG-TAT-PT in Balb/c nude mice bearing NY-ESO-1 negative xenografts, calculated from SPECT image analysis. The SPECT intensity was calculated by quantification of regions of interest using Inveon Research Workspace software (Siemens, Erlangen, Germany). The relative SPECT intensity was normalised to the amount of radioactivity administered. The bar charts show mean and standard deviation of data from 3 mice per treatment group.

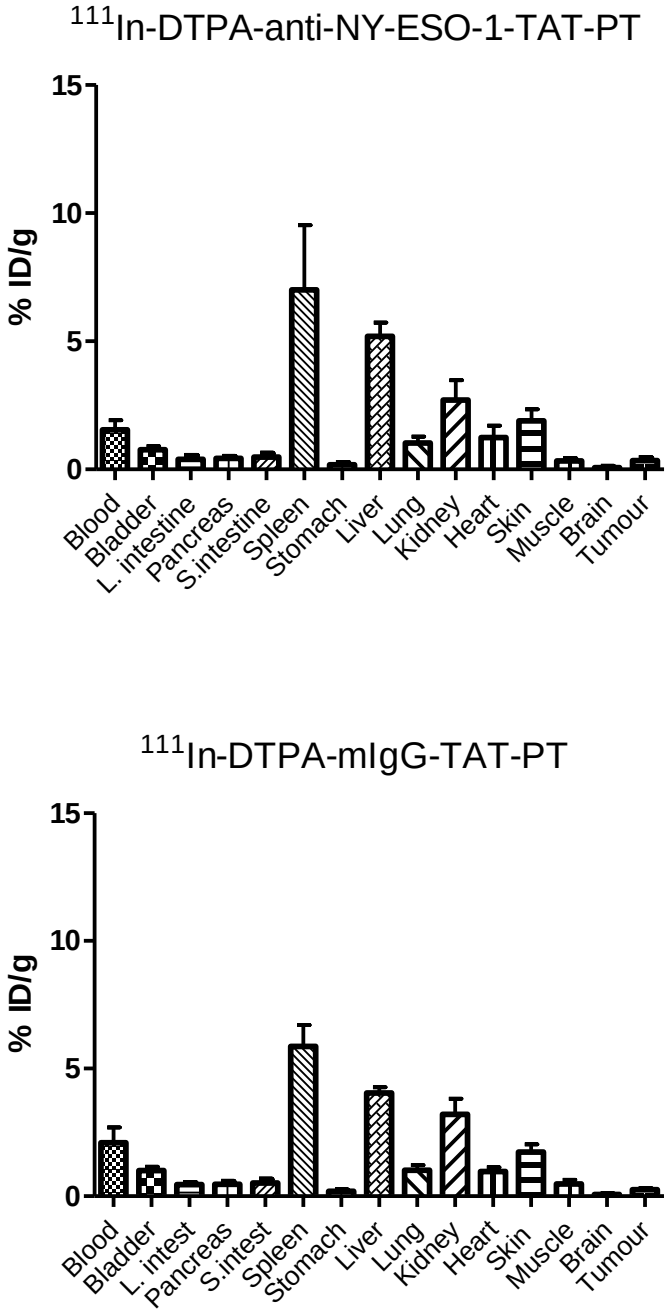

Figure 5.8: Biodistribution of ^{111}In-DTPA-anti-NY-ESO-1-TAT-PT and ^{111}In-DTPA-anti-mIgG-TAT-PT in Balb/c nude mice bearing NY-ESO-1 negative xenografts, calculated by quantification of radioactivity in the organs. Mice were culled 72 h after injection of RICs, and the organs removed. Radioactivity in the organs was quantified using a Gamma counter and results expressed as % of injected dose per gram. The bar charts show mean and standard deviation of data from 3 mice per treatment group. ID/g refers to injected dose per gram weight of animal.

5.5. Biodistribution of ^{111}In-DTPA-anti-NY-ESO-1-TAT-PT in BALB/c nude mice bearing NY-ESO-1 expressing xenografts

The objective of this experiment was to investigate whether ^{111}In-DTPA-anti-NY-ESO-1-TAT-PT accumulates in NY-ESO-1 expressing xenografts. To generate NY-ESO-1 positive xenografts, SK-MEL-37 cells were injected subcutaneously into the right flank of BALB/c nude mice. Mice were scanned using the nanoSPECT/CT at 24 h, 48 h, 72 h and 120 h following intravenous injection of ^{111}In-DTPA-anti-NY-ESO-1-TAT-PT and control probe, ^{111}In-DTPA-mIgG-TAT-PT (Figure 5.9). Accumulation of radioactivity in tumours was clearly detectable in 2 out of 3 mice at 48 h and 72 h after injection with ^{111}In-DTPA-anti-NY-ESO-1-TAT-PT (indicated by red circles in Figure 5.9), whereas the control probe did not accumulate in tumours at any time points.

Analysis of the SPECT images was performed by quantification of regions of interest at the 24 h, 48 h and 72 h time points post-injection (Figure 5.10). At the 120 h time point, the signal was too low to be quantified, which was considered to be due to the decay of the ^{111}In radionuclide and clearance of the probe from the blood circulation. Consistent with the results highlighted in Sections 5.3 and 5.4, the SPECT signal for both RICs was relatively high in liver and spleen. The SPECT intensity in the tumour after injection with ^{111}In-DTPA-anti-NY-ESO-1-TAT-PT was higher than that in the muscle, heart and bladder at 48 h ($P < 0.05$, 1 way ANOVA) and 72 h post injection ($P < 0.01$, 1 way ANOVA), whereas after administration of the control probe, signal intensity in the tumour was comparable to that in the muscle, heart and bladder. Further evidence of the accumulation of the ^{111}In-DTPA-anti-NY-ESO-1-TAT-PT probe in the tumour was provided by calculation of the tumour to muscle ratio for both probes. The tumour to muscle

ratio of ^{111}In-DTPA-anti-NY-ESO-1-TAT-PT was significantly higher than that of ^{111}In-DTPA-mIgG-TAT-PT at 24, 48 and 72 h post injection ($P < 0.01$, $P < 0.001$, $P < 0.001$ respectively, 2 way ANOVA).

Following the acquisition of SPECT/CT images at 120 h post-injection, mice were euthanized and the organs removed. The radioactivity in the organs was measured using a gamma counter (Figure 5.11). The results from this study were consistent with the previous data generated in non-tumour bearing and NY-ESO-1 negative tumour bearing mice as radiolabelled probes were observed to accumulate primarily in the liver and spleen. The uptake of ^{111}In-DTPA-anti-NY-ESO-1-TAT-PT and ^{111}In-DTPA-mIgG-TAT-PT by tumour at 120 h post-injection was 1.50 % ± 0.08% ID/g and 0.083 % ± 0.008% ID/g respectively, which further confirmed the increased tumour uptake of the antigen specific ^{111}In-DTPA-anti-NY-ESO-1-TAT-PT compared to the control probe.

It should be pointed out that these data are considered preliminary at this point, and a further study carried out in a larger number of mice is planned, with the aim of providing conclusive evidence of the accumulation of the antigen specific RIC into NY-ESO-1-positive xenografts. However this study provides promising indications that NY-ESO-1 expression is a major determinant of ^{111}In-DTPA-anti-NY-ESO-1-TAT-PT uptake of into tumours.

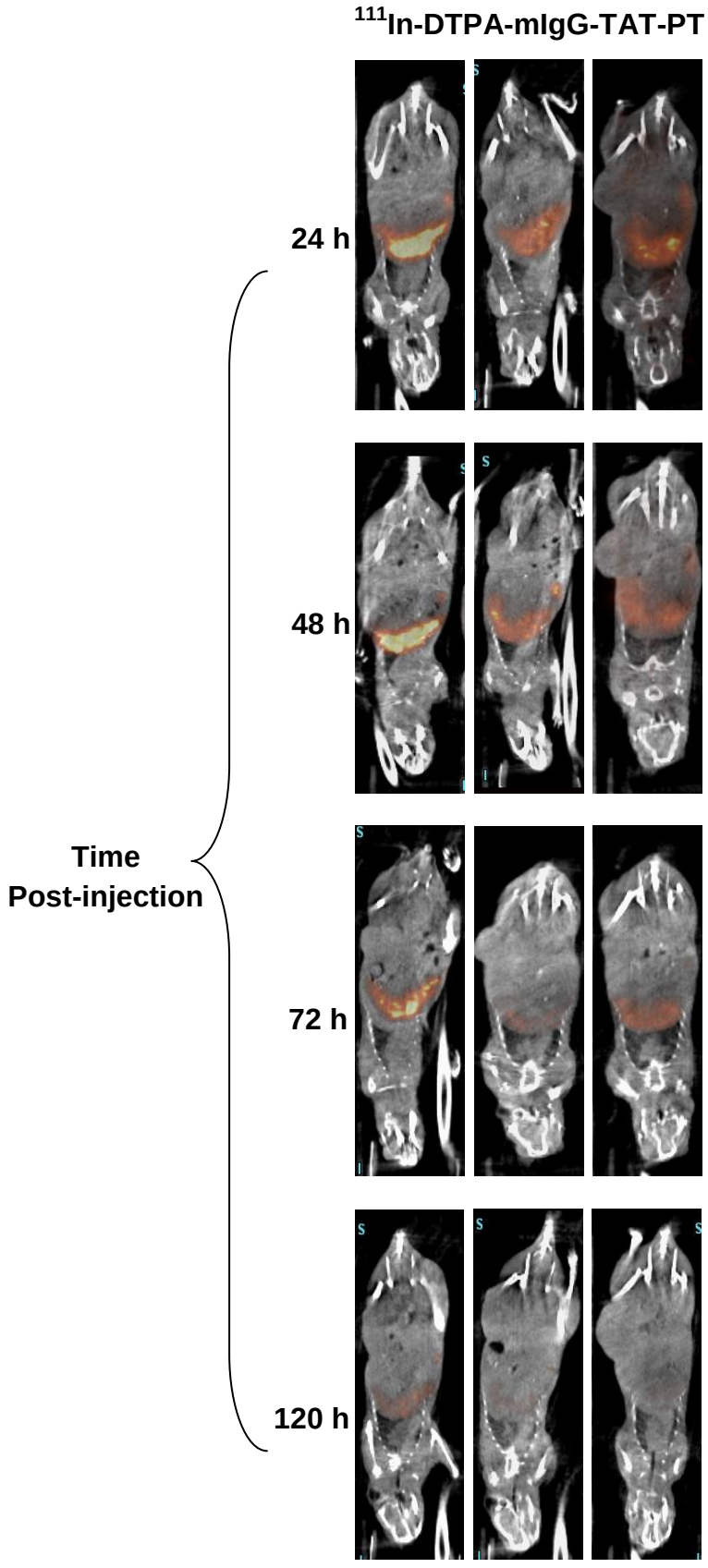
^{111}In-DTPA-mIgG-TAT-PT
24 h
48 h
72 h
120 h
Time
Post-injection

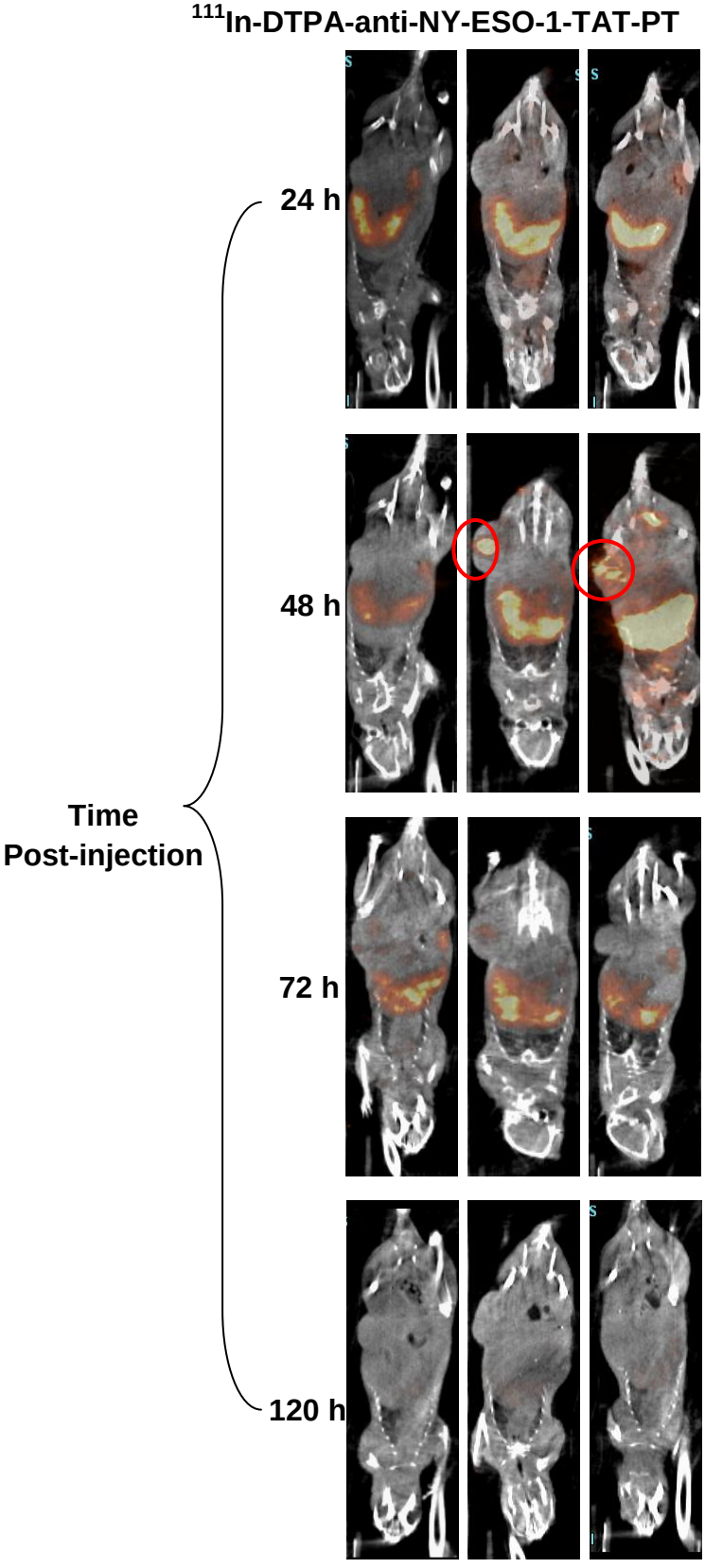

Figure 5.9. The intensity projection SPECT/CT images obtained at 24 h, 48 h, 72 h and 120 h after tail vein injection ^{111}In-DTPA-anti-NY-ESO-1-TAT-PT (10 µg, 0.5 MBq/µg), and control probe ^{111}In-DTPA-mIgG-TAT-PT (10 µg, 0.5 MBq/µg) in BALB/c nude mice bearing NY-ESO-1 expressing xenografts. 3 mice were used per treatment group. All images at each time are normalised to optimise display using Inveon Research Workspace (Siemens, Erlangen, Germany).

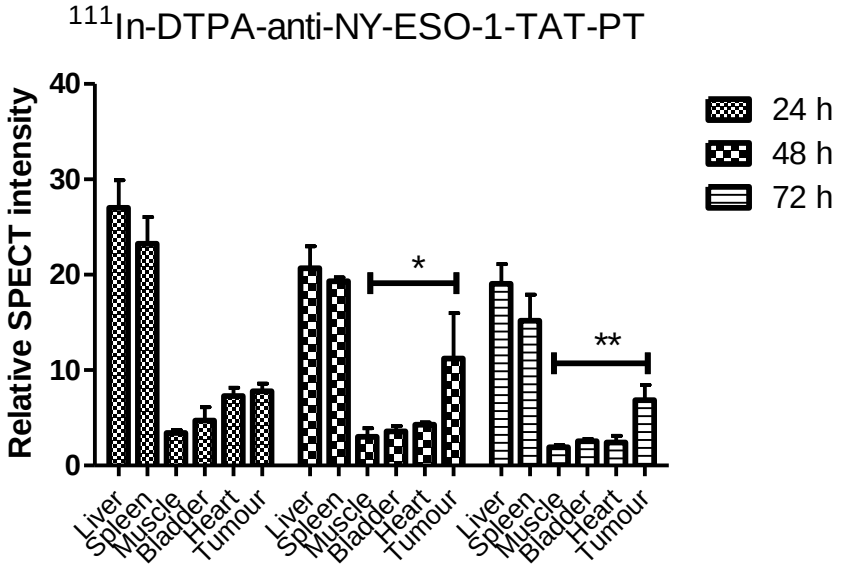
111In-DTPA-anti-NY-ESO-1-TAT-PT
Relative SPECT intensity
40
30
20
10
0
24 h
48 h
72 h
*
**
Liver
Spleen
Muscle
Bladder
Heart
Tumour

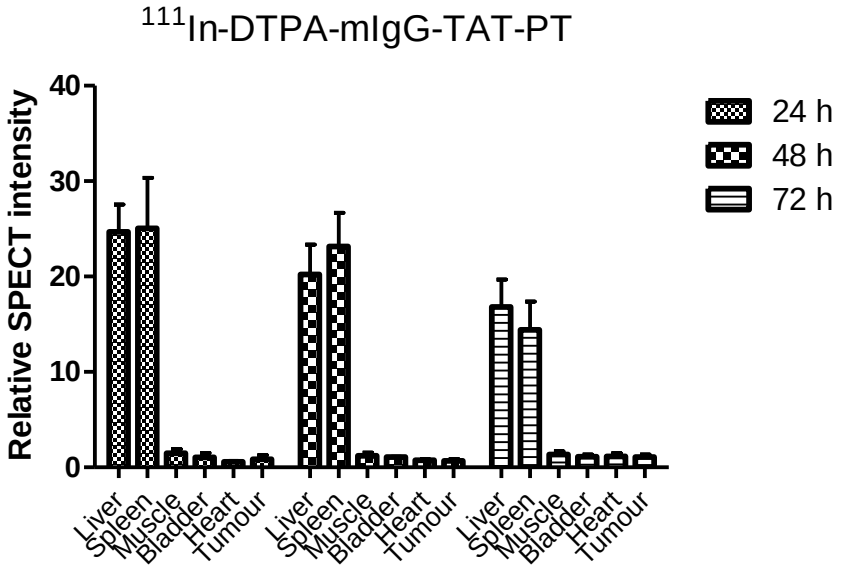
111In-DTPA-mIgG-TAT-PT
Relative SPECT intensity
40
30
20
10
0
24 h
48 h
72 h
Liver
Spleen
Muscle
Bladder
Heart
Tumour

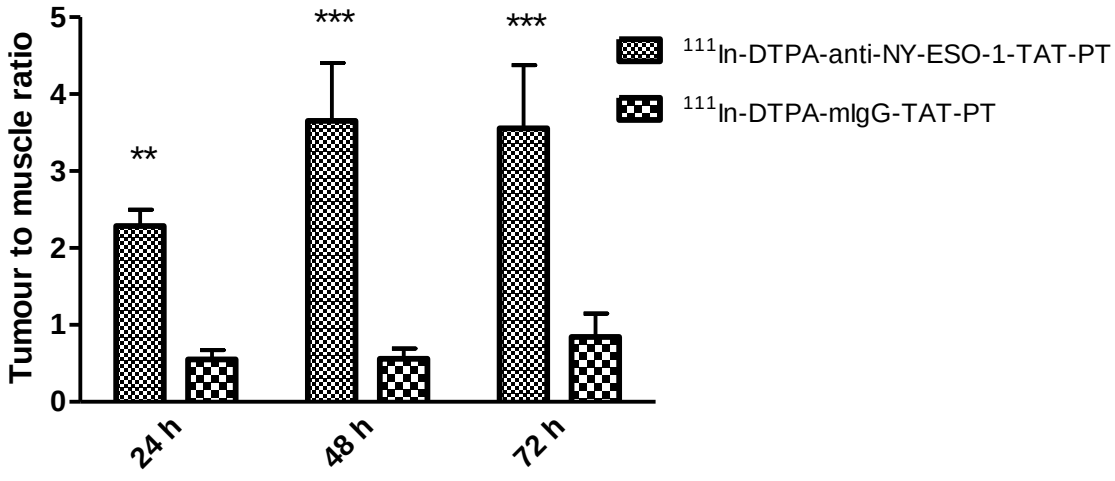

Figure 5.10. Biodistribution of ^{111}In-DTPA-anti-NY-ESO-1-TAT-PT and control probe, ^{111}In-DTPA-mIgG-TAT-PT, in Balb/c nude mice bearing NY-ESO-1 positive xenografts, calculated from SPECT image analysis (top and middle). Tumour to muscle ratios of ^{111}In-DTPA-anti-NY-ESO-1-TAT-PT and control probe, ^{111}In-DTPA-mIgG-TAT-PT, in Balb/c nude mice bearing NY-ESO-1 positive xenografts (bottom). The SPECT intensity was calculated by quantification of ROI using Inveon Research Workspace software (Siemens, Erlangen, Germany). The relative SPECT intensity was normalised to the amount of radioactivity administered. The bar charts show mean and standard deviation of data from three mice per treatment group. 24, 48 and 72 h post injection ($P < 0.01$, $P < 0.001$, $P < 0.001$ respectively, 2 way ANOVA)

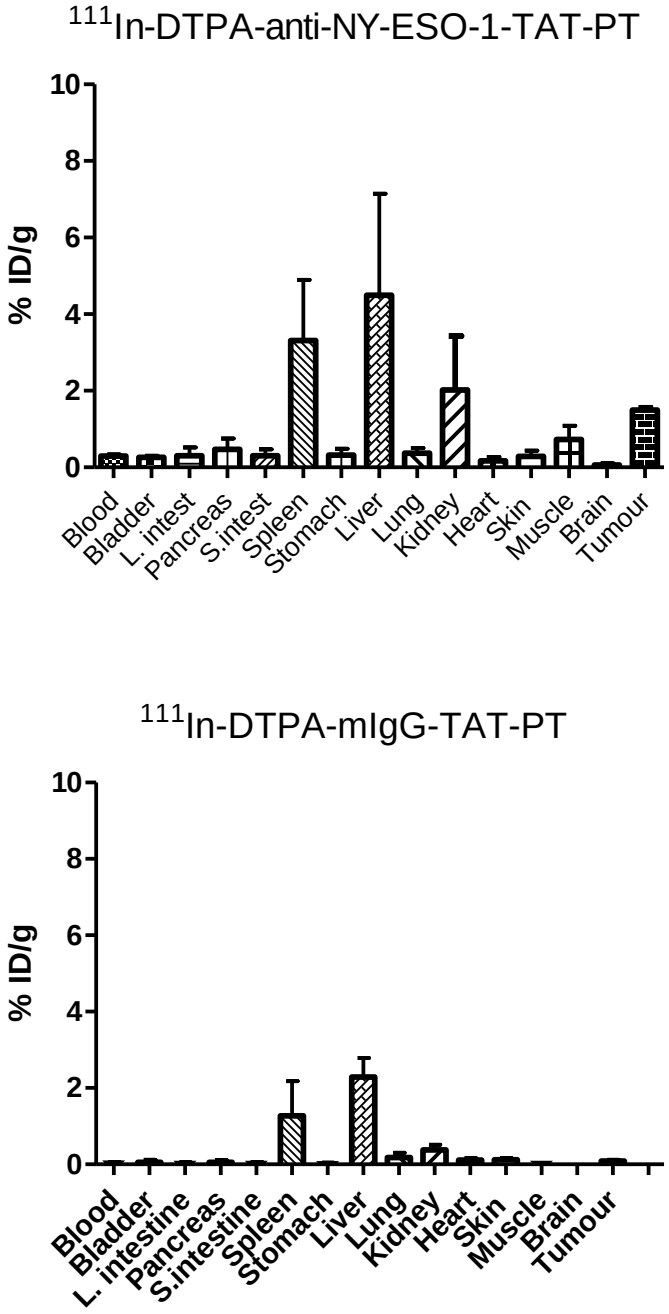

Figure 5.11. Biodistribution of ^{111}In-DTPA-anti-NY-ESO-1-TAT-PT and ^{111}In-DTPA-mIgG-TAT-PT in Balb/c nude mice bearing NY-ESO-1 positive xenografts, calculated by quantification of radioactivity in the organs. Mice were culled 120 h after injection of radioimmunoconjugates, and the organs removed. Radioactivity in the organs was quantified using a gamma counter and results expressed as % ID/g. The bar charts show mean and standard deviation of data from three mice per treatment group. ID/g refers to injected dose per gram weight of animal.

5.6. Discussion

Uptake of the RICs in liver and spleen was observed in all biodistribution experiments. Studies in the published literature have demonstrated that the choice of metal chelator used in the radiolabelling process may influence uptake of ^{111}In in the liver, possibly due to conformational change in the antibody conjugate (Knogler et al., 2006). In one study, the uptake of the radioactivity was reduced from 17 % to 9 % ID/g by conjugating the antibody to SCN-Bn-DTPA rather than cDTPA prior to radiolabelling (Esteban et al., 1987). Moreover, Fc receptors expressed by Kupffer cells, a type of macrophage cell located in the liver, were shown to be responsible for eliminating the IgG type antibodies in cooperation with liver endothelial cells (Lovdal et al., 2000). In mice, the spleen stores a large population of monocytes, which can be transformed into dendritic cells or macrophages upon injury, and the spleen also plays an important role in lymphocyte and macrophage homing (Swirski et al., 2009, Krause et al., 2012). Therefore, it is possible that RICs were engulfed by macrophages via Fc receptor binding, and were transported to the spleen, leading to the accumulation of radioactivity in this organ.

Accumulation of the RICs was also observed in the kidney, which is consistent with published data using RICs for imaging. For example, a biodistribution study of ^{111}In-labelled anti-p27-TAT, showed that uptake in the kidney was nearly 9% of ID/g (Cornelissen et al., 2009). The accumulation of radioactivity in the kidney is likely a result of free ^{111}In, released due to the instability of binding between ^{111}In and cDTPA. ^{111}In can be bound by transferrin and transported to the kidney (Schuhmacher et al., 1990). The slow blood clearance of the RICs could be due to the fact that large IgG molecules are difficult to filter through the glomerular

membrane, thereby prolonging the retention of RICs in the circulation (Vegt et al., 2010). Intact IgG antibodies can be engineered into smaller fragments including Fab (50 kDa), $F(ab)_2$ (100 kDa), single chain variable fragments (~ 30 kDa), diabodies (~ 60 kDa) and minibodies (~ 80 kDa), which have more rapid blood clearance. However, an accelerated blood clearance and removal of the Fc portion should be carefully weighed, as the Fc portion is important in initiating antibody-dependent cell-mediated cytotoxicity (ADCC), and rapid clearance of probes from blood could reduce the potency for cancer treatments.

The preliminary data generated in the SK-MEL-37 xenograft experiment indicates that accumulation of the antigen-specific RIC in tumours occurs *in vivo*. This will be investigated further in a subsequent study.

Chapter 6

Discussion

Chapter 6: Discussion

6.1. NY-ESO-1 and targeted immunotherapy

Antibodies recognise the cognate antigen with exquisite specificity, and this characteristic has been exploited in the development of antigen specific monoclonal antibodies for therapeutic applications. Conjugation of radionuclides to monoclonal antibodies (mAb) led to the development of ^{90}Y-ibritumomab tiuxetan (Biogen IDEC) and ^{131}I-tositumomab (GlaxoSmithKline), both of which have been approved by the Food and Drug Administration (FDA) for the treatment of refractory or relapsed low-grade, follicular, or transformed B-cell non-Hodgkin's lymphoma (NHL) (Jacene et al., 2007). These antibodies bind to the CD20 antigen on the surface of malignant B cells, and the radionuclides induce DNA damage.

NY-ESO-1 is a member of a class of molecules termed cancer testis antigens. These molecules are normally only expressed in human germ cells, but are also expressed in a wide range of tumour derived from different tissues (Simpson et al., 2005). The expression of NY-ESO-1 protein in tumour cells but not in other somatic cells makes it an ideal target for radioimmunotargeting approaches. However NY-ESO-1, like the majority of tumour antigens identified to date [2-4], is an intracellular protein that is found exclusively in the cytoplasm and nucleus, hindering it from being a potential candidate for conventional mAb therapy. This thesis explores the possibility of targeting NY-ESO-1 by conjugation of a monoclonal antibody against NY-ESO-1 to the cell-penetrating peptide, TAT, which extends the application of targeted mAb therapy to intracellular molecules.

6.2. Synthesis of radiopharmaceuticals

Efficient conjugation of the cell-penetrating peptide, TAT, to antibody can be achieved using 1-Ethyl-3-(3-dimethylaminopropyl) carbodiimide hydrochloride (EDC), which results in activation of carboxyl groups for direct reaction with primary amines via amide bond formation. *N*-hydroxysulfosuccinimide (Sulfo-NHS) is added along with EDC to improve coupling efficiency by creating dry-stable amine-reactive intermediates. Consideration was given to the number of molecules of TAT that would bind to one molecule of antibody. There is a lack of published data on this issue, and it was necessary to achieve efficient TAT-mediated nuclear translocation without disruption of the antigen-binding site on the antibody. The final experimental conditions involved incubation of 12-fold molar excess of TAT with anti-NY-ESO-1 monoclonal antibody for 2 h, achieving 2-3 molecules of TAT conjugated to one molecule of antibody. TAT conjugation did not affect the binding affinity of anti-NY-ESO-1-TAT antibody, as demonstrated by competitive binding assays. Attempts at conjugation of 2-(4-isothiocyanatobenzyl)-diethylenetriaminepentaacetic acid (*p*-SCN-Bn-DTPA) to anti-NY-ESO-1-TAT, to allow subsequent ^{111}In-labelling, were unsuccessful, which was surprising given that the use of this technique is well documented in the literature (Mirzadeh et al., 1990, Reilly et al., 1992, Pham et al., 1995, Cornelissen et al., 2011a). It is possible that the conjugation efficiency was reduced by steric hindrance due to the large BnDTPA molecule, or that the BnDTPA was subject to hydrolysis. Because of the difficulties experienced in conjugating BnDTPA to anti-NY-ESO-1 antibody, an alternative strategy using an oxidant instead of a metal chelator was used in radiolabelling antibody at the beginning of this project.

During the method development process, it was discovered that cyclic DTPA (cDTPA) anhydride could be successfully conjugated to anti-NY-ESO-1-TAT, allowing the antibody to be labelled with ^{111}In. The limitations of the use of cDTPA are that the antibody conjugate is less stable, and interaction between the multiple free carboxyl groups on DTPA and the lysine groups on antibodies can bring two antibodies into close proximity (Arano et al., 1996, Reilly et al., 1992).

6.3. Delivery of radiolabelled anti-NY-ESO-1-TAT across the cell membrane

Cell-penetrating peptides (CPPs) are one of the widely used strategies for intracellular delivery of various cargoes such as proteins, peptides, antibodies, genes and nanoparticles, due to their low toxicity and independence of membrane receptor and cell type. TAT, a CPP derived from the transcription transactivating protein encoded by human immunodeficiency virus (HIV), has been shown to be capable of penetrating the cell membrane. TAT possesses a nuclear localisation sequence, an important property for use in this study, as the ^{111}In-anti-NY-ESO-1-TAT must be delivered to the nucleus for the Auger electron emitters, ^{111}In and ^{123}I, to cause maximum cytotoxicity. Previous studies using ^{111}In-labelled EGF have demonstrated that the radiation-absorbed dose to the nucleus is 2-fold and 35-fold greater when ^{111}In decays in the nucleus rather than in the cytoplasm or on the cell surface (Reilly et al., 2000). TAT conjugation has been reported to improve cellular uptake of antibodies both *in vitro* and *in vivo*. Therefore TAT conjugation offers a means to specifically target intracellular epitopes in tumour cells for radiotherapeutic or diagnostic applications.

After successful development of the ^{111}In-anti-NY-ESO-1-TAT radioimmunoconjugate (RIC)**,** it was necessary to determine if it would internalise into the NY-ESO-1 expressing cell line, SK-MEL-37, *in vitro*. However, the

results clearly indicated that conjugation of TAT to ^{123}I-labelled anti-NY-ESO-1 antibody did not significantly enhance cellular uptake. It was previously reported that heparan sulfate proteoglycans on the cell surface play an important role in translocation of molecules across cell membrane by interacting with CPPs. Syndecan-4 (SDC-4), a heparan sulfate proteoglycan present on the cell surface, was shown to be associated with cationic CPPs such as TAT, suggesting that TAT acts as a ligand for SCD-4 during the translocation process. In the literature, low levels of cellular uptake of TAT were observed in the K562 myelogenous leukemia cell line, which does not express heparin sulphate proteoglycans. Transfection of SDC-4 into K562 cells significantly enhanced the uptake of TAT, which further supports an important role of heparan sulfate proteoglycans in mediating TAT internalisation. It is possible that there is low expression of SDC-4 in SK-MEL-37 cells and this may explain why TAT failed to facilitate the uptake of RICs into these cells. Due to a lack of literature detailing the expression of SDC-4 in SK-MEL-37 cells, more experiments are needed to confirm or refute this hypothesis.

Due to the failure of TAT conjugation to increase internalisation of the ^{111}In-NY-ESO-1 in SK-MEL-37 cells, the use of a protein delivery reagent was investigated. The use of cationic amphiphilic liposomal compound SAINT2:DOPE for protein delivery in the presence of serum was first demonstrated by Van der Gun *et* a*l* in 2007 (van der Gun et al., 2007). Cytosine-5 methyltransferase, which methylates cytosines in CpG dinucleotides, was successfully delivered into the nucleus by use of this protein transfection reagent. However, it is possible that, because the cytosine-5 methyltransferase is a small protein with molecular weight below 60 KDa, it could passively diffuse across the nuclear pores after delivery into the

cytoplasm (Wang and Brattain, 2007). The protein transfection reagent known as SAINT-PhD used in this study is the advanced version of SAINT2:DOPE according to the manufacturer (Synvolux Therapeutics, BV, Groningen, Netherlands). There was no activation of the immune system or cytotoxicity observed when this reagent was used in both *in vitro* and *in vivo* models (Hoekstra, 2001, Audouy et al., 2002). In this study it was decided to pursue a strategy combining the use of protein transfection reagent and TAT conjugation. The prediction was that radiolabelled anti-NY-ESO-1-TAT antibody would be transported across the cell membrane by the protein transfection reagent, SAINT-PhD, and subsequently translocated to the nucleus through the action of the nuclear localisation sequence present in TAT.

6.4. Cytotoxic effect of radiolabelled anti-NY-ESO-1-TAT-PT on melanoma cells

The results demonstrate that cell viability and clonogenic survival were reduced when SK-MEL-37 cells were exposed to ^{111}In or ^{123}I-labelled anti-NY-ESO-1-TAT-PT. The cytotoxicity of radiolabelled anti-NY-ESO-1-TAT-PT antibody towards SK-MEL-37 cells was positively correlated with the specific activity of the radionuclide and the molar concentration of the RIC. There was a slight decrease in cell viability and clonogenic survival in cells incubated with high concentration of non-specific radiolabelled mIgG-TAT-PT, suggesting that in a clinical setting the concentration of RIC would have to be adjusted so as to achieve cytotoxicity of the tumour cells without damaging surrounding tissue. No evidence of cytotoxicity was observed in SK-MEL-37 cells incubated with protein transfection reagent alone, which was consistent with other studies (Hoekstra, 2001).

Incubation of the NY-ESO-1 negative melanoma cell line SK-MEL-23 with the RIC had no significant effect on survival fraction, indicating a specific antibody targeted effect. This evidence was further supported by reducing the NY-ESO-1 expression in SK-MEL-37 cells using siRNA. However the radiolabelled anti-NY-ESO-1-TAT-PT associated cytotoxicity was only partially reversed by NY-ESO-1 protein knockdown. This could be due to the radiolabelled anti-NY-ESO-1-TAT-PT binding to another cancer testis antigen known as LAGE-1, which shares 84% homology with NY-ESO-1 at the protein level (Chen et al., 1997). In order to confirm the role of LAGE-1, further experiments knocking down both proteins should be performed.

An increase in the number of γH2AX foci was detected in the nuclei of SK-MEL-37 cells exposed to radiolabelled anti-NY-ESO-1-TAT-PT, confirming the presence of DNA damage. The Histone isoform, H2AX, is phosphorylated in response to DNA double strand (dsDNA) breaks, which occur following exposure to ionising radiation or chemotherapeutic agents (Cornelissen et al., 2012). SK-MEL-37 cells exhibited substantial basal levels of γH2AX foci, suggesting the possibility of a mutation in a DNA repair protein, such as p53 and BRCA1, resulting in genomic instability (Yu et al., 2006). It has also been previously reported that high endogenous expression of γH2AX foci in several melanoma cell lines was associated with telomere dysfunction, thus driving genomic instability (Warters et al., 2005).

6.5. *In vivo* effect of radiolabelled anti-NY-ESO-1-TAT-PT

Following the observation of a cytotoxic effect of the radiolabelled anti-NY-ESO-1-TAT-PT *in vitro*, the efficacy *in vivo* was investigated using xenograft models. The biodistribution of the radioimmunoconjugate in BALB/c nude mice bearing

NY-ESO-1 expressing and NY-ESO-1 negative xenografts was studied. The results showed high liver and spleen uptake, and slow blood clearance, which was considered to be due to the pharmacokinetic properties of the large molecular weight whole IgG antibody and the binding to Fc receptor of immune effector cells via Fc portion. Intact IgG antibodies can be engineered into smaller fragments including the generation of Fab (50 kDa), $F(ab)_2$ (100 kDa), Single chain variable fragments (~ 30 kDa), diabodies (~ 60 kDa) and minibodies (~ 80 kDa), which enhances blood clearance. However, an accelerated blood clearance and removal of the Fc portion needs to be carefully evaluated as the Fc portion is important in initiating antibody-dependent cell-mediated cytotoxicity (ADCC), and rapid clearance of probes from blood could potentially reduce the potency for cancer treatments.

In BALB/c nude mice bearing NY-ESO-1 expressing xenografts, the biodistribution data showed that ^{111}In-DTPA-anti-NY-ESO-1-TAT-PT accumulated and was retained in tumours 48 h post injection in 2 out of 3 mice, whereas no accumulation was observed in the BALB/c nude mice injected with the control, ^{111}In-DTPA-mIgG-TAT-PT. This appears to confirm the targeting of the radioimmunoconjugate *in vivo*.

6.6. The immune system and radiolabelled anti-NY-ESO-1-TAT-PT

The immune system protects against diseases by distinguishing foreign or abnormal antigens from the organism's own healthy cells. Tumour cells are able to evade detection by the immune system through their ability to generate and maintain an immunosuppressive microenvironment. Several mechanisms are used to achieve this immunosuppression, including, downregulation of major histocompatibility complex class 1 molecules (MHC 1), upregulation of anti-

inflammatory cytokine such as interleukin-4,5, and 10, upregulation of indoleamine 2, 3-dioxygenase (IDO) depleting tryptophan (which causes T cells to become hyporesponsive), and promoting the generation of $CD4^+CD25^+$ regulatory T cells (T_{reg} cells) (Drake et al., 2006, Kim et al., 2005). These are major challenges in developing effective immunotherapies for cancer treatments.

In a clinical setting, it is envisaged that radiolabelled anti-NY-ESO-1-TAT-PT would be administered to a patient with an NY-ESO-1 expressing tumour. The radioimmunoconjugate would be delivered to the nucleus of the tumour cells by the protein transfection reagent and TAT, and DNA damage would be caused by the release of Auger electrons. The destruction of tumour cells by Auger electron mediated DNA damage would lead to the release of NY-ESO-1, which could be subsequently be taken up antigen presenting cells such as dendritic cells (DCs) (Formenti and Demaria, 2009, Noguchi et al., 2012). Once activated, DCs migrate to the lymph nodes where naive T cells are primed to shape the adaptive immune system. NY-ESO-1 antigen released from tumour cells that are damaged or killed by radiolabelled anti-NY-ESO-1-TAT-PT, might be bound by endogenous, circulating anti-NY-ESO-1 antibody . Natural killer (NK) cells expressing CD16 are recruited by the Fc portion of antibodies, triggering antibody dependent cell mediated cytotoxicity (ADCC). Therefore, it is possible that the anti-tumour response would be be enhanced by the release of NY-ESO-1 antigens following treatment with RICs, thereby providing a patient specific anti-tumour effect.

Over the last few years, there has been intensive research into the development of cancer vaccines against NY-ESO-1, as it is one of the most immunogenic cancer testis antigens identified to date (Ademuyiwa et al., 2012).

6.7. Imaging approaches using radiolabelled NY-ESO-1

The analysis of the serum level of tumour markers is used for cancer detection, and prediction of outcome. There are several organ-specific tumour markers that are used in the clinic. For instance, an elevated level of prostate specific antigen is indicative of the presence of prostate cancer (Seamonds et al., 1986). However, some of the commonly used tumour markers for detecting gastrointestinal and gynaecological cancer, including carcinoembryonic antigen (CEA), CA19-9, and CA125, may be raised in non-malignant conditions or sometimes are not raised even when cancer is present. As a result, misleading information might results in failure to detect tumours (Kilpatrick and Lind, 2009). Therefore, more specific tumour markers need to be identified in order to make an accurate diagnosis.

Since NY-ESO-1 is highly immunogenic, anti-NY-ESO-1 antibody can be found in the sera of patients with NY-ESO-1 expressing tumours but not in healthy individuals (Stockert et al., 1998). It was therefore initially thought that early detection of cancer could be achieved by measuring the level of anti-NY-ESO-1 antibody. However, the NY-ESO-1 humoral response is modest, with, for example, only a 3.4% increase in patients with stage 1 gastric cancer. Therefore evaluation of the level of anti-NY-ESO-1 antibody in serum is of limited utility for the early detection of tumours (Fujiwara et al., 2013).

It was previously reported that NY-ESO-1/LAGE-1 protein was detected in 9 of 24 (37.5%) tissue samples from patients with stage 1 and 2 diffuse large B-cell lymphoma (DLBCL) (Hudolin et al., 2013). Furthermore, high expression (66 of 110) of NY-ESO-1 protein was detected in patients with stage 1 and 2 triple negative breast cancer (Ademuyiwa et al., 2012). The expression of NY-ESO-1 protein in early stage tumours suggests a possibile role for radiolabelled anti-NY-

ESO-1 antibody as an imaging probe. The ^{111}In or ^{123}I-labelled anti-NY-ESO-1-TAT-PT developed in this study are candidates for imaging NY-ESO-1 expressing tumours. Single-photon emission computed tomography (SPECT) is used to detect the γ-rays emitted by the radionuclides attached to anti-NY-ESO-1-TAT-PT, thus marking the location of the tumours. To increase their potential imaging application, it would be possible to use different radionuclides such as ^{89}Zr for PET imaging. This study was primarily designed to investigate the cytotoxicity of anti-NY-ESO-1 RICs, so further work is required to explore their use for imaging.

6.8.Conclusion

Monoclonal antibodies are increasingly investigated for cancer therapy due to their high affinity and target specificity. However, many of tumour-associated antigens are intracellular, limiting the use of immunotargeting approaches. This study has shown that it is possible to deliver radiolabelled antibody across the cell membrane using serum insensitive and non-toxic protein transfection reagent to target the endogenous tumour-associated antigen, NY-ESO-1. Cell-penetrating peptide, TAT, which possesses a nuclear localisation sequence, translocates the radiolabelled anti-NY-ESO-1 antibody into the nucleus of SK-MEL-37 cells, to allow Auger electron mediated DNA damage. The clonogenic survival of SK-MEL-37 cells was significantly reduced by incubation with radiolabelled anti-NY-ESO-1-TAT-PT and was positively correlated with the specific activity and concentration of radiolabelled probes. The successful development of ^{111}In-labelled anti-NY-ESO-1-TAT-PT *in vitro*, justified the subsequent study of this radiolabelled probe in animal models. The biodistribution data demonstrated that ^{111}In-DTPA-anti-NY-ESO-1-TAT-PT accumulated and was retained in mice

bearing NY-ESO-1 expressing xenografts. Furthermore, there was no significant uptake of the probe by testis, suggesting that neither protein transfection reagent or TAT penetrate the blood testis barrier, thus minimising non-specific binding to healthy cells.

The objectives of this study, as stated in Chapter 1, were achieved. This thesis demonstrates the development and synthesis of a radiolabelled antibody against cancer testis antigen, NY-ESO-1, which retained intact binding affinity after conjugation to TAT peptide. The internalisation and cytotoxicity of these RICs were evaluated and promising data obtained from *in vitro* experiments, leading on to the investigation of these RICs in animal models of cancer. The accumulation of the RIC in xenografts *in vivo* suggests the possibility for use of the construct in a clinical setting.

Chapter 7

Summary

Chapter 7: Summary

Antibodies bind with high specificity to their target antigen, and this characteristic has been exploited in the development of antigen specific monoclonal antibodies for therapeutic applications. For a therapeutic antibody to exert selective cytotoxic effects on tumours, the antigen should show a restricted expression profile in normal tissues, but abundant expression in tumour cells. NY-ESO-1 is a member of a class of molecules termed cancer testis antigens, the expression of which is restricted to germ cells and a wide range of tumour tissues. However NY-ESO-1, like the majority of tumour antigens identified to date, is an intracellular protein, presenting a challenge for the delivery of an antibody-based therapy.

This study has demonstrated that it is possible to engineer the internalisation and nuclear localisation of radiolabelled anti-NY-ESO-1 antibody by conjugation to protein transfection reagent and the cell-penetrating peptide TAT. The resulting radioimmunoconjugates (RICs) were shown to be cytotoxic to NY-ESO-1 expressing tumour cells *in vitro*, and preliminary *in vivo* data indicates that the ^{111}In-labelled RIC accumulates in NY-ESO-1 tumours. These results suggest that anti-NY-ESO-1 RICs could be of benefit for clinical cancer therapy.

Bibliography

ADEMUYIWA, F. O., BSHARA, W., ATTWOOD, K., MORRISON, C., EDGE, S. B., AMBROSONE, C. B., O CONNOR, T. L., LEVINE, E. G., MILIOTTO, A. & RITTER, E. 2012. NY-ESO-1 cancer testis antigen demonstrates high immunogenicity in triple negative breast cancer. *PloS one,* 7**,** e38783.

AKCAKANAT, A., KANDA, T., KOYAMA, Y., WATANABE, M., KIMURA, E., YOSHIDA, Y., KOMUKAI, S., NAKAGAWA, S., ODANI, S. & FUJII, H. 2004. NY-ESO-1 expression and its serum immunoreactivity in esophageal cancer. *Cancer chemotherapy and pharmacology,* 54**,** 95-100.

ALISON, M. R. 2001. Cancer. *eLS.* John Wiley & Sons, Ltd.

APRELIKOVA, O., PANDOLFI, S., TACKETT, S., FERREIRA, M., SALNIKOW, K., WARD, Y., RISINGER, J. I., BARRETT, J. C. & NIEDERHUBER, J. 2009. Melanoma antigen-11 inhibits the hypoxia-inducible factor prolyl hydroxylase 2 and activates hypoxic response. *Cancer Research,* 69**,** 616-624.

ARANO, Y., UEZONO, T., AKIZAWA, H., ONO, M., WAKISAKA, K., NAKAYAMA, M., SAKAHARA, H., KONISHI, J. & YOKOYAMA, A. 1996. Reassessment of diethylenetriaminepentaacetic acid (DTPA) as a chelating agent for indium-111 labeling of polypeptides using a newly synthesized monoreactive DTPA derivative. *Journal of medicinal chemistry,* 39**,** 3451-3460.

AUDOUY, S. A. L., DE LEIJ, L. F. M. H., HOEKSTRA, D. & MOLEMA, G. 2002. In vivo characteristics of cationic liposomes as delivery vectors for gene therapy. *Pharmaceutical research,* 19**,** 1599-1605.

AYYOUB, M., TAUB, R. N., KEOHAN, M.-L., HESDORFFER, M., METTHEZ, G., MEMEO, L., MANSUKHANI, M., HIBSHOOSH, H., HESDORFFER, C. S. & VALMORI, D. 2004. The frequent expression of cancer/testis antigens provides opportunities for immunotherapeutic targeting of sarcoma. *Cancer Immun,* 4.

BAN TH., J. P. & OLIVE, P. L. 2003. Expression of phosphorylated histone H2AX as a surrogate of cell killing by drugs that create DNA double-strand breaks. *Cancer Research,* 63**,** 4347-4350.

BASKAR, R., LEE, K. A., YEO, R. & YEOH, K.-W. 2012. Cancer and Radiation Therapy: Current Advances and Future Directions. *Int J Med Sci,* 9(3)**,** 193-199.

BECHARA, C. & SAGAN, S. Cell-penetrating peptides: 20 years later, where do we stand? *FEBS Letters*.

BERRIDGE, M. V., HERST, P. M. & TAN, A. S. 2005. Tetrazolium dyes as tools in cell biology: new insights into their cellular reduction. *Biotechnology annual review,* 11**,** 127-152.

BLEIBERG, H. & DE GRAMONT, A. 1998. Oxaliplatin plus 5-fluorouracil: clinical experience in patients with advanced colorectal cancer. *Seminars in oncology,* 25**,** 32-39.

BLEND, M. J., GREAGER, J. A., ATCHER, R. W., BROWN, J. M., BRECHBIEL, M. W., GANSOW, O. A. & DAS GUPTA, T. K. 1988. Improved sarcoma imaging and reduced hepatic activity with indium-111-SCN-Bz-DTPA linked to MoAb 19-24. *Journal of nuclear medicine,* 29**,** 1810-1816.

BOLLI, M., SCHULTZ-THATER, E., ZAJAC, P., GULLER, U., FEDER, C., SANGUEDOLCE, F., CARAFA, V., TERRACCIANO, L., HUDOLIN, T. & SPAGNOLI, G. C. 2005. NY-ESO-1/LAGE-1 coexpression with MAGE-A cancer/testis antigens: A tissue microarray study. *International journal of cancer,* 115**,** 960-966.

BONNER, W. M., REDON, C. E., DICKEY, J. S., NAKAMURA, A. J., SEDELNIKOVA, O. A., SOLIER, S. & POMMIER, Y. 2008. gammaH2AX and cancer. *Nature Reviews Cancer,* 8**,** 957-967.

BRECHBIEL, M. W., GANSOW, O. A., ATCHER, R. W., SCHLOM, J., ESTEBAN, J., SIMPSON, D. & COLCHER, D. 1986. Synthesis of 1-(p-isothiocyanatobenzyl) derivatives of DTPA and EDTA. Antibody labeling and tumor-imaging studies. *Inorganic Chemistry,* 25**,** 2772-2781.

BROOKS, H., LEBLEU, B. & VIV S, E. 2005. Tat peptide-mediated cellular delivery: back to basics. *Advanced Drug Delivery Reviews,* 57**,** 559-577.

BUCHEGGER, F., ANTONESCU, C., DELALOYE, A. B., HELG, C., KOVACSOVICS, T., KOSINSKI, M., MACH, J. P. & KETTERER, N. 2006a. Long-term complete responses after 131I-tositumomab therapy for relapsed or refractory indolent non-Hodgkin's lymphoma. *Br J Cancer,* 94**,** 1770-1776.

BUCHEGGER, F., PERILLO-ADAMER, F., DUPERTUIS, Y. & BISCHOF DELALOYE, A. 2006b. Auger radiation targeted into DNA: a therapy perspective. *European Journal of Nuclear Medicine and Molecular Imaging,* 33**,** 1352-1363.

CABALLERO, O. L. & CHEN, Y.-T. 2009. Cancer/testis (CT) antigens: Potential targets for immunotherapy. *Cancer Science,* 100**,** 2014-2021.

CARTER, P. 2001. Improving the efficacy of antibody-based cancer therapies. *Nat Rev Cancer,* 1**,** 118-129.

CASTANHO, M. A. R. B., PRIETO, M. & JAMESON, D. M. 1999. The pentaene macrolide antibiotic filipin prefers more rigid DPPC bilayers: a fluorescence pressure dependence study. *Biochimica et Biophysica Acta (BBA)-Biomembranes,* 1419**,** 1-14.

CHABNER, B. A. & ROBERTS, T. G. 2005. Chemotherapy and the war on cancer. *Nature Reviews Cancer,* 5**,** 65-72.

CHEN, H. S., QIN, L. L., CONG, X., WANG, Y., FEI, R., JIANG, D., CAO, J., SU, J. J., WEI, L. & CHEN, W. F. 2003. Expression of tumor-specific cancer/testis antigens in hepatocellular carcinoma]. *Zhonghua gan zang bing za zhi= Zhonghua ganzangbing zazhi= Chinese journal of hepatology,* 11**,** 145.

CHEN, Y.-T., SCANLAN, M. J., SAHIN, U., TURECI, O., GURE, A. O., TSANG, S., WILLIAMSON, B., STOCKERT, E., PFREUNDSCHUH, M. & OLD, L. J. 1997. A testicular antigen aberrantly expressed in human cancers detected by autologous antibody screening. *Proceedings of the National Academy of Sciences,* 94**,** 1914-1918.

CHEN, Y. T., STOCKERT, E., CHEN, Y., GARIN-CHESA, P., RETTIG, W. J., VAN DER BRUGGEN, P., BOON, T. & OLD, L. J. 1994. Identification of the MAGE-1 gene product by monoclonal and polyclonal antibodies. *Proceedings of the National Academy of Sciences,* 91**,** 1004-1008.

CHIRIVA-INTERNATI, M., PANDEY, A., SABA, R., KIM, M., SAADEH, C., LUKMAN, T., CHIARAMONTE, R., JENKINS, M., COBOS, E. & JUMPER, C. 2012. Cancer Testis Antigens: A Novel Target in Lung Cancer. *International reviews of immunology,* 31**,** 321-343.

CLYNES, R. A., TOWERS, T. L., PRESTA, L. G. & RAVETCH, J. V. 2000. Inhibitory Fc receptors modulate in vivo cytoxicity against tumor targets. *Nature medicine,* 6**,** 443-446.

CORNELISSEN, B., DARBAR, S., KERSEMANS, V., ALLEN, D., FALZONE, N., BARBEAU, J., SMART, S. & VALLIS, K. A. 2012. Amplification of DNA damage by a gammaH2AX-targeted radiopharmaceutical. *Nuclear Medicine and Biology,* 39**,** 1142-1151.

CORNELISSEN, B., HU, M., MCLARTY, K., COSTANTINI, D. & REILLY, R. M. 2007. Cellular penetration and nuclear importation properties of 111In-labeled and 123I-labeled HIV-1 tat peptide immunoconjugates in BT-474 human breast cancer cells. *Nuclear Medicine and Biology,* 34**,** 37-46.

CORNELISSEN, B., KERSEMANS, V., DARBAR, S., THOMPSON, J., SHAH, K., SLEETH, K., HILL, M. A. & VALLIS, K. A. 2011a. Imaging DNA damage in vivo using gammaH2AX-Targeted immunoconjugates. Cancer Res.

CORNELISSEN, B., KERSEMANS, V., MCLARTY, K., TRAN, L., VALLIS, K. A. & REILLY, R. M. 2009. In vivo monitoring of intranuclear p27/kip1 protein expression in breast cancer cells during trastuzumab (Herceptin) therapy. *Nuclear medicine and biology,* 36**,** 811-819.

CORNELISSEN, B., WALLER, A., TARGET, C., KERSEMANS, V., SMART, S. & VALLIS, K. 2011b. 111In-BnDTPA-F3: an Auger electron-emitting radiotherapeutic agent that targets nucleolin. EJNMMI Research

COUCHMAN, J. R. 2003. Syndecans: proteoglycan regulators of cell-surface microdomains? *Nat Rev Mol Cell Biol,* 4**,** 926-938.

DALKARA, D., CHANDRASHEKHAR, C. & ZUBER, G. 2006. Intracellular protein delivery with a dimerizable amphiphile for improved complex stability and prolonged protein release in the cytoplasm of adherent cell lines. *Journal of controlled release,* 116**,** 353-359.

DE MATTEIS, M. A. & GODI, A. 2004. PI-loting membrane traffic. *Nature cell biology,* 6**,** 487-492.

DELANEY, G., JACOB, S., FEATHERSTONE, C. & BARTON, M. 2005. The role of radiotherapy in cancer treatment. *Cancer,* 104**,** 1129-1137.

DESHAYES, S. B., MORRIS, M., HEITZ, F. D. R. & DIVITA, G. 2008. Delivery of proteins and nucleic acids using a non-covalent peptide-based strategy. *Advanced Drug Delivery Reviews,* 60**,** 537-547.

DHODAPKAR, M. V., OSMAN, K., TERUYA-FELDSTEIN, J., FILIPPA, D., HEDVAT, C. V., IVERSEN, K., KOLB, D., GELLER, M. D., HASSOUN, H. & KEWALRAMANI, T. 2003. Expression of cancer/testis (CT) antigens MAGE-A1, MAGE-A3, MAGE-A4, CT-7, and NY-ESO-1 in malignant gammopathies is heterogeneous and correlates with site, stage and risk status of disease. *Cancer Immun,* 3**,** 9.

DI PAOLO, G. & DE CAMILLI, P. 2006. Phosphoinositides in cell regulation and membrane dynamics. *Nature,* 443**,** 651-657.

DIETZ, G. P. H. & BΔHR, M. 2004. Delivery of bioactive molecules into the cell: the Trojan horse approach. *Molecular and Cellular Neuroscience,* 27**,** 85-131.

DOBRYNIN, P., MATYUNINA, E., MALOV, S. V. & KOZLOV, A. P. The novelty of human Cancer/Testis Antigen encoding genes in evolution. *International Journal of Genomics,* 2013**,** 7.

DRAKE, C. G., JAFFEE, E. & PARDOLL, D. M. 2006. Mechanisms of immune evasion by tumors. *Advances in immunology,* 90**,** 51-81.

ESTEBAN, J. M., SCHLOM, J., GANSOW, O. A., ATCHER, R. W., BRECHBIEL, M. W., SIMPSON, D. E. & COLCHER, D. 1987. New method for the chelation of indium-111 to monoclonal antibodies: biodistribution and imaging of athymic mice bearing human colon carcinoma xenografts. *Journal of nuclear medicine: official publication, Society of Nuclear Medicine,* 28**,** 861-870.

FIRE, A., XU, S., MONTGOMERY, M. K., KOSTAS, S. A., DRIVER, S. E. & MELLO, C. C. 1998. Potent and specific genetic interference by double-stranded RNA in Caenorhabditis elegans. *nature,* 391**,** 806-811.

FOMENKO, V. V., POLYNOVA, T. N., PORAI-KOSHITS, M. A., VARLAMOVA, G. L. & PECHUROVA, N. I. 1973. Crystal structure of copper (II) diethylenetriaminepentaacetate monohydrate. *Journal of Structural Chemistry,* 14**,** 529.

FORMENTI, S. C. & DEMARIA, S. 2009. Systemic effects of local radiotherapy. *The lancet oncology,* 10**,** 718-726.

FOSSA, A., BERNER, A., FOSSA, S. D., HERNES, E., GAUDERNACK, G. & SMELAND, E. B. 2004. NY-ESO-1 protein expression and humoral immune responses in prostate cancer. *The Prostate,* 59**,** 440-447.

FRANKEN, N. A. P., RODERMOND, H. M., STAP, J., HAVEMAN, J. & VAN BREE, C. 2006. Clonogenic assay of cells in vitro. *Nat. Protocols,* 1**,** 2315-2319.

FUJITA, S., WADA, H., JUNGBLUTH, A. A., SATO, S., NAKATA, T., NOGUCHI, Y., DOKI, Y., YASUI, M., SUGITA, Y. & YASUDA, T. 2004. NY-ESO-1 expression and immunogenicity in esophageal cancer. *Clinical cancer research,* 10**,** 6551-6558.

FUJIWARA, S., WADA, H., KAWADA, J., KAWABATA, R., TAKAHASHI, T., FUJITA, J., HIRAO, T., SHIBATA, K., MAKARI, Y. & IIJIMA, S. 2013. NY-ESO-1 antibody as a novel tumour marker of gastric cancer. *British journal of cancer,* 108**,** 1119-1125.

GNJATIC, S., NISHIKAWA, H., JUNGBLUTH, A. A., GURE, A. O., RITTER, G., JAGER, E., KNUTH, A., CHEN, Y.-T., OLD, L. J. & GEORGE F. VANDE WOUDE, A. G. K. 2006. NY-ESO-1: Review of an Immunogenic Tumor Antigen. *Advances in Cancer Research.* Academic Press.

GOLDSMITH, S. J. Radioimmunotherapy of lymphoma: Bexxar and Zevalin. Seminars in nuclear medicine, 2010. Elsevier, 122-135.

HALL, E. J. 1997. *Radiobiology for the radiologist 4th edition*.

HAMMOND, S. M., BERNSTEIN, E., BEACH, D. & HANNON, G. J. 2000. An RNA-directed nuclease mediates post-transcriptional gene silencing in Drosophila cells. *nature,* 404**,** 293-296.

HANAHAN, D. & WEINBERG, R. A. 2000. The Hallmarks of Cancer. *Cell,* 100**,** 57-70.

HAYAMA, S., DAIGO, Y., KATO, T., ISHIKAWA, N., YAMABUKI, T., MIYAMOTO, M., ITO, T., TSUCHIYA, E., KONDO, S. & NAKAMURA, Y. 2006. Activation of CDCA1-KNTC2, members of

centromere protein complex, involved in pulmonary carcinogenesis. *Cancer research,* 66**,** 10339-10348.

HEITZ, F., MORRIS, M. C. & DIVITA, G. 2009. Twenty years of cell-penetrating peptides: from molecular mechanisms to therapeutics. *British Journal of Pharmacology,* 157**,** 195-206.

HOEKSTRA, S. A. D. 2001. Cationic lipid-mediated transfection in vitro and in vivo. *Molecular membrane biology,* 18**,** 129-143.

HOFMANN, O., CABALLERO, O. L., STEVENSON, B. J., CHEN, Y.-T., COHEN, T., CHUA, R., MAHER, C. A., PANJI, S., SCHAEFER, U., KRUGER, A., LEHVASLAIHO, M., CARNINCI, P., HAYASHIZAKI, Y., JONGENEEL, C. V., SIMPSON, A. J. G., OLD, L. J. & HIDE, W. 2008. Genome-wide analysis of cancer/testis gene expression. *Proceedings of the National Academy of Sciences,* 105**,** 20422-20427.

HU, M., CHEN, P., WANG, J., CHAN, C., SCOLLARD, D. & REILLY, R. 2006. Site-specific conjugation of HIV-1 tat peptides to IgG: a potential route to construct radioimmunoconjugates for targeting intracellular and nuclear epitopes in cancer. *European Journal of Nuclear Medicine and Molecular Imaging,* 33**,** 301-310.

HUDOLIN, T., KASTELAN, Z., ILIC, I., LEVARDA-HUDOLIN, K., BASIC-JUKIC, N., RIEKEN, M., SPAGNOLI, G. C., JURETIC, A. & MENGUS, C. 2013. Immunohistochemical analysis of the expression of MAGE-A and NY-ESO-1 cancer/testis antigens in diffuse large B-cell testicular lymphoma. *Journal of translational medicine,* 11**,** 123.

J GER, E., CHEN, Y.-T., DRIJFHOUT, J. W., KARBACH, J., RINGHOFFER, M., J GER, D., ARAND, M., WADA, H., NOGUCHI, Y., STOCKERT, E., OLD, L. J. & KNUTH, A. 1998. Simultaneous humoral and cellular immune response against Cancer–Testis Antigen NY-ESO-1: Definition of human histocompatibility leukocyte antigen (HLA)-A2–binding Peptide Epitopes *The Journal of Experimental Medicine,* 187**,** 265-270.

J GER, E., GNJATIC, S., NAGATA, Y., STOCKERT, E., J GER, D., KARBACH, J., NEUMANN, A., RIECKENBERG, J., CHEN, Y.-T., RITTER, G., HOFFMAN, E., ARAND, M., OLD, L. J. & KNUTH, A. 2000. Induction of primary NY-ESO-1 immunity: CD8+ T lymphocyte and antibody responses in peptide-vaccinated patients with NY-ESO-1+ cancers. *Proceedings of the National Academy of Sciences,* 97**,** 12198-12203.

J GER, E., STOCKERT, E., ZIDIANAKIS, Z., CHEN, Y.-T., KARBACH, J., J GER, D., ARAND, M., RITTER, G., OLD, L. J. & KNUTH, A. 1999. Humoral immune responses of cancer patients against "Cancer-Testis" antigen NY-ESO-1: Correlation with clinical events. *International Journal of Cancer,* 84**,** 506-510.

J RVER, P. & LANGEL, Ü. 2006. Cell-penetrating peptides—A brief introduction. *Biochimica et Biophysica Acta (BBA)-Biomembranes,* 1758**,** 260-263.

JACENE, H. A., FILICE, R., KASECAMP, W. & WAHL, R. L. 2007. Comparison of 90Y-ibritumomab tiuxetan and 131I-tositumomab in clinical practice. *Journal of Nuclear Medicine,* 48**,** 1767-1776.

JACKS, T. & WEINBERG, R. A. 2002. Taking the study of cancer cell survival to a new dimension. *Cell,* 111**,** 923-925.

JONES, S. W., CHRISTISON, R., BUNDELL, K., VOYCE, C. J., BROCKBANK, S., NEWHAM, P. & LINDSAY, M. A. 2005. Characterisation of cell-penetrating peptide-mediated peptide delivery. *British journal of pharmacology,* 145**,** 1093-1102.

JUNGBLUTH, A. A., ANTONESCU, C. R., BUSAM, K. J., IVERSEN, K., KOLB, D., COPLAN, K., CHEN, Y. T., STOCKERT, E., LADANYI, M. & OLD, L. J. 2001a. Monophasic and biphasic synovial sarcomas abundantly express cancer/testis antigen ny-eso-1 but not mage-A1 or CT7. *International journal of cancer,* 94**,** 252-256.

JUNGBLUTH, A. A., CHEN, Y. T., STOCKERT, E., BUSAM, K. J., KOLB, D., IVERSEN, K., COPLAN, K., WILLIAMSON, B., ALTORKI, N. & OLD, L. J. 2001b. Immunohistochemical analysis of NY-ESO-1 antigen expression in normal and malignant human tissues. *International Journal of Cancer,* 92**,** 856-860.

KANG, Y., HONG, J. A., CHEN, G. A., NGUYEN, D. M. & SCHRUMP, D. S. 2007. Dynamic transcriptional regulatory complexes including BORIS, CTCF and Sp1 modulate NY-ESO-1 expression in lung cancer cells. *Oncogene,* 26**,** 4394-4403.

KARAGIANNIS, T. C. 2007. Comparison of different classes of radionuclides for potential use in radioimmunotherapy. *Hellenic Journal of Nuclear Medicine,* 10**,** 82-88.

KAWASHIMA, I., OZAWA, H., KOTANI, M., SUZUKI, M., KAWAN, T., GOMIBUCHI, M. & TAI, T. 1993. Characterization of ganglioside expression in human melanoma cells: immunological and biochemical analysis. *Journal of biochemistry,* 114**,** 186-193.

KEENEY, S., GIROUX, C. N. & KLECKNER, N. 1997. Meiosis-specific DNA double-strand breaks are catalyzed by Spo11, a member of a widely conserved protein family. *Cell,* 88**,** 375-384.

KILPATRICK, E. S. & LIND, M. J. 2009. Appropriate requesting of serum tumour markers. *BMJ,* 339.

KIM, D.-H., BEHLKE, M. A., ROSE, S. D., CHANG, M.-S., CHOI, S. & ROSSI, J. J. 2004. Synthetic dsRNA Dicer substrates enhance RNAi potency and efficacy. *Nature biotechnology,* 23**,** 222-226.

KIM, R., EMI, M. & TANABE, K. 2005. Cancer cell immune escape and tumor progression by exploitation of anti-inflammatory and pro-inflammatory responses. *Cancer biology & therapy,* 4**,** 924-933.

KNOGLER, K., GR NBERG, J., NOVAK-HOFER, I., ZIMMERMANN, K. & SCHUBIGER, P. A. 2006. Evaluation of 177Lu-DOTA-labeled aglycosylated monoclonal anti-L1-CAM antibody chCE7: influence of the number of chelators on the in vitro and in vivo properties. *Nuclear Medicine and Biology,* 33**,** 883-889.

KONISHI, J., TOYOOKA, S., AOE, M., OMURA, Y., WASHIO, K., TSUKUDA, K. & SHIMIZU, N. 2004. The relationship between NY-ESO-1 mRNA expression and clinicopathological features in non-small cell lung cancer. *Oncology reports,* 11**,** 1063-1067.

KORANGY, F., ORMANDY, L. A., BLECK, J. R. S., KLEMPNAUER, J. R., WILKENS, L., MANNS, M. P. & GRETEN, T. F. 2004. Spontaneous tumor-specific humoral and cellular immune responses to NY-ESO-1 in hepatocellular carcinoma. *Clinical cancer research,* 10**,** 4332-4341.

KRAUSE, M. M.-R., SCHLEGELBERGER, B., HERLING, M., HALLEK, M. & FINGERLE-ROWSON, G. N. 2012. Delayed development of chronic lymphocytic leukemia in the absence of macrophage migration inhibitory factor.

KUBUSCHOK, B., XIE, X., JESNOWSKI, R., PREUSS, K. D., ROMEIKE, B. F. M., NEUMANN, F., REGITZ, E., PISTORIUS, G., SCHILLING, M. & SCHEUNEMANN, P. 2004. Expression of cancer testis antigens in pancreatic carcinoma cell lines, pancreatic adenocarcinoma and chronic pancreatitis. *International journal of cancer,* 109**,** 568-575.

KURASHIGE, T., NOGUCHI, Y., SAIKA, T., ONO, T., NAGATA, Y., JUNGBLUTH, A., RITTER, G., CHEN, Y.-T., STOCKERT, E. & TSUSHIMA, T. 2001. NY-ESO-1 Expression and Immunogenicity Associated with Transitional Cell Carcinoma Correlation with Tumor Grade. *Cancer research,* 61**,** 4671-4674.

LADURON, S., DEPLUS, R., ZHOU, S., KHOLMANSKIKH, O., GODELAINE, D. L., DE SMET, C., HAYWARD, S. D., FUKS, F. O., BOON, T. & DE PLAEN, E. 2004. MAGE-A1 interacts with adaptor SKIP and the deacetylase HDAC1 to repress transcription. *Nucleic Acids Research,* 32**,** 4340-4350.

LETH , B., LUCAS, S., MICHAUX, L., DE SMET, C., GODELAINE, D., SERRANO, A., DE PLAEN, E. & BOON, T. 1998. LAGE-1, a new gene with tumor specificity. *International Journal of Cancer,* 76**,** 903-908.

LI, M., YUAN, Y.-H., HAN, Y., LIU, Y.-X., YAN, L., WANG, Y. & GU, J. 2005. Expression profile of cancer-testis genes in 121 human colorectal cancer tissue and adjacent normal tissue. *Clinical cancer research,* 11**,** 1809-1814.

LI, M. C., HERTZ, R. & BERGENSTAL, D. M. 1958. Therapy of Choriocarcinoma and Related Trophoblastic Tumors with Folic Acid and Purine Antagonists. *New England Journal of Medicine,* 259**,** 66-74.

LOVDAL, T., ANDERSEN, E., BRECH, A. & BERG, T. 2000. Fc receptor mediated endocytosis of small soluble immunoglobulin G immune complexes in Kupffer and endothelial cells from rat liver. *Journal of cell science,* 113**,** 3255-3266.

LUBBERT, M. 2000. DNA methylation inhibitors in the treatment of leukemias, myelodysplastic syndromes and hemoglobinopathies: clinical results and possible mechanisms of action. *Current topics in microbiology and immunology,* 249**,** 135-164.

MALUMBRES, M. & BARBACID, M. 2003. RAS oncogenes: the first 30 years. *Nat Rev Cancer,* 3**,** 459-465.

MARTIN, O. A. & BONNER, W. M. 2006. gammaH2AX in Cancer Cells: A potential biomarker for cancer diagnostics, prediction and recurrence. *Cell Cycle,* 5**,** 2909-2913.

MASHINO, K., SADANAGA, N., TANAKA, F., YAMAGUCHI, H., NAGASHIMA, H., INOUE, H., SUGIMACHI, K. & MORI, M. 2001. Expression of multiple cancer-testis antigen genes in gastrointestinal and breast carcinomas. *British journal of cancer,* 85**,** 713.

MEDINA-KAUWE, L. K., XIE, J. & HAMM-ALVAREZ, S. 2005. Intracellular trafficking of nonviral vectors. *Gene Therapy,* 12**,** 1734-1751.

MILLETTI, F. 2012. Cell-penetrating peptides: classes, origin, and current landscape. *Drug Discovery Today,* 17**,** 850-860.

MIRZADEH, S., BRECHBIEL, M. W., ATCHER, R. W. & GANSOW, O. A. 1990. Radiometal labeling of immunoproteins: covalent linkage of 2-(4-isothiocyanatobenzyl) diethylenetriaminepentaacetic acid ligands to immunoglobulin. *Bioconjugate chemistry,* 1**,** 59-65.

MITAL, P., HINTON, B. T. & DUFOUR, J. M. 2011. The blood-testis and blood-epididymis barriers are more than just their tight junctions. *Biology of reproduction,* 84**,** 851-858.

MORSCHHAUSER, F., RADFORD, J., VAN HOOF, A., VITOLO, U., SOUBEYRAN, P., TILLY, H., HUIJGENS, P. C., KOLSTAD, A., D €™AMORE, F. & DIAZ, M. G. 2008. Phase III trial of consolidation therapy with yttrium-90-ibritumomab tiuxetan compared with no

additional therapy after first remission in advanced follicular lymphoma. *Journal of Clinical Oncology,* 26**,** 5156-5164.

MOUNKES, L. C., ZHONG, W., CIPRES-PALACIN, G., HEATH, T. D. & DEBS, R. J. 1998. Proteoglycans mediate cationic liposome-DNA complex-based gene delivery in vitro and in vivo. *Journal of Biological Chemistry,* 273**,** 26164-26170.

NAGAO, T., HIGASHITSUJI, H., NONOGUCHI, K., SAKURAI, T., DAWSON, S., MAYER, R. J., ITOH, K. & FUJITA, J. 2003. MAGE-A4 interacts with the liver oncoprotein gankyrin and suppresses its tumorigenic Activity. *Journal of Biological Chemistry,* 278**,** 10668-10674.

NAHTA, R., YU, D., HUNG, M.-C., HORTOBAGYI, G. N. & ESTEVA, F. J. 2006. Mechanisms of Disease: understanding resistance to HER2-targeted therapy in human breast cancer. *Nat Clin Prac Oncol,* 3**,** 269-280.

NAKADA, T., NOGUCHI, Y., SATOH, S., ONO, T., SAIKA, T., KURASHIGE, T., GNJATIC, S., RITTER, G., CHEN, Y.-T. & STOCKERT, E. 2003. NY-ESO-1 mRNA expression and immunogenicity in advanced prostate cancer. *Cancer Immun,* 3.

NGAMWONGSATIT, P., BANADA, P. P., PANBANGRED, W. & BHUNIA, A. K. 2008. WST-1-based cell cytotoxicity assay as a substitute for MTT-based assay for rapid detection of toxigenic *Bacillus* species using CHO cell line. *Journal of Microbiological Methods,* 73**,** 211-215.

NICHOLAOU, T., EBERT, L., DAVIS, I. D., ROBSON, N., KLEIN, O., MARASKOVSKY, E., CHEN, W. & CEBON, J. 2006. Directions in the immune targeting of cancer: Lessons learned from the cancer-testis Ag NY-ESO-1. *Immunol Cell Biol,* 84**,** 303-317.

NOGUCHI, T., KATO, T., WANG, L., MAEDA, Y., IKEDA, H., SATO, E., KNUTH, A., GNJATIC, S., RITTER, G. & SAKAGUCHI, S. 2012. Intracellular tumor-associated antigens represent effective targets for passive immunotherapy. *Cancer research,* 72**,** 1672-1682.

ODUNSI, K., JUNGBLUTH, A. A., STOCKERT, E., QIAN, F., GNJATIC, S., TAMMELA, J., INTENGAN, M., BECK, A., KEITZ, B. & SANTIAGO, D. 2003. NY-ESO-1 and LAGE-1 cancer-testis antigens are potential targets for immunotherapy in epithelial ovarian cancer. *Cancer research,* 63**,** 6076-6083.

PARK, S., LIM, Y., LEE, D., CHO, B., BANG, Y.-J., SUNG, S., KIM, H.-Y., KIM, D.-K., LEE, Y.-S. & SONG, Y. 2003. Identification and characterization of a novel cancer/testis antigen gene CAGE-1. *Biochimica et Biophysica Acta (BBA)-Gene Structure and Expression,* 1625**,** 173-182.

PARRIZAS, M., SALTIEL, A. R. & LEROITH, D. 1997. Insulin-like Growth Factor 1 inhibits Apoptosis using the Phosphatidylinositol 3'-Kinase and

Mitogen-activated Protein Kinase Pathways. *Journal of Biological Chemistry,* 272**,** 154-161.

PENG, J.-R., CHEN, H.-S., MOU, D.-C., CAO, J., CONG, X., QIN, L.-L., WEI, L., LENG, X.-S., WANG, Y. & CHEN, W.-F. 2005. Expression of cancer/testis (CT) antigens in Chinese hepatocellular carcinoma and its correlation with clinical parameters. *Cancer letters,* 219**,** 223-232.

PHAM, D. T., KASPERSEN, F. M. & BOS, E. S. 1995. Electrophoretic method for the quantitative determination of a benzyl-DTPA ligand in DTPA monoclonal antibody conjugates. *Bioconjugate chemistry,* 6**,** 313-315.

POUGET, J.-P., NAVARRO-TEULON, I., BARDIES, M., CHOUIN, N., CARTRON, G., PELEGRIN, A. & AZRIA, D. 2011. Clinical radioimmunotherapy-the role of radiobiology. *Nat Rev Clin Oncol,* 8**,** 720-734.

PRASAD, M. L., JUNGBLUTH, A. A., PATEL, S. G., IVERSEN, K., HOSHAW €WOODARD, S. & BUSAM, K. J. 2004. Expression and significance of cancer testis antigens in primary mucosal melanoma of the head and neck. *Head & neck,* 26**,** 1053-1057.

PRESSMAN, D. 1949. The Zone of Localization of Antibodies. IV The in Vivo Disposition of Anti-Mouse-Kidney Serum and Anti-Mouse-Plasma Serum As Determined by Radioactive Tracers. *The Journal of Immunology,* 63**,** 375-388.

PRESSMAN, D., HILL, R. F. & FOOTE, F. W. 1949. The zone of localization of anti-mouse-kidney serum as determined by radioautographs. *Science,* 109**,** 65-66.

PRESSMAN, D. & KORNGOLD, L. 1953. The in vivo localization of anti-Wagner-osteogenic-sarcoma antibodies. *Cancer,* 6**,** 619-623.

PRISE, K. M., SCHETTINO, G., FOLKARD, M. & HELD, K. D. 2005. New insights on cell death from radiation exposure. *The Lancet Oncology,* 6**,** 520-528.

RAYNE, F., DEBAISIEUX, S., YEZID, H., LIN, Y.-L., METTLING, C., KONATE, K., CHAZAL, N., AROLD, S. T., PUGNI RE, M. & SANCHEZ, F. 2010. Phosphatidylinositol-(4, 5)-bisphosphate enables efficient secretion of HIV-1 Tat by infected T-cells. *The EMBO journal,* 29**,** 1348-1362.

REILLY, R., LEE, N., HOULE, S., LAW, J. & MARKS, A. 1992. In vitro stability of EDTA and DTPA immunoconjugates of monoclonal antibody 2G3 labeled with indium-111. *International journal of radiation applications and instrumentation. Part A. Applied radiation and isotopes,* 43**,** 961-967.

REILLY, R. M., KIARASH, R., CAMERON, R. G., PORLIER, N., SANDHU, J., HILL, R. P., VALLIS, K., HENDLER, A. & GARIÃ©PY, J. 2000. 111In-labeled EGF is selectively radiotoxic to human breast cancer cells overexpressing EGFR. *Journal of nuclear medicine: official publication, Society of Nuclear Medicine,* 41**,** 429-438.

RICHARD, J. P., MELIKOV, K., BROOKS, H., PREVOT, P., LEBLEU, B. & CHERNOMORDIK, L. V. 2005. Cellular uptake of unconjugated TAT peptide involves clathrin-dependent endocytosis and heparan sulfate receptors. *Journal of Biological Chemistry,* 280**,** 15300-15306.

RICHARD, J. P., MELIKOV, K., VIVES, E., RAMOS, C., VERBEURE, B., GAIT, M. J., CHERNOMORDIK, L. V. & LEBLEU, B. 2003. Cell-penetrating Peptides: A reevaluation of the mechanism of cellular uptake. *Journal of Biological Chemistry,* 278**,** 585-590.

RODOLFO, M., LUKSCH, R., STOCKERT, E., CHEN, Y.-T., COLLINI, P., RANZANI, T., LOMBARDO, C., DALERBA, P., RIVOLTINI, L., ARIENTI, F., FOSSATI-BELLANI, F., OLD, L. J., PARMIANI, G. & CASTELLI, C. 2003. Antigen-specific immunity in neuroblastoma patients: Antibody and T-Cell recognition of NY-ESO-1 tumor antigen. *Cancer Research,* 63**,** 6948-6955.

ROGAKOU, E. P., BOON, C., REDON, C. & BONNER, W. M. 1999. Megabase chromatin domains involved in DNA double-strand breaks in vivo. *The Journal of cell biology,* 146**,** 905-916.

ROSS, M. T., GRAFHAM, D. V., COFFEY, A. J., SCHERER, S., MCLAY, K., MUZNY, D., PLATZER, M., HOWELL, G. R., BURROWS, C., BIRD, C. P., FRANKISH, A., LOVELL, F. L., HOWE, K. L., ASHURST, J. L., FULTON, R. S., SUDBRAK, R., WEN, G., JONES, M. C., HURLES, M. E., ANDREWS, T. D., SCOTT, C. E., SEARLE, S., RAMSER, J., WHITTAKER, A., DEADMAN, R., CARTER, N. P., HUNT, S. E., CHEN, R., CREE, A., GUNARATNE, P., HAVLAK, P., HODGSON, A., METZKER, M. L., RICHARDS, S., SCOTT, G., STEFFEN, D., SODERGREN, E., WHEELER, D. A., WORLEY, K. C., AINSCOUGH, R., AMBROSE, K. D., ANSARI-LARI, M. A., ARADHYA, S., ASHWELL, R. I. S., BABBAGE, A. K., BAGGULEY, C. L., BALLABIO, A., BANERJEE, R., BARKER, G. E., BARLOW, K. F., BARRETT, I. P., BATES, K. N., BEARE, D. M., BEASLEY, H., BEASLEY, O., BECK, A., BETHEL, G., BLECHSCHMIDT, K., BRADY, N., BRAY-ALLEN, S., BRIDGEMAN, A. M., BROWN, A. J., BROWN, M. J., BONNIN, D., BRUFORD, E. A., BUHAY, C., BURCH, P., BURFORD, D., BURGESS, J., BURRILL, W., BURTON, J., BYE, J. M., CARDER, C., CARREL, L., CHAKO, J., CHAPMAN, J. C., CHAVEZ, D., CHEN, E., CHEN, G., CHEN, Y., CHEN, Z., CHINAULT, C., CICCODICOLA, A., CLARK, S. Y., CLARKE, G., CLEE, C. M., CLEGG, S., CLERC-BLANKENBURG, K., CLIFFORD, K., COBLEY, V., COLE, C. G., CONQUER, J. S., CORBY, N., CONNOR, R. E., DAVID, R., DAVIES, J., DAVIS, C., DAVIS, J., DELGADO, O.,

DESHAZO, D., et al. 2005. The DNA sequence of the human X chromosome. *Nature,* 434**,** 325-337.

SCANLAN, M. J., GURE, A. O., JUNGBLUTH, A. A., OLD, L. J. & CHEN, Y.-T. 2002. Cancer/testis antigens: an expanding family of targets for cancer immunotherapy. *Immunological reviews,* 188**,** 22.

SCANLAN, M. J., SIMPSON, A. J. & OLD, L. J. 2004. The cancer/testis genes: review, standardization, and commentary. *Cancer Immun,* 4**,** 1-15.

SCHUHMACHER, J., KLIV NYI, G., MATYS, R., KIRCHGEBNER, H., HAUSER, H., MAIER-BORST, W. & MATZKU, S. 1990. Uptake of Indium-111 in the Liver of Mice Following Administration of Indium-111-DTPA-Labeled Monoclonal Antibodies: Influence of Labeling Parameters, Physiologic Parameters, and Antibody Dose. *Journal of Nuclear Medicine,* 31**,** 1084-1093.

SCOTT, A. M., WOLCHOK, J. D. & OLD, L. J. 2012. Antibody therapy of cancer. *Nature Reviews Cancer,* 12**,** 278-287.

SEAMONDS, B., YANG, N., ANDERSON, K., WHITAKER, B., SHAW, L. M. & BOLLINGER, J. R. 1986. Evaluation of prostate-specific antigen and prosttic acid phosphatase as prostate cancer markers. *Urology,* 28**,** 472-479.

SHARMA, P., GNJATIC, S., JUNGBLUTH, A. A., WILLIAMSON, B., HERR, H., STOCKERT, E., DALBAGNI, G., DONAT, S. M., REUTER, V. E. & SANTIAGO, D. 2003. Frequency of NY-ESO-1 and LAGE-1 expression in bladder cancer and evidence of a new NY-ESO-1 T-cell epitope in a patient with bladder cancer. *Cancer Immun,* 3**,** 19-26.

SIMPSON, A. J. G., CABALLERO, O. L., JUNGBLUTH, A., CHEN, Y.-T. & OLD, L. J. 2005. Cancer/testis antigens, gametogenesis and cancer. *Nat Rev Cancer,* 5**,** 615-625.

SLAMON, D. J., GODOLPHIN, W., JONES, L. A., HOLT, J. A., WONG, S. G., KEITH, D. E., LEVIN, W. J., STUART, S. G., UDOVE, J., ULLRICH, A. & ET, A. 1989. Studies of the HER-2/neu proto-oncogene in human breast and ovarian cancer. *Science,* 244**,** 707-712.

STARK, G. R., KERR, I. M., WILLIAMS, B. R. G., SILVERMAN, R. H. & SCHREIBER, R. D. 1998. How cells respond to interferons. *Annual review of biochemistry,* 67**,** 227-264.

STEGMEIER, F., WARMUTH, M., SELLERS, W. R. & DORSCH, M. Targeted Cancer Therapies in the Twenty-First Century: Lessons From Imatinib. *Clin Pharmacol Ther,* 87**,** 543-552.

STERN, M. & HERRMANN, R. 2005. Overview of monoclonal antibodies in cancer therapy: present and promise. *Critical Reviews in Oncology/Hematology,* 54**,** 11-29.

STOCKERT, E., J GER, E., CHEN, Y.-T., SCANLAN, M. J., GOUT, I., KARBACH, J., ARAND, M., KNUTH, A. & OLD, L. J. 1998. A survey of the humoral immune response of cancer patients to a panel of human tumor antigens. *The Journal of experimental medicine,* 187**,** 1349-1354.

SUGITA, Y., WADA, H., FUJITA, S., NAKATA, T., SATO, S., NOGUCHI, Y., JUNGBLUTH, A. A., YAMAGUCHI, M., CHEN, Y.-T. & STOCKERT, E. 2004. NY-ESO-1 expression and immunogenicity in malignant and benign breast tumors. *Cancer research,* 64**,** 2199-2204.

SUZUKI, T., FUTAKI, S., NIWA, M., TANAKA, S., UEDA, K. & SUGIURA, Y. 2002. Possible existence of common internalization mechanisms among arginine-rich peptides. *Journal of Biological Chemistry,* 277**,** 2437-2443.

SWIRSKI, F. K., NAHRENDORF, M., ETZRODT, M., WILDGRUBER, M., CORTEZ-RETAMOZO, V., PANIZZI, P., FIGUEIREDO, J.-L., KOHLER, R. H., CHUDNOVSKIY, A. & WATERMAN, P. 2009. Identification of splenic reservoir monocytes and their deployment to inflammatory sites. *Science,* 325**,** 612-616.

T RECI, Ö., MACK, U., LUXEMBURGER, U., HEINEN, H., KRUMMENAUER, F., SESTER, M., SESTER, U., SYBRECHT, G. W. & SAHIN, U. 2006. Humoral immune responses of lung cancer patients against tumor antigen NY-ESO-1. *Cancer Letters,* 236**,** 64-71.

TAJIMA, K., OBATA, Y., TAMAKI, H., YOSHIDA, M., CHEN, Y.-T., SCANLAN, M. J., OLD, L. J., KUWANO, H., TAKAHASHI, T. & TAKAHASHI, T. 2003. Expression of cancer/testis (CT) antigens in lung cancer. *Lung Cancer,* 42**,** 23-33.

TANIURA, H., KOBAYASHI, M. & YOSHIKAWA, K. 2005. Functional domains of necdin for protein-protein interaction, nuclear matrix targeting, and cell growth suppression. *Journal of cellular biochemistry,* 94**,** 804-815.

VALABREGA, G., MONTEMURRO, F. & AGLIETTA, M. 2007. Trastuzumab: mechanism of action, resistance and future perspectives in HER2-overexpressing breast cancer. *Annals of Oncology,* 18**,** 977-984.

VALERIE, K., YACOUB, A., HAGAN, M. P., CURIEL, D. T., FISHER, P. B., GRANT, S. & DENT, P. 2007. Radiation-induced cell signaling: inside-out and outside-in. *Molecular Cancer Therapeutics,* 6**,** 789-801.

VAN DER BRUGGEN, P., TRAVERSARI, C., CHOMEZ, P., LURQUIN, C., DE PLAEN, E., VAN DEN EYNDE, B., KNUTH, A. & BOON, T. 1991. A gene encoding an antigen recognized by cytolytic T lymphocytes on a human melanoma. *Science,* 254**,** 1643-1647.

VAN DER GUN, B. T. F., MONAMI, A., LAARMANN, S., RASK , T., ŚLASKA-KISS, K., WEINHOLD, E., WASSERKORT, R., DE LEIJ, L. F. M. H., RUITERS, M. H. J. & KISS, A. 2007. Serum insensitive,

intranuclear protein delivery by the multipurpose cationic lipid SAINT-2. *Journal of Controlled Release,* 123**,** 228-238.

VAN RHEE, F., SZMANIA, S. M., ZHAN, F., GUPTA, S. K., POMTREE, M., LIN, P., BATCHU, R. B., MORENO, A., SPAGNOLI, G. & SHAUGHNESSY, J. 2005. NY-ESO-1 is highly expressed in poor-prognosis multiple myeloma and induces spontaneous humoral and cellular immune responses. *Blood,* 105**,** 3939-3944.

VAUGHAN, H. A., SVOBODOVA, S., MACGREGOR, D., STURROCK, S., JUNGBLUTH, A. A., BROWNING, J., DAVIS, I. D., PARENTE, P., CHEN, Y.-T. & STOCKERT, E. 2004. Immunohistochemical and molecular analysis of human melanomas for expression of the human cancer-testis antigens NY-ESO-1 and LAGE-1. *Clinical cancer research,* 10**,** 8396-8404.

VEGT, E., DE JONG, M., WETZELS, J. F. M., MASEREEUW, R., MELIS, M., OYEN, W. J. G., GOTTHARDT, M. & BOERMAN, O. C. 2010. Renal toxicity of radiolabeled peptides and antibody fragments: mechanisms, impact on radionuclide therapy, and strategies for prevention. *Journal of Nuclear Medicine,* 51**,** 1049-1058.

VIV S, E., BRODIN, P. & LEBLEU, B. 1997. A truncated HIV-1 Tat protein basic domain rapidly translocates through the plasma membrane and accumulates in the cell nucleus. *Journal of Biological Chemistry,* 272**,** 16010-16017.

WANG, H. Y., LEE, D. A., PENG, G., GUO, Z., LI, Y., KINIWA, Y., SHEVACH, E. M. & WANG, R.-F. 2004a. Tumor-Specific Human $CD4^+$ Regulatory T Cells and Their Ligands: Implications for Immunotherapy. *Immunity,* 20**,** 107-118.

WANG, R. & BRATTAIN, M. G. 2007. The maximal size of protein to diffuse through the nuclear pore is larger than 60kDa. *FEBS letters,* 581**,** 3164-3170.

WANG, Y., LIANG, Z., YUAN, Y. H., HAN, Y., LIU, Y. X., LIU, N., CHEN, Y. T., RITTER, G., OLD, L. J. & ZHANG, L. J. 2004b. Expression of multiple cancer-testis antigen genes in non-small cell lung cancer treated by chemotherapy prior surgery]. *Zhonghua yi xue za zhi,* 84**,** 464.

WARTERS, R. L., ADAMSON, P. J., POND, C. D. & LEACHMAN, S. A. 2005. Melanoma cells express elevated levels of phosphorylated histone H2AX foci. *Journal of investigative dermatology,* 124**,** 807-817.

WENDER, P. A., MITCHELL, D. J., PATTABIRAMAN, K., PELKEY, E. T., STEINMAN, L. & ROTHBARD, J. B. 2000. The design, synthesis, and evaluation of molecules that enable or enhance cellular uptake: Peptoid molecular transporters. *Proceedings of the National Academy of Sciences,* 97**,** 13003-13008.

WITZIG, T. E., GORDON, L. I., CABANILLAS, F., CZUCZMAN, M. S., EMMANOUILIDES, C., JOYCE, R., POHLMAN, B. L., BARTLETT, N. L., WISEMAN, G. A., PADRE, N., GRILLO-LÃ ŀPEZ, A. J., MULTANI, P. & WHITE, C. A. 2002. Randomized Controlled Trial of Yttrium90–Labeled Ibritumomab Tiuxetan Radioimmunotherapy Versus Rituximab Immunotherapy for Patients With Relapsed or Refractory Low-Grade, Follicular, or Transformed B-Cell Non-Hodgkin's Lymphoma. *Journal of Clinical Oncology,* 20**,** 2453-2463.

WITZIG, T. E., MOLINA, A., GORDON, L. I., EMMANOUILIDES, C., SCHILDER, R. J., FLINN, I. W., DARIF, M., MACKLIS, R., VO, K. & WISEMAN, G. A. 2007. Long-term responses in patients with recurring or refractory B-cell non-Hodgkin lymphoma treated with yttrium 90 ibritumomab tiuxetan. *Cancer,* 109**,** 1804-1810.

XING, B. C., YUAN, Y. H., HU, Z. G., LIU, Y. X., HAN, Y., LIU, N., CHEN, W. F. & WANG, Y. 2004. Expression of NY-ESO-1/LAGE-1 genes in hepatocellular carcinoma and autologous humoral responses induced thereby]. *Zhonghua yi xue za zhi,* 84**,** 1980.

YE, D., XU, D., SINGER, A. U. & JULIANO, R. L. 2002. Evaluation of strategies for the intracellular delivery of proteins. *Pharmaceutical research,* 19**,** 1302-1309.

YIN, L.-M., WEI, Y., WANG, Y., XU, Y.-D. & YANG, Y.-Q. 2013. Long term and standard incubations of WST-1 reagent reflect the same inhibitory trend of cell viability in rat airway smooth muscle cells. *International journal of medical sciences,* 10**,** 68.

YU, T., MACPHAIL, S. H., BANATH, J. P., KLOKOV, D. & OLIVE, P. L. 2006. Endogenous expression of phosphorylated histone H2AX in tumors in relation to DNA double-strand breaks and genomic instability. *DNA repair,* 5**,** 935-946.

YUANFANG, L. & CHUANCHU, W. 1991. Radiolabeling of monoclonal antibodies with metal chelates. *Pure Appl. Chem,* 63**,** 427.

ZAMORE, P. D., TUSCHL, T., SHARP, P. A. & BARTEL, D. P. 2000. RNAi: double-stranded RNA directs the ATP-dependent cleavage of mRNA at 21 to 23 nucleotide intervals. *cell,* 101**,** 25-33.

ZASSLER, B., BLASIG, I. E. & HUMPEL, C. 2005. Protein delivery of caspase-3 induces cell death in malignant C6 glioma, primary astrocytes and immortalized and primary brain capillary endothelial cells. *Journal of neuro-oncology,* 71**,** 127-134.

ZELPHATI, O. & SZOKA, F. C. 1996. Mechanism of oligonucleotide release from cationic liposomes. *Proceedings of the National Academy of Sciences,* 93**,** 11493-11498.

ZELPHATI, O., WANG, Y., KITADA, S., REED, J. C., FELGNER, P. L. & CORBEIL, J. 2001. Intracellular delivery of proteins with a new lipid-mediated delivery system. *Journal of Biological Chemistry,* 276**,** 35103-35110.

ZENG, G., WANG, X., ROBBINS, P. F., ROSENBERG, S. A. & WANG, R.-F. 2001. CD4+ T cell recognition of MHC class II-restricted epitopes from NY-ESO-1 presented by a prevalent HLA DP4 allele: Association with NY-ESO-1 antibody production. *Proceedings of the National Academy of Sciences,* 98**,** 3964-3969.

ZHANG, W. M., XIAO, G., XIE, D., ZHANG, M., GUO, A. L. & WEN, J. M. 2005. Correlation of NY-ESO-1 gene and protein expression to metastasis and clinicopathologic features of hepatocellular carcinoma. *Ai zheng,* 24**,** 622-626.

ZITVOGEL, L., APETOH, L., GHIRINGHELLI, F. O. & KROEMER, G. 2008. Immunological aspects of cancer chemotherapy. *Nature Reviews Immunology,* 8**,** 59-73.

ZOU, W. 2006. Regulatory T cells, tumour immunity and immunotherapy. *Nature Reviews Immunology,* 6**,** 295-307.

ZUHORN, I. S., KALICHARAN, R. & HOEKSTRA, D. 2002. Lipoplex-mediated transfection of mammalian cells occurs through the cholesterol-dependent clathrin-mediated pathway of endocytosis. *Journal of Biological Chemistry,* 277**,** 18021-18028.